



Calhoun: The NPS Institutional Archive

Theses and Dissertations

Thesis Collection

1981-12

Local heat transfer coefficients around a cylinder in oscillating flow

Brunson, Fred W.

Monterey, California. Naval Postgraduate School

<http://hdl.handle.net/10945/20585>



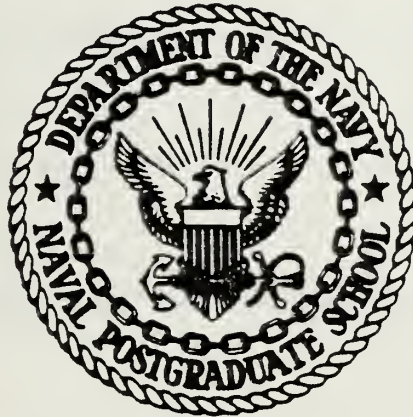
Calhoun is a project of the Dudley Knox Library at NPS, furthering the precepts and goals of open government and government transparency. All information contained herein has been approved for release by the NPS Public Affairs Officer.

Dudley Knox Library / Naval Postgraduate School
411 Dyer Road / 1 University Circle
Monterey, California USA 93943

<http://www.nps.edu/library>

NAVAL POSTGRADUATE SCHOOL

Monterey, California



THESIS

LOCAL HEAT TRANSFER COEFFICIENTS
AROUND A CYLINDER IN OSCILLATING FLOW

by

Fred W. Brunson, Jr.

December 1981

Thesis Advisors: J.A. Miller and P.F. Pucci

Approved for Public Release, Distribution Unlimited

T204554

REPORT DOCUMENTATION PAGE		READ INSTRUCTIONS BEFORE COMPLETING FORM
1. REPORT NUMBER	2. GOVT ACCESSION NO.	3. RECIPIENT'S CATALOG NUMBER
4. TITLE (and Subtitle) Local Heat Transfer Coefficients Around a Cylinder in Oscillating Flow		5. TYPE OF REPORT & PERIOD COVERED Master's Thesis December 1981
		6. PERFORMING ORG. REPORT NUMBER
7. AUTHOR(s) Fred W. Brunson, Jr.		8. CONTRACT OR GRANT NUMBER(s)
9. PERFORMING ORGANIZATION NAME AND ADDRESS Naval Postgraduate School Monterey, California 93940		10. PROGRAM ELEMENT, PROJECT, TASK AREA & WORK UNIT NUMBERS
11. CONTROLLING OFFICE NAME AND ADDRESS Naval Postgraduate School Monterey, California 93940		12. REPORT DATE December 1981
		13. NUMBER OF PAGES 146
14. MONITORING AGENCY NAME & ADDRESS (if different from Controlling Office)		15. SECURITY CLASS. (of this report) Unclassified
		15a. DECLASSIFICATION/DOWNGRADING SCHEDULE
16. DISTRIBUTION STATEMENT (of this Report) Approved for Public Release, Distribution Unlimited		
17. DISTRIBUTION STATEMENT (of the abstract entered in Block 20, if different from Report)		
18. SUPPLEMENTARY NOTES		
19. KEY WORDS (Continue on reverse side if necessary and identify by block number) Heat Transfer, Oscillating Flow, Cylinder, Normal Flow, Yawed Cylinder		
20. ABSTRACT (Continue on reverse side if necessary and identify by block number) Local and average heat transfer coefficients were determined for a right circular cylinder in an oscillating flow. Spanwise plati- num heater strips were used to heat the cylinder isothermally over the lower 180 degrees from the front to rear stagnation point. The four inch diameter cylinder was positioned both normal to and at 45 degrees to the flow direction. Data was gathered for diameter Reynolds numbers from 100,000 to 300,000. Large amplitude oscil- lations were imposed upon the mean flow using a rotating shutter		

arrangement. Frequencies of 0, 5, 10, 22, 50, 100 and 126 Hertz were investigated. For normal flows, local heat transfer coefficients in the wake and average Nusselt numbers were enhanced above values for steady flow, for runs having large amplitude. In the 45 degree flows, no significant change in heat transfer was noted with oscillating flow.

Approved for Public Release, Distribution Unlimited

Local Heat Transfer Coefficients
Around a Cylinder in Oscillating Flow

by

Fred W. Brunson, Jr.
Lieutenant, United States Navy
B.S.M.E., University of Illinois, 1974

Submitted in partial fulfillment of the
requirements for the degree of

MASTER OF SCIENCE IN MECHANICAL ENGINEERING

from the

NAVAL POSTGRADUATE SCHOOL
December 1981

ABSTRACT

Local and average heat transfer coefficients were determined for a right circular cylinder in an oscillating flow. Spanwise platinum heater strips were used to heat the cylinder isothermally over the lower 180 degrees from the front to rear stagnation point. The four inch diameter cylinder was positioned both normal to and at 45 degrees to the flow direction.

Data was gathered for diameter Reynolds numbers from 100,000 to 300,000. Large amplitude oscillations were imposed upon the mean flow using a rotating shutter arrangement. Frequencies of 0, 5, 10, 22, 50, 100 and 126 Hertz were investigated.

For normal flows, local heat transfer coefficients in the wake and average Nusselt numbers were enhanced above values for steady flow, for runs having large amplitude. In the 45° flows, no significant change in heat transfer was noted with oscillating flow.

TABLE OF CONTENTS

I.	INTRODUCTION	12
	A. NORMAL CYLINDER	12
II.	DESCRIPTION OF APPARATUS	15
	A. MODEL	15
	B. WIND TUNNEL	16
III.	EXPERIMENTAL PROCEDURE	21
	A. CALIBRATION OF MODEL	21
	B. ADJUSTMENT OF SURFACE HEATERS	22
	C. FREESTREAM CONDITIONS	23
	D. DATA REDUCTION	23
IV.	RESULTS AND DISCUSSION	25
	A. STEADY FLOW	25
	B. NONSTEADY FLOW	26
	C. NUSSELT NUMBER CORRELATION	28
V.	CONCLUSIONS	29
	APPENDIX A - Data Reduction	30
	APPENDIX B - Sample Calculation	32
	APPENDIX C - Radiation	36
	APPENDIX D - Conduction Losses	38
	APPENDIX E - Uncertainty Analysis	42
	APPENDIX F - Predictor - Corrector Equation	48

LIST OF REFERENCES	143
INITIAL DISTRIBUTION LIST	146

LIST OF TABLES

I.	Summary of Average Heat Transfer Results	103
II.	Summary of Local Heat Transfer Results	105

LIST OF FIGURES

Figure

1.	Sketch of the Model	50
2.	Cross Sectional Sketch of the Model	51
3.	Photograph of the Model	52
4.	Photograph of the Wind Tunnel Test Facility	53
5.	Photograph of the Wind Tunnel Test Section and Instrumentation	54
6.	Plan View of the Wind Tunnel	55
7.	Photograph of the Rotating Shutter Valves	56
8.	Photograph of the Model Mounted in the Tunnel	57
9.	Sketch of Calibration and Working Circuits	58
10.	Typical Velocity Waveforms	59
11.	Sketch of Teledeltos Paper Model	60
12.	Sketch of the Lumped Resistance Model	61
13.	Local Heat Transfer Coefficients in Steady Flow	62
14.	Local Heat Transfer Coefficients in Steady Flow	63
15.	Local Heat Transfer Coefficients in Steady Flow	64
16.	Local Heat Transfer Coefficients in Steady Flow	65
17.	Local Heat Transfer Coefficients in Steady Flow	66
18.	Local Heat Transfer Coefficients in Steady Flow	67

19.	Comparison of Published Steady Flow Results to Experimental	68
20.	Local Heat Transfer Coefficients in Oscillating Flow that Showed Unaltered Results	69
21.	Local Heat Transfer Coefficients in Oscillating Flow that Showed Unaltered Results	70
22.	Local Heat Transfer Coefficients in Oscillating Flow that Showed Unaltered Results	71
23.	Local Heat Transfer Coefficients in Oscillating Flow that Showed Unaltered Results	72
24.	Local Heat Transfer Coefficients in Oscillating Flow that Showed Unaltered Results	73
25.	Local Heat Transfer Coefficients in Oscillating Flow that Showed Unaltered Results	74
26.	Local Heat Transfer Coefficients in Oscillating Flow that Showed Unaltered Results	75
27.	Local Heat Transfer Coefficients in Oscillating Flow that Showed Unaltered Results	76
28.	Local Heat Transfer Coefficients in Oscillating Flow that Showed Unaltered Results	77
29.	Local Heat Transfer Coefficients in Oscillating Flow that Showed Unaltered Results	78
30.	Local Heat Transfer Coefficients in Oscillating Flow that Showed Unaltered Results	79
31.	Local Heat Transfer Coefficients in Oscillating Flow that Showed Unaltered Results	80
32.	Local Heat Transfer Coefficients in Oscillating Flow that Showed Unaltered Results	81
33.	Local Heat Transfer Coefficients in Oscillating Flow that Showed Unaltered Results	82
34.	Local Heat Transfer Coefficients in Oscillating Flow that Showed Unaltered Results	83
35.	Local Heat Transfer Coefficients in Oscillating Flow that Showed Unaltered Results	84

36.	Local Heat Transfer Coefficients in Oscillating Flow that Showed Unaltered Results . . .	85
37.	Local Heat Transfer Coefficients in Oscillating Flow that Showed Unaltered Results . . .	86
38.	Local Heat Transfer Coefficients in Oscillating Flow that Showed Unaltered Results . . .	87
39.	Local Heat Transfer Coefficients in Oscillating Flow that Showed Unaltered Results . . .	88
40.	Local Heat Transfer Coefficients in Oscillating Flow that Showed Enhanced Heat Transfer .	89
41.	Local Heat Transfer Coefficients in Oscillating Flow that Showed Enhanced Heat Transfer .	90
42.	Local Heat Transfer Coefficients in Oscillating Flow that Showed Enhanced Heat Transfer .	91
43.	Local Heat Transfer Coefficients in Oscillating Flow that Showed Enhanced Heat Transfer .	92
44.	Local Heat Transfer Coefficients in Oscillating Flow that Showed Enhanced Heat Transfer .	93
45.	Local Heat Transfer Coefficients in Oscillating Flow that Showed Enhanced Heat Transfer .	94
46.	Local Heat Transfer Coefficients in Oscillating Flow that Showed Enhanced Heat Transfer .	95
47.	Local Heat Transfer Coefficients in Oscillating Flow that Showed Enhanced Heat Transfer .	96
48.	Local Heat Transfer Coefficients in Oscillating Flow that Showed Degraded Heat Transfer	97
49.	Local Heat Transfer Coefficients in Oscillating Flow that Showed Degraded Heat Transfer	98
50.	Local Heat Transfer Coefficients in Oscillating Flow that Showed Degraded Heat Transfer	99
51.	Local Heat Transfer Coefficients in Oscillating Flow that Showed Degraded Heat Transfer	100
52.	Variation of Average Nusselt number with Reynolds number	101

53.	Variation of Average Nusselt number with Reynolds number	102
-----	---	-----

I. INTRODUCTION

A. NORMAL CYLINDER

Forced convective heat transfer from a cylinder in uniform flow has been a topic of interest to researchers since the turn of the century. In 1914 Professor L.V. King presented his relationship to describe the heat transfer from a cylinder in laminar crossflow as a function of air velocity:

$$Nu = A_1 + B_1 N_{Re}^{0.5}$$

Although slightly modified by Collis and Williams in 1959, it still serves today and is the basic equation of hot wire anemometry. Numerous other correlations are available and are a standard part of the heat transfer literature [Ref. 1].

A topic of increasingly greater interest to researchers and designers is the effect of an oscillating flow on forced convection. Gas turbine designers are intensely interested in upgrading the performance of gas turbine blades through materials research and blade cooling. Gas turbine blades experience a hot, oscillating flow environment as they pass through the wakes of upstream blades.

Heat exchange designers involved in waste heat recovery from diesel engine exhausts are also concerned with the effect of flow oscillations on the exchange of heat to and from cylinders.

Little data has been made available to date for a cylinder in oscillating flow. Data is available for heat transfer from a flat plate in oscillating flow [Refs. 1, 2 and 3] and for an airfoil in oscillating flow [Ref. 4]. Data for a cylinder in other than uniform flow is generally for a vibrating cylinder with or without a net flow [Ref. 5] or for a cylinder with screen induced turbulence of less than about ten percent [Refs. 6, 7, 8 and 9]. This study concerns itself with the effect of oscillations on the order of fifty percent of the freestream velocity on local heat transfer rates.

Yawed cylinders are of interest to aerodynamicists because of the correlation of a yawed cylinder to a swept back aircraft wing. Researchers and designers may also encounter yawed cylinders in heat exchangers and other applications.

No information is currently available on the effect of flow oscillations on a yawed cylinder. Viteri [Ref. 10] determined the average heat transfer coefficients of yawed cylinders in uniform flow, and Kraabel [Ref. 11] determined the local heat transfer coefficients around yawed cylinders in uniform flow. These papers provide a basis for validation of the yawed cylinder results reported here.

It has been demonstrated by Miller [Ref. 2] that augmented convective heat transfer can be attributed to the reduction of laminar to turbulent transition Reynolds numbers. Despard [Ref. 12] showed that freestream oscillations promote laminar boundary layer separation in the presence of an adverse pressure

gradient. Banning [Ref. 13] produced data that revealed that the starting vortex associated with periodic separation from an airfoil in oscillating flow produced an unexpectedly strong boundary layer reattachment which markedly improved the aerodynamic performance of the foil.

In summary, the effects of early laminar to turbulent boundary layer transition and the destabilized boundary layer produced slightly augmented heat transfer while periodic vortices shed from the separation point can cause periodic reattachment of the hydrodynamic boundary layer. This can be expected to greatly enhance the heat transfer in the afterbody region.

The purpose of this investigation is to determine the effect of large flow oscillations on the local heat transfer coefficients around both normal and yawed cylinders. Additionally it is desired to develop a correlation formula for the average Nusselt number in oscillating flow that includes the effect of yaw angle, Reynolds number, and flow frequency and amplitude.

II. DESCRIPTION OF APPARATUS

A. MODEL

The model used in the investigation was a four inch diameter cylinder. It was fabricated from one half inch wall thickness fiberglass-phenolic tubing two feet long. The 12 inch mid-span section was instrumented with 16 platinum heater/resistance thermometers oriented parallel to the axis of the cylinder and spaced 12 degrees apart from center-to-center. A sketch of the model showing the orientation of the heater strips is shown in Figure 1.

The platinum strips used were 12 inches long by one-quarter of an inch wide by one-thousandth of an inch thick. Each strip subtended an arc of 7.16 degrees of the circumference of the cylinder. The strips were spot welded to brass studs that were machined flush with the cylinder on the outside and protruded into the interior of the model for attachment of the voltage sensing and current carrying wires. Figure 2 shows a cross section of the cylinder wall through the studs and strips. Voltage drop across the platinum strip was measured using the voltage sensing wires attached to each stud. Platinum was used to both heat the cylinder and determine the surface temperature of the cylinder because of its large linear resistivity-temperature relationship. The resistance of the strips was determined from the voltage drop across the strip which was

then to be used to find the temperature. The amount of heat convected at each location was proportional to the power dissipated by the strip which was equal to the product of the current squared and the strip resistance.

The entire outside of the cylinder, including the platinum strips, was covered with a thin layer of hard epoxy. The hard epoxy layer was machined and polished on a lathe to reduce the thickness over the strips to less than one-hundredth of an inch and to produce a smooth heat transfer surface. A photograph of the completed model showing the mounting stud and bracket and electrical leads is shown in Figure 3.

Two copper-constantan thermocouples were mounted on the inside surface of the cylinder at 90 degrees and 270 degrees from the front stagnation point. These thermocouples were used to monitor the interior wall temperature of the cylinder in order to estimate the heat loss to the inside of the cylinder.

B. WIND TUNNEL

The experiment was carried out in the oscillating flow wind tunnel of the Naval Postgraduate School. Photographs of the facility are shown in Figures 4 and 5. The oscillating flow wind tunnel is a low speed, open circuit wind tunnel with the inlet bell extending out of the building. The tunnel inlet bell is eight feet square and the test section is two feet square, providing a 16.1 contraction ratio. Three high solidity screens located in the inlet section upstream of the nozzle

produce freestream turbulence intensities of less than 0.5 percent of the freestream velocity for uniform flow.

The wind tunnel drive consists of two axial flow fans in series, each of which has an internal, 100 horsepower, direct connected, 1750 RPM motor. The fan blades are internally adjustable through a pitch range of 25 to 55 degrees, providing a wide operating base. A set of variable inlet vanes, located immediately upstream of each fan, are externally adjusted to provide control of test section velocity. These vanes, of radial configuration, preswirl the air in the direction of fan rotation to reduce fan capacity. The total range of freestream velocities possible is from ten to 250 feet per second.

A plan view sketch of the wind tunnel showing the location of the fans and inlet vanes in relation to the test section is shown in Figure 6.

Two fundamental methods are available to superimpose oscillating flow, on a mean velocity. Both Nickerson [14] and Hori [15] introduced oscillations by oscillating their models in a steady flow environment. This method severely restricts the range of attainable frequencies because of mechanical complications and instrumentation difficulties.

The other approach is to provide an oscillating flow environment over a stationary model. Hill [16] used a sliding shutter to impose oscillations on the freestream but was limited to low frequencies because of mechanical difficulties. Feiler and Yeager [17] used a siren mounted upstream of an eight inch

diameter wind tunnel to expose small models to frequencies ranging from 34 to 300 Hz. with root-mean-squared amplitudes of up to 65 percent of the mean velocity. The most successful method of obtaining oscillating flows with a large range of frequencies, amplitudes and flow velocities in a moderate sized tunnel is that employed by Karlson [18] and later by Miller [19]. A rotating shutter valve, immediately downstream of the test section is used to superimpose a periodic variation of velocity on the mean flow. The method used in this investigation is identical to that used by Miller.

The shutters consist of four horizontal, equally spaced, shafts mounted in a plane just downstream of the test section. The shafts are slotted to receive blades of various widths, forming a set of four butterfly valves spanning the wind tunnel. Figure 7 is a picture of the shutter valve assembly. The shutters are driven synchronously by a pulley and belt arrangement and a vari-drive motor and gearcase, and can be varied from 0.1 - 250 Hz. The amplitude of the oscillation is a function of the width of shutter blades, frequency of rotation of the shutters and the freestream velocity. Five sets of blades are available producing tunnel blockages of 33, 50, 66, 83 and 100 percent of the flow area in the fully closed position. In this investigation blades providing 66 and 100 percent blockage were used resulting in amplitudes of 5 to 69 percent of the mean freestream velocity.

The test section of the tunnel is fabricated from two-two inch thick, 25 inch wide by 18 feet long pieces of aluminum as the upper and lower walls and three-two inch thick stress relieved lucite panels on each side as side walls. The front panels are hinged at the top and can be hydraulically opened and closed for access to the test section.

For this investigation the rear center, lucite panel has been replaced by a two inch thick plywood panel to facilitate mounting the model. The model was mounted by a chordwise extension held in a rotatable clamp mounted flush in the center of the plywood panel. The other end of the model is supported by a 3/8 inch thick "Y" shaped, faired bracket, that is affixed to the tunnel ceiling and floor, and rests against the front lucite panel. The model is shown in place with the "Y" bracket clearly visible in Figure 8. Electrical leads were taken out through the plywood back panel where they were connected to the power supplies and the voltage drop sensing circuits. The model was yawed by affixing extension pieces to each end that were angled and sized to completely span the tunnel at each angle of yaw.

Power to heat the strips was controlled by sixteen variacs that powered 16 individual DC power supplies (see working circuit, Figure 9). A precision shunt ($R=0.001$) was placed in series with each strip and the voltage drop across the known resistance was used to determine the current. The voltage drop across each strip was measured using the potential sensing

leads that were attached to the studs on the inside of the model. Instantaneous velocity measurements for the purpose of free-stream turbulence determination in uniform flows and amplitude and frequency measurement in oscillating flows were made using a linearized constant temperature hot-wire anemometer described in Reference 20. An oscilloscope and a Ballantine True R.M.S. meter were used to monitor hot-wire signals. Mean velocity of the free stream was measured using a Prandtl Probe and a water-filled micromanometer.

Figure 10 shows a pair a typical velocity wave forms. The vertical axis is velocity and the horizontal axis is time. The roughness of the upper tracing is typical of low amplitude oscillations which are significantly more difficult to produce in true sinusodial form.

The freestream temperature and the model internal wall temperature were measured using copper-constantan thermocouples and a Newport digital temperature indicator.

The frequency of oscillation was also monitored with an optical chopper driven by a shutter valve shaft and a digital counter.

III. EXPERIMENTAL PROCEDURE

A. CALIBRATION OF MODEL

The platinum strips were calibrated as resistance thermometers by determining their electrical resistance as a function of temperature in an electric oven. Seven separate temperatures were used, evenly spaced between ambient (60°F) and 200°F. Although the platinum heater-thermometer strips were extremely pure and are expected to have a linear resistance-temperature characteristic, calibration was carried out to determine the exact slope and intercept of each strip.

The calibration circuit employed (see Figure 9) was powered by a low impedance DC voltmeter calibration standard. This proved to be an extremely precise, drift free power supply. The voltage drop across the precision resistance ($1.0 \pm 0.15\%$) was recorded as was the voltage drop across the heater strip itself. The current was then computed from the voltage drop across the precision resistance divided by one ohm, and the resistance of the strip for that temperature was computed from the voltage drop across the strip divided by the current. Temperatures in the oven were monitored with a Newport Laboratories Digital Temperature Indicator and a copper-constantan thermocouple.

After determining the resistances as a function of the temperature a straight line was fitted to the data using linear regression. The resulting equations were used throughout the

subsequent experimentation and data reduction to determine surface temperatures.

B. ADJUSTMENT OF SURFACE HEATERS

Before each series of runs the heater strips were energized and the wind tunnel was run with a low velocity uniform flow in order to allow the model substrate to come to thermal equilibrium. Once this was accomplished the shutters were turned on and adjusted to the desired frequency and the velocity was adjusted to the magnitude corresponding to the Reynolds number desired. At this point the model was again allowed to come to thermal equilibrium.

Once this initial thermal equilibrium was achieved the voltage drop and current through each strip was recorded and inserted into a predictor-corrector program (see Appendix F). This program calculated a new required voltage drop based on desired strip temperature, current strip temperature, and the known resistance-temperature calibration curve for that strip; the strip was then adjusted to the new desired voltage drop through adjustment of its power supply. Following adjustment of the strips the model was again allowed to return to thermal equilibrium.

These adjustments were performed as many times as necessary until all the strips were at the same temperature, ensuring an isothermal heat transfer surface that minimized heat conduction between strips.

The temperature for a particular run was determined from a sampling of the strip temperatures before the first set of adjustments was made and was selected to minimize the number of adjustments required. In every case however the temperature was chosen to be over 110°F in order to maintain at least a 50° temperature difference between the strip and the ambient temperature.

C. FREESTREAM CONDITIONS

A series of runs was made with both the 45° yawed model and the normal model covering a wide range of operating conditions. Each model was tested with both the six inch blades (100 percent tunnel blockage) and the four inch blades (66 percent tunnel blockage), resulting in oscillation amplitudes from five to 69 percent of freestream mean velocity. Each combination of frequency and amplitude was run at two freestream velocities corresponding to nominal diametral Reynolds numbers of 300,000 and 150,000. Frequencies investigated were 0, 5, 10, 22, 50, 100 and 125 Hz.

D. DATA REDUCTION

The data reduction technique is described in Appendix A and a sample calculation is presented in Appendix B. A detailed energy balance is necessary in order to determine what portion of the total Joulian heat generated by platinum resistance heater is transferred from the surface by convection. Part of the energy was conducted through the thin epoxy coating and

convected directly to the freestream or was radiated into the environment. The balance of the energy was conducted into the substrate of the cylinder where some was conducted and convected into the center of the cylinder, some was lost to the ends of the cylinder, and some was conducted to the gaps between the strips where it was convected to the freestream or was radiated to the environment.

The energy lost from the substrate side of the surface heaters is hard to determine analytically since it consists of both conduction to the intraheater gaps and subsequent loss by convection and radiation as well as conduction to the inner surface of the model. Therefore a two-dimensional Teledeltos paper model was constructed to determine the relationship between the thermal resistances to the inner and outer surfaces. This procedure and the results are discussed in Appendix D. The results of the Teledeltos paper experiment were placed in equation form and solved iteratively for the external convection heat transfer coefficient, h , for each strip.

The other major loss of energy from the system is by radiation to the environment. These losses can be appreciable and an accounting for this loss was developed as part of the data reduction program. Details are described in Appendix C.

IV. RESULTS AND DISCUSSION

A. STEADY FLOW

Six steady flow runs were made, two with the model normal to the flow at $N_{Re} = 150,000$ and $300,000$ and four runs with the model at 45° to the flow at $N_{Re} = 35,000, 100,000, 150,000,$ and $300,000$. The results of these runs are shown graphically in Figures 13 through 18. Results of the model at 90° (normal to the flow) at $N_{Re} = 150,000$ are compared in Figure 19 with the theory of Froessling [Ref. 24] and the experimental results of Schmidt [Ref. 25] for $N_{Re} = 170,000$. The discrepancy between theory and both of the experimental results is expected and is a consequence of the effect of freestream turbulence near the stagnation point [Ref. 26].

Comparison of the results of the present experiment with those of Schmidt indicates two interesting points. The two agree within 20 percent up to an angle of 150° from the stagnation point, beyond which they diverge markedly, differing by 70 percent at 180° . This sharp increase in heat transfer above that noted by Schmidt is typical of all the results observed in the present investigation and shows no correlation with frequency number or Reynolds number. Agreement within 20 percent is good however and this lends a high degree of confidence in the experimental techniques and results.

No local heat transfer data is available for the steady flow case with 45° yaw. However, the data of Viteri [Ref. 10] can be interpolated to arrive at an average Nusselt number of 128.3 at a Reynolds number of 31,900. At a Reynolds number of 35,630 the present experiment produced an average Nusselt number of 122.1. This close agreement lends confidence in at least the average Nusselt Numbers obtained in the 45° yawed case.

B. NONSTEADY FLOW

Two thirds of the nonsteady freestream conditions did not produce substantial alteration in heat transfer when compared to the steady flow case. Figures 20 through 25 depict the cases with the 90° model that show little or no altered heat transfer, and Figures 26 through 39 depict those of the 45° model. In each of these figures the steady flow data has been plotted along with the nonsteady data for comparison.

Twelve of the 38 freestream conditions investigated produced substantially altered local heat transfer rates. These results are shown graphically in Figures 40 through 49 for the 90° model, and Figures 50 and 51 for the 45° model. The changes in local Nusselt number took place almost exclusively in the afterbody region of the model, and resulted from altered separation and flow patterns in the wake of the cylinder. Figure 40 is a typical example of these results and demonstrates enhanced heat transfer in the wake area of the 90° model. The data reported in Figures 48 through 51 exhibit diminished heat transfer rates. Figure 50 is typical of this class of data.

In order to simplify the analysis of the results, the average Nusselt number was calculated for each freestream condition (see Table I). Figures 52 and 53 report average Nusselt numbers versus Reynolds number for the 90° model and the 45° model respectively. In the 90° case (Figure 52) a curve has been drawn representing $Nu = N_{Re}^{0.5716}$ and the Amplitude and Strouhal numbers have been annotated for each data point. Of interest is the fact that data with higher Amplitude numbers are those which tend to exhibit augmented average heat transfer rates. Moreover, higher Amplitude numbers seem to correspond to greater heat transfer augmentation. Although the data is sparse, a pattern of larger Nusselt numbers for larger Amplitude numbers at the same Reynolds number seems to exist. Three apparent anomalies exist associated with the data from run numbers 15, 17 and 20. It is possible that an error in recording the amplitude data was made and that the Amplitude numbers for runs 17 and 20 were reversed. If this were true then both runs 17 and 20 would conform to the apparent pattern. When the Frequency numbers, Nusselt numbers and Reynolds numbers of runs 15 and 17 are compared, it is seen that they are very similar but that the Amplitude numbers are considerably different. If the previously noted pattern for higher Nusselt number for higher Amplitude number is true then the Amplitude number of run 15 is suspect and may be too low.

Average Nusselt number data taken for the 45° model is shown in Figure 53. No apparent pattern of heat transfer alteration is evident in this plot even though Amplitude numbers as high as 0.44 and 0.65 appear in the data.

C. NUSSELT NUMBER CORRELATION

The data obtained in this investigation is too sparse to allow a correlation between heat transfer rate and freestream conditions to emerge. Only a possible pattern is suggested by the results and more data covering a wide range of Reynolds numbers and Amplitude numbers is necessary to produce such a correlation.

V. CONCLUSIONS

Although there is insufficient data to draw any definite conclusions or to derive a correlation, several trends may be observed. In the 90° case, significant increases in the local Nusselt numbers are seen in the wake region and are due to changes in the separation and wake structure. Moreover, augmentation of local Nusselt numbers seems to increase with increasing frequency as suggested by the data shown in Figures 40 through 47. Increases in average Nusselt numbers is apparently related to the Amplitude numbers as discussed above and shown in Figure 52. With the exception of the three points associated with runs 15, 17 and 20, discussed in Chapter IV, the pattern exhibited is for higher average Nusselt numbers to be associated with greater amplitudes.

In the case of the 45° yawed cylinder, no general patterns are discernable and it appears that local Nusselt numbers exhibit no significant change over a wide range of frequencies and amplitudes.

This investigation has served to initiate a study of heat transfer from a cylinder in oscillating flow. Additionally it has validated the techniques to be used for further study. More extensive data collection will be required before definitive conclusions can be drawn or correlations made.

APPENDIX A

DATA REDUCTION

The data was reduced to the form shown in Table 2 by a specially written Fortran computer program on an IBM 360 computer at the Naval Postgraduate School.

The raw data consisted of pitot-static tube ΔP (inches H_2O), freestream temperature, T_F , ($^{\circ}F$), internal model temperatures (heater side and "other" side, $^{\circ}F$), frequency of oscillation (Hz), amplitude ratio (%) and the voltage drop across (volts) and current passing through (amperes) each strip. The total power dissipated by each strip is simply:

$$P = 3.4149 \times E \times I$$

where 3.4149 is a conversion factor from watts to BTU/Hr.

From the measured current (I) and voltage drop (E) each individual strip temperature is determined by comparing its resistance to its known temperature versus resistance characteristics. The resistance of a strip is:

$$R = \frac{E}{I}$$

From the linear temperature-resistance relationship obtained during calibration, the strip temperature can be obtained:

$$T_S = \frac{R-C}{S}$$

where C and S are the known ordinate intercept and slope obtained from the individual resistance versus temperature calibration curve.

The other unknown temperature required by the data reduction program is the inner wall temperature, T_I . The inner wall temperatures are known at two points. Thermocouples are mounted on the wall at locations 90° and 270° from the stagnation point at mid-span (see Figure 2). The inner wall temperature is assumed to vary linearly between these two measured values.

With this information h, the heat transfer coefficient may be calculated. The following formula (developed in Appendix D) is used:

$$q_s = \frac{T_s - T_F}{R_D} \left[1 + \frac{R_D}{R_O} \right] + \frac{T_s - T_I}{R_D} \left[\frac{R_I}{R_D} \right]$$

h is contained in the expressions for R_D , R_O/R_D , and R_I/R_D as is shown in Appendix D. This equation was solved iteratively to obtain h.

With the local h for each strip, the local Nusselt number is calculated from:

$$Nu = \frac{hD}{k}$$

APPENDIX B

SAMPLE CALCULATION

For the purpose of this sample calculation strip Nr 6 from data run Nr 20 was selected.

The information recorded is:

Voltage drop	E = 1.62 Volts
Current	I = 7.47 Amps
Pitot-Static Pressure	HW = 4.16 inches H ₂ O
Ambient Temperature	TA = 64.0°F
Inside Temperature:	
Heater Side	TIHTR = 105.0°F
Other Side	TIOTH = 77.0°F
Frequency	Freq = 50.0 CPS
Amplitude Ratio	N _A = 0.31
Blades	Medium (4")
Model	90° to stream
Barometric Pressure	30.04 inches Hg

Freestream Mean Velocity

$$\begin{aligned} V &= \left[2g_{HW} \left(\frac{\gamma_{water}}{\gamma_{air}} \right) - 1 \right]^{1/2} \\ &= \left[2 \left(32.2 \frac{ft}{s^2} \right) (4.16 \text{ in H}_2\text{O}) \left(\frac{1. ft}{12. in} \right) \left\{ \frac{62.4 \frac{lb_f}{ft^3}}{0.07654 \frac{lb_f}{ft^3}} - 1 \right\} \right]^{1/2} \\ &= 134.4 \frac{ft}{sec} \end{aligned}$$

Freestream Reynolds number:

$$N_{Re} = \frac{VD}{\nu} = \frac{134.8 \frac{ft}{s} (0.333 ft)}{0.000166 ft^2/s}$$

$$= 269,800$$

Temperature of the strip:

$$T = \frac{\frac{E}{I} - C}{S}$$

$$\frac{E}{I} = \frac{1.622 Volts}{7.47 Amps} = 0.2171 ohms$$

$$C = 0.173955807$$

$$S = 0.000390625$$

Therefore,

$$T = \frac{0.2171 - 0.173955807}{0.000390625} = 110.5^{\circ}F$$

Total Heat Dissipated by the strip:

$$q_s = EI = (3.4149 \frac{Btu}{Volt-Amp-hr})(1.622 Volts)(7.47 Amps)$$

$$= 41.38 Btu$$

Also:

$$q_s = \frac{1}{R_D} \left[(T_S - T_F) \left(1 + \frac{R_D}{R_O} \right) + (T_S - T_I) \left(\frac{R_D}{R_I} \right) \right]$$

$$R_D = \frac{k + \ell h_r}{k h_T A}$$

$$\frac{R_O}{R_D} = a_1 + a_2 h_T$$

$$\frac{R_I}{R_D} = b_1 h_T + b_2 h_T^2 + b_3 h_T^3$$

After substitution, the equation may be solved for h_T .
 (the constants a_1 , a_2 , b_1 , b_2 and b_3 are given in Appendix D).
 By iteration:

$$h_t = 36.9 \frac{\text{Btu}}{\text{hr} - \text{ft}^2 - ^\circ\text{F}}$$

The radiant heat transfer coefficient:

$$h_r = \epsilon \sigma (T_S + T_A)(T_S^2 + T_A^2)$$

Assuming T_A is the same as the fluid temperature:

$$\begin{aligned} h_r &= (0.73)(0.1718 \times 10^{-8})(570.5 + 524.0) \\ &\quad \times (570.5^2 + 524.0^2) \\ &= 0.824 \frac{\text{Btu}}{\text{hr} - \text{ft}^2 - ^\circ\text{F}} \end{aligned}$$

Therefore, the local convective heat transfer coefficient is:

$$\begin{aligned} h &= h_T - h_r \\ &= 36.9 - 0.824 \\ &= 36.1 \frac{\text{Btu}}{\text{hr} - \text{ft}^2 - ^\circ\text{F}} \end{aligned}$$

The local Nusselt number:

$$\text{Nu} = \frac{hd}{k} = \frac{(36.1)(0.333)}{0.014738}$$

$$= 815.9$$

APPENDIX C

RADIATION

For a uniformly convex gray body with emissivity ϵ , at a temperature T , radiating into an enclosure of temperature T_∞ , the net radiant heat exchange is:

$$q_r = \sigma \epsilon A (T^4 - T_\infty^4)$$

where σ is the Stefan-Boltzmann constant, and A is the surface area of the emitter.

The above equation can be put in the same form as the convection equation:

$$q_r = h_r A (T - T_\infty)$$

where h_r is the effective radiation heat transfer coefficient given by:

$$h_r = \epsilon \sigma (T + T_\infty)(T^2 + T_\infty^2)$$

Taking $\epsilon = 0.73$ for epoxy coating over aluminum [Ref. 22] and the following typical temperatures:

$$T = 120^\circ\text{F} = 580^\circ\text{R}$$

$$T_\infty = 60^\circ\text{F} = 520^\circ\text{R}$$

Gives:

$$\begin{aligned} h_r &= 0.73 (0.1714)(10^{-8})(580 + 520)(580^2 + 520^2) \\ &= 0.835 \frac{\text{Btu}}{\text{hr} \cdot \text{ft}^2 \cdot \text{F}} \end{aligned}$$

This value falls within two to 10 percent of the total heat transfer coefficient and therefore cannot be neglected. Therefore, the convective heat transfer coefficient, h , is obtained by subtracting the radiant heat transfer coefficient, h_r , from the experimentally derived total heat transfer coefficient, that is,

$$h = h_T - h_r \quad .$$

APPENDIX D

CONDUCTION LOSSES

Although the thermal resistance of the fiberglass substrate is very high compared to the thermal resistance between the strip and the fluid, some heat is lost to the interior of the model. This heat loss must be deducted from the total heat input in order to arrive at the actual heat transferred to the air. Heat loss due to conduction in the longitudinal axis direction and radially through the small brass studs was neglected.

A Teledeltos paper model was used to estimate the heat loss to the interior of the model. Symmetry was used to reduce the size of the required model (see Figure 11).

Teledeltos paper is a graphite covered paper having a nominal resistivity of 1000 ohms per inch square and is highly isotropic. Teledeltos paper is extremely useful for two-dimensional heat conduction modeling in cases such as this which have boundary conditions and a physical shape that are inconvenient for an exact solution.

The heater strip itself is simulated with a strip of silver conductive paint that is placed on the paper in exactly the same position as the platinum strip is on the actual model. The inside of the model segment is considered isothermal so the analogous surface of the Teledeltos paper model was

held at uniform potential with a conductive strip of silver paint. The left and right hand adiabatic boundaries, between strips, are easily modeled by leaving them bare. The convective boundary at the gap between strips is modeled by allowing the Teledeltos paper to extend beyond the actual cylinder surface for a distance to simulate the convection resistance. The required distance is determined by:

$$L = \frac{k}{h} S$$

where k is the conductivity of the actual substrate, h , is the convective coefficient being modeled and S is the scale factor, in this case, $S = 48$. Additionally the excess length was slit into eight equal width strips lengthwise to force the flux lines parallel to each other and perpendicular to the surface. In order to model h 's of 10, 20, 50 and 100 Btu/hr·ft²·F, L 's of 14.4, 7.2, 2.88 and 1.44 inches respectively were used.

A strip temperature of 120°F with an inner temperature of 100°F and a fluid temperature of 60°F were used. These temperatures were scaled to appropriate voltages that would avoid excessive Joulian heating of the Teledeltos paper.

In operation the voltages were measured at 17 equally spaced intervals along the line corresponding to the cylinder surface and at five equally spaced points along a line corresponding to 0.08 inches from the inner surface. This allows the determination of the ratio of heat loss to the inside of

the model, compared to the heat loss indirectly through the air (via the substrate).

Considering the lumped electrical resistance network analogous to the heat transfer problem (see Figure 12) it is noted that the power input to the strip is equal to the sum of the losses to the air, to the inside of the cylinder to the gap between the strips, or:

$$q_s = q_D + q_O + q_I$$

since in general:

$$q = \frac{\Delta T}{R_{TH}}$$

this becomes:

$$q_s = \frac{T_S - T_F}{R_D} + \frac{T_S - T_F}{R_O} + \frac{T_S - T_I}{R_I}$$

Where T_S , T_F and T_I are the temperatures of the strip, the fluid and the inside respectively and R_D , R_O and R_I are the thermal resistances from the strip to the air, from the strip through the gap to the air ($R_O = R_a + R_b$) and through the substrate to the inside of the cylinder respectively (see Figure 12).

This equation can be manipulated into the following form:

$$q_s = \frac{T_S - T_F}{R_D} \left[1 + \frac{R_D}{R_O} \right] + \frac{T_S - T_I}{R_D} \left[\frac{R_D}{R_I} \right]$$

The resistance to heat loss from the strip directly to the air, R_D , is due to the thin layer of epoxy on the strip and the convection film resistance. The conduction resistance due to the epoxy is equal to ℓ/kA where ℓ is the thickness of the epoxy layer, k is the thermal conductivity of the epoxy and A is the surface area of the strip. The convective resistance is equal to $1/hA$, where h is the convection heat transfer coefficient. Summing these we obtain:

$$R_D = \frac{k + \ell h}{khA}$$

The quantities R_O/R_D and R_I/R_D are derived experimentally from the Teledeltos paper analogue and are in the form of polynomial equations in h :

$$\frac{R_O}{R_D} = 1.546744 + 0.0320672 h$$

$$\frac{R_I}{R_D} = 0.106105h + 0.0047559h^2 + 0.0000079h^3$$

These resistances were used in the heat transfer equation to solve for h (see Appendix B).

APPENDIX E

UNCERTAINTY ANALYSIS

For the purpose of this analysis, the method of Kline and McClintock [Ref. 23] will be used, assuming that all variables have a normal Gaussian distribution. Possible dimensional error in strip size, placement and other dimensions were considered so small as to be negligible. The tabulated values of k and e were assumed to be correct. All temperatures measured with thermocouples were assumed to have an uncertainty, due to readout error, of 0.1 degree F.

The strip temperature uncertainties derive from the ± 0.003 mV uncertainty in reading the digital voltmeter used in calibration and the ± 0.002 V and ± 0.01 amp uncertainty in reading the meters during data runs.

The uncertainty in measured resistances during calibration is

$$\Delta R = R \left[\left(\frac{\Delta I}{I} \right)^2 + \left(\frac{-\Delta V}{V} \right)^2 \right]^{1/2}$$
$$= \pm 0.00031 \text{ ohms}$$

The resistances obtained in calibration are used to obtain a straight line equation for temperature vs resistance.

$$R = S \cdot T + C$$

The uncertainty of C is assumed to be of the same order as R. The uncertainty of S is:

$$\Delta S = S \left[\left(\frac{\Delta R}{R} \right)^2 + \left(\frac{-\Delta T}{T} \right)^2 \right]^{1/2}$$

$$= \pm 0.00000064$$

Since the strip temperature during a data run is given by:

$$T = \frac{\frac{E}{I} - C}{S}$$

The uncertainty of T is given by:

$$\Delta T_S = T_S \left[\left(\frac{\Delta E}{E} \right)^2 + \left(\frac{-\Delta I}{I} \right)^2 + \left(\frac{-\Delta S}{S} \right)^2 \right]^{1/2}$$

$$+ T \left[\left(\frac{\Delta C}{C} \right)^2 + \left(\frac{-\Delta S}{S} \right)^2 \right]^{1/2}$$

$$= \pm 0.54^\circ \text{F}$$

The values of R_0/R_D were obtained from a Teledeltos paper model. Uncertainties in measuring a potential difference between any two points on the Teledeltos paper was ± 0.02 volts. This corresponds to a uncertainty in temperature of $\pm 0.2^\circ$. For R_0/R_D is given by:

$$\frac{R_0}{R_D} = \frac{ADT}{SADT}$$

where ADT is the direct convection surface area times $(T_S - T_F)$
 and SADT is the indirect convection area times $(T_{\text{local}} - T_F)$.
 (T_{local} is determined from the Teledeltos paper model.)

The uncertainty of SADT is given by:

$$\begin{aligned}\Delta \text{SADT} &= \text{SADT} \left(\frac{\Delta(\Delta T)}{\Delta T} \right) \\ &= \pm 0.0011\end{aligned}$$

Similarly for ADT:

$$\begin{aligned}\Delta \text{ADT} &= \text{ADT} \left(\frac{\Delta(\Delta T)}{\Delta T} \right) \\ &= \pm 0.0021\end{aligned}$$

Now

$$\begin{aligned}\Delta \frac{R_O}{R_D} &= \frac{R_O}{R_D} \left[\left(\frac{\Delta \text{ADT}}{\text{ADT}} \right)^2 + \left(\frac{\Delta \text{SADT}}{\text{SADT}} \right)^2 \right]^{1/2} \\ &= \pm 0.0088\end{aligned}$$

R_I/R_D is given by:

$$\frac{R_I}{R_D} = \frac{\text{ADT}}{\text{IADT}} \frac{h}{k} \frac{(T_S - T_I)}{(T_S - T_F)} \Delta y$$

The uncertainty of IADT is given by:

$$\begin{aligned}\Delta \text{IADT} &= \text{IADT} \left(\frac{\Delta(\Delta T)}{\Delta T} \right) \\ &= \pm 0.032\end{aligned}$$

Thus the uncertainty of R_I/R_D is given by:

$$\Delta \frac{R_I}{R_D} = \frac{R_I}{R_D} \left[\left(\frac{\Delta A D T}{A D T} \right)^2 + \left(\frac{\Delta I A D T}{I A D T} \right)^2 + \left(\frac{\Delta \Delta T}{T_S - T_I} \right)^2 + \left(\frac{\Delta \Delta T}{T_S - T_F} \right)^2 \right]^{1/2}$$

$$= \pm 0.024$$

q is given by:

$$q = EI$$

The uncertainty in q is given by:

$$\Delta q = q \left[\left(\frac{\Delta E}{E} \right)^2 + \left(\frac{\Delta I}{I} \right)^2 \right]^{1/2}$$

$$= \pm 0.052 \frac{\text{Btu}}{\text{hr}}$$

Because of the complexity of the formula used to determine h,

h was found by iteration of the following implicit equation:

$$q = \frac{h k A}{k + h \lambda} \left[(T_S - T_F) \left(1 + \frac{1}{A_1 + A_2 h} \right) + (T_S - T_I) \left(\frac{1}{B_1 h + B_2 h^2 + B_3 h^3} \right) \right]$$

The uncertainty of h was determined by:

$$\Delta h = \left[\left(\frac{\Delta T_S 2h}{2T_S} \right)^2 + \left(\frac{\Delta T_F 2h}{2T_F} \right)^2 + \left(\frac{\Delta T_I 2h}{2T_I} \right)^2 \right. \\ \left. + \left(\Delta \left(\frac{R_O}{R_D} \right) \frac{2h}{2(R_O/R_D)} \right)^2 + \left(\Delta \left(\frac{R_I}{R_D} \right) \frac{2h}{2(R_I/R_D)} \right)^2 \right]^{1/2}$$

The partial derivatives were evaluated numerically and were found to be:

$$\frac{2h}{2T_S} = -0.9137 \qquad \frac{2h}{2T_F} = 1.375$$

$$\frac{2h}{2T_F} = 0.0698 \qquad \frac{2h}{2(R_O/R_D)} = 4.7619$$

$$\frac{2h}{2(R_I/R_D)} = 0.01$$

therefore:

$$\Delta h = \pm 0.51 \frac{\text{Btu}}{\text{Hr} \cdot \text{ft}^2 \cdot \text{F}}$$

The mean velocity is given by:

$$V_M = \left[2gH \left(\frac{\gamma_{\text{water}}}{\gamma_{\text{air}}} - 1 \right) \right]^{1/2}$$

The only parameter here that is open to uncertainty (due to the assumption that property values are correct) is the H, or height of water column in the micromanometer. Since $\Delta H = \pm 0.02$ inches:

$$\Delta V_M = \frac{V_M}{2} \left(\frac{\Delta H}{H} \right)$$

$$= \pm 0.324 \text{ ft/s}$$

since:

$$N_{Re} = \frac{VD}{\nu}$$

$$\Delta N_{Re} = N_{Re} \left(\frac{\Delta V_M}{V_M} \right)$$

$$= \pm 635.$$

Nusselt number is by definition:

$$Nu = \frac{hD}{k}$$

therefore:

$$\Delta Nu = Nu \left(\frac{\Delta h}{h} \right)$$

$$= \pm 11.3$$

APPENDIX F

PREDICTOR - CORRECTOR EQUATION

In order to simplify and shorten the process of adjusting strip voltages to obtain an isothermal surface as described in Chapter 3, a predictor-corrector program was developed and implemented on a TI-59 with PC-100C thermal printer. The program listing is included at the end of this Appendix.

The program requires entry of the ambient temperature and desired temperature of the strips. Then the strip number is entered and the program prompts for initial voltage drop and initial current of the strip. The program computes strip temperature using the formula:

$$T = \frac{\frac{E}{I} - C}{S}$$

where C and S are taken from the calibration curves.

Next the program calculates the voltage drop that would be expected at the desired strip temperature using:

$$E_D = \left[\frac{R_D E_i I_i (T_D - T_F)}{(T_D - T_F) + \left[\frac{\frac{E_i}{I_i} - R_D}{S} \right]} \right]^{1/2}$$

Where R_D = required resistance, from calibration

T_F = Fluid temperature

S = Slope of calibration curve

The variac on the test rig is then adjusted to produce this voltage drop across the strip. The strip must be allowed to come to thermal equilibrium after an adjustment is made. The calibration curves assume thermal equilibrium and are meaningless when temperature transients are taking place.

The program listed requires 204 program storage locations and 76 memory storage registers. The TI-59 must be repartitioned to obtain adequate storage registers by entering 8 (2nd) OP 17. This provides 319 program storage locations and 79 data registers. All of the data listed must be entered to take advantage of the full capability of the program.

After the program and stored data are loaded the ambient temperature is specified by entering the temperature and pressing key "B". The desired strip temperature can then be entered and the key "C" depressed. The program is now ready for use.

In use the number of the desired strip is entered and key "A" depressed. The printer will then prompt "E?" and the initial voltage drop should be entered and the "R/S" key depressed. The program will echo the current on the printer and will proceed to print the current temperature and desired voltage drop. The program will then pause and is ready for the next strip number.

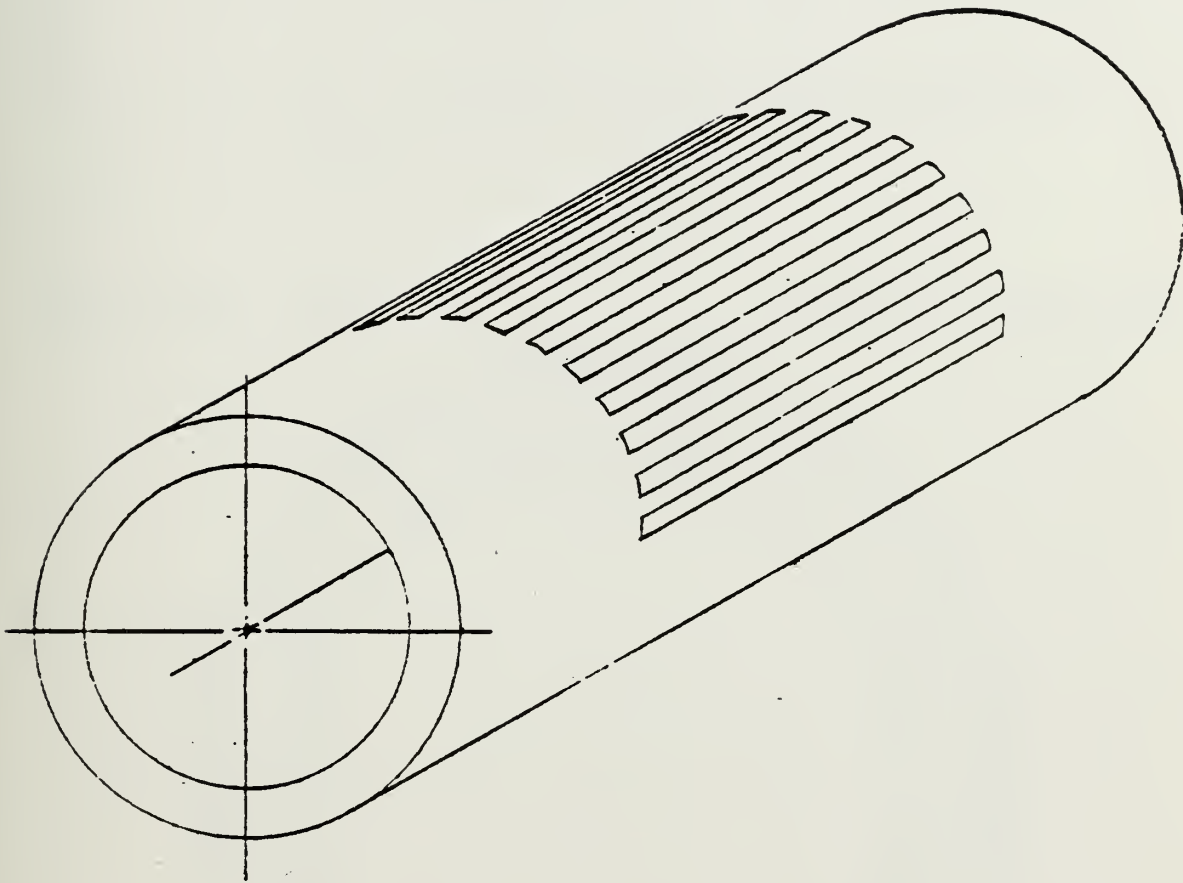


FIGURE 1 - SKETCH OF THE MODEL

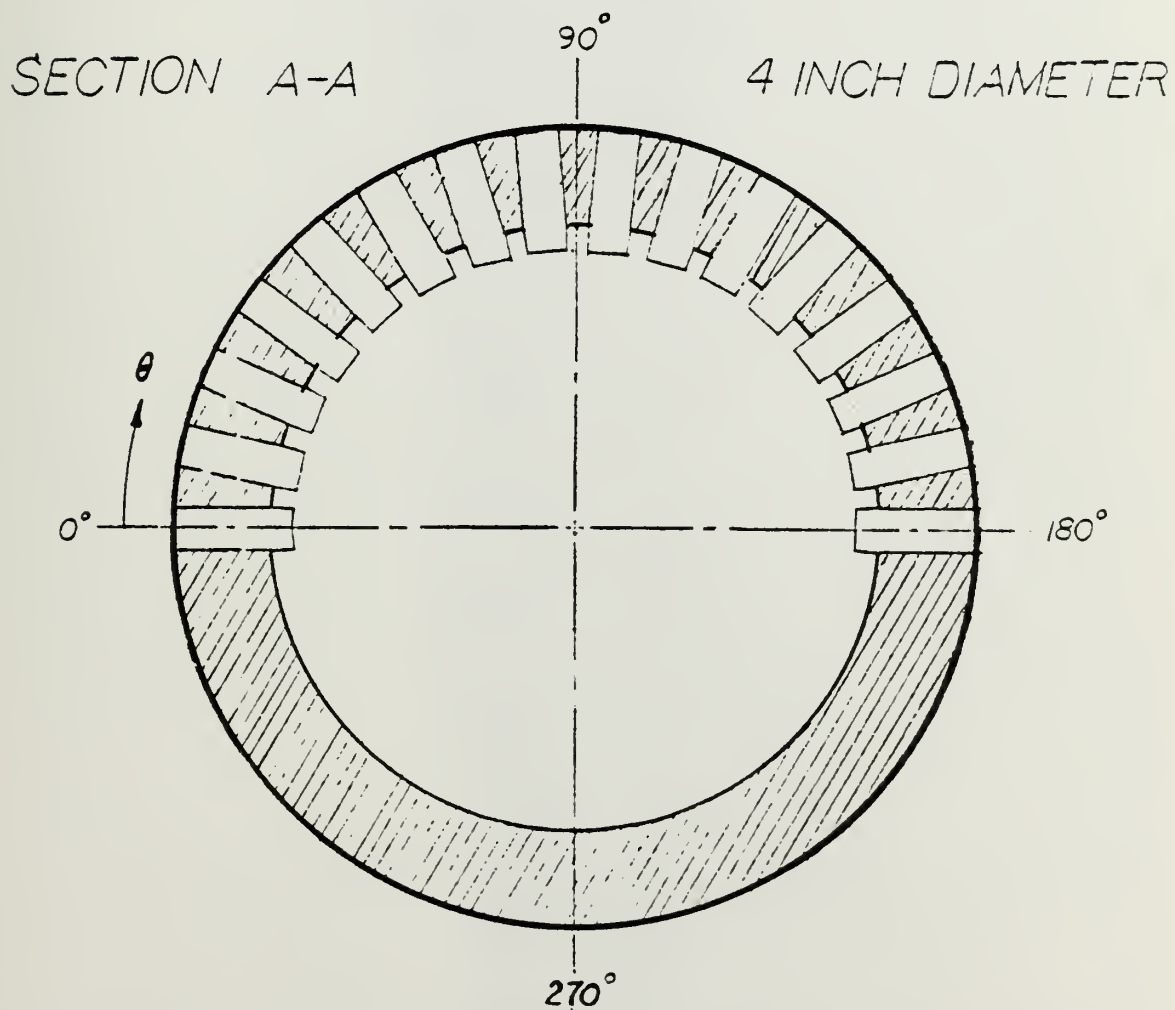
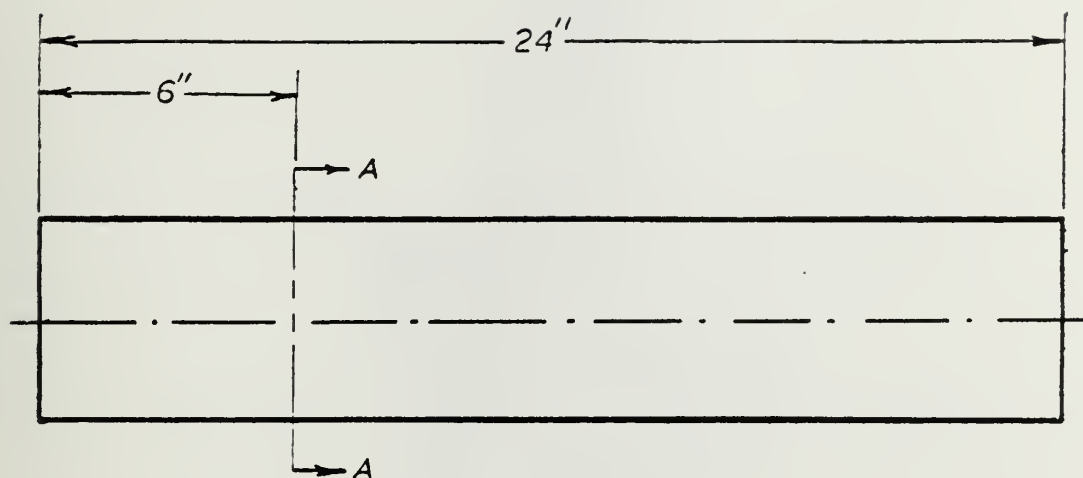


FIGURE 2 - CROSS-SECTIONAL SKETCH OF THE MODEL

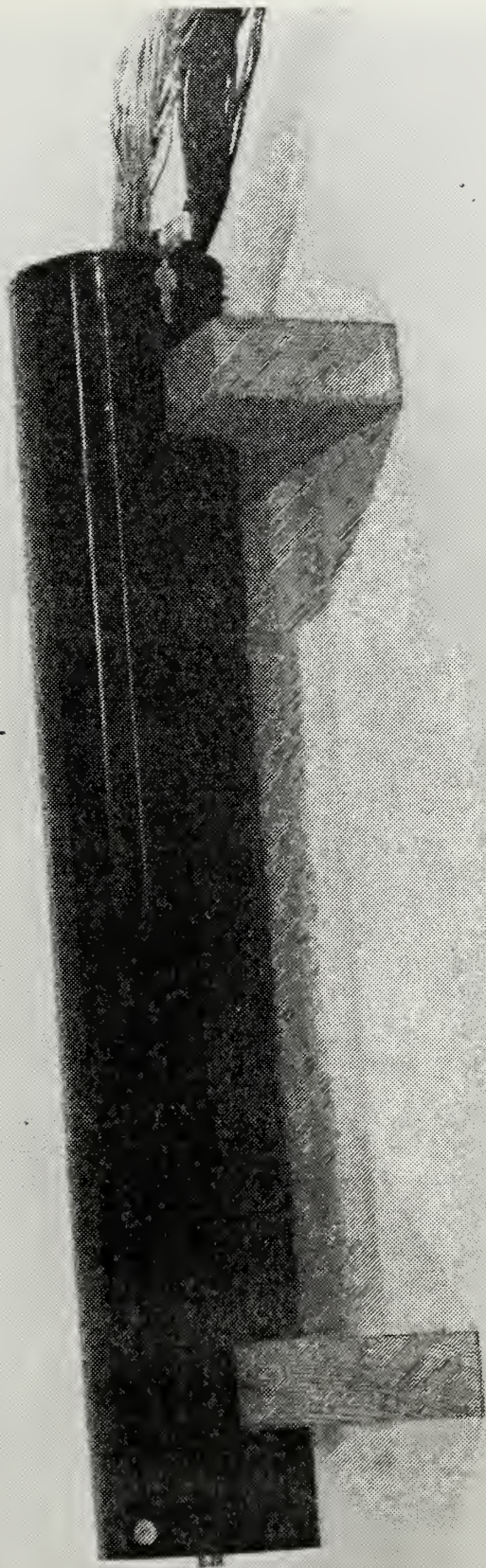


FIGURE 3 - PHOTOGRAPH OF THE MODEL

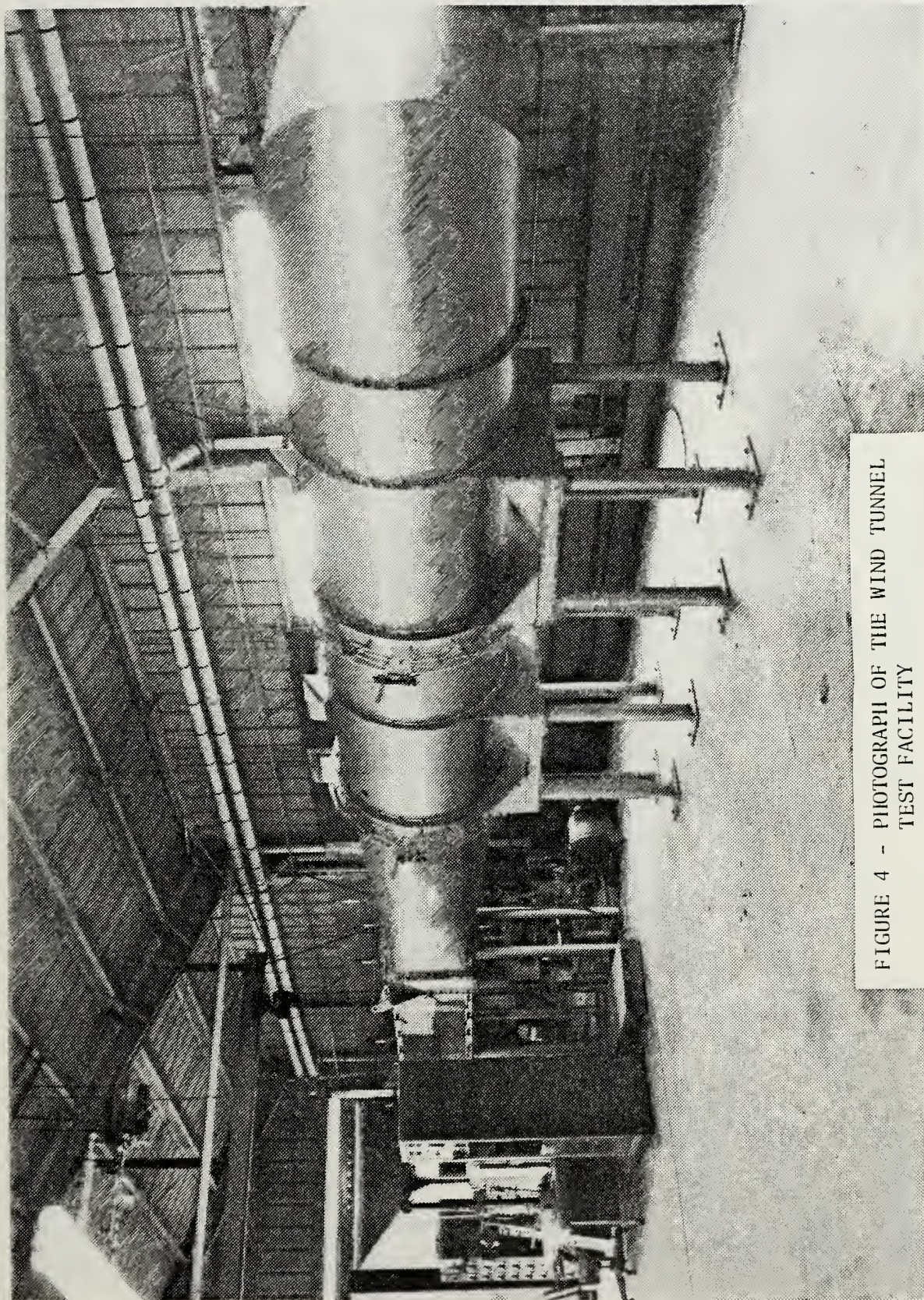


FIGURE 4 - PHOTOGRAPH OF THE WIND TUNNEL
TEST FACILITY

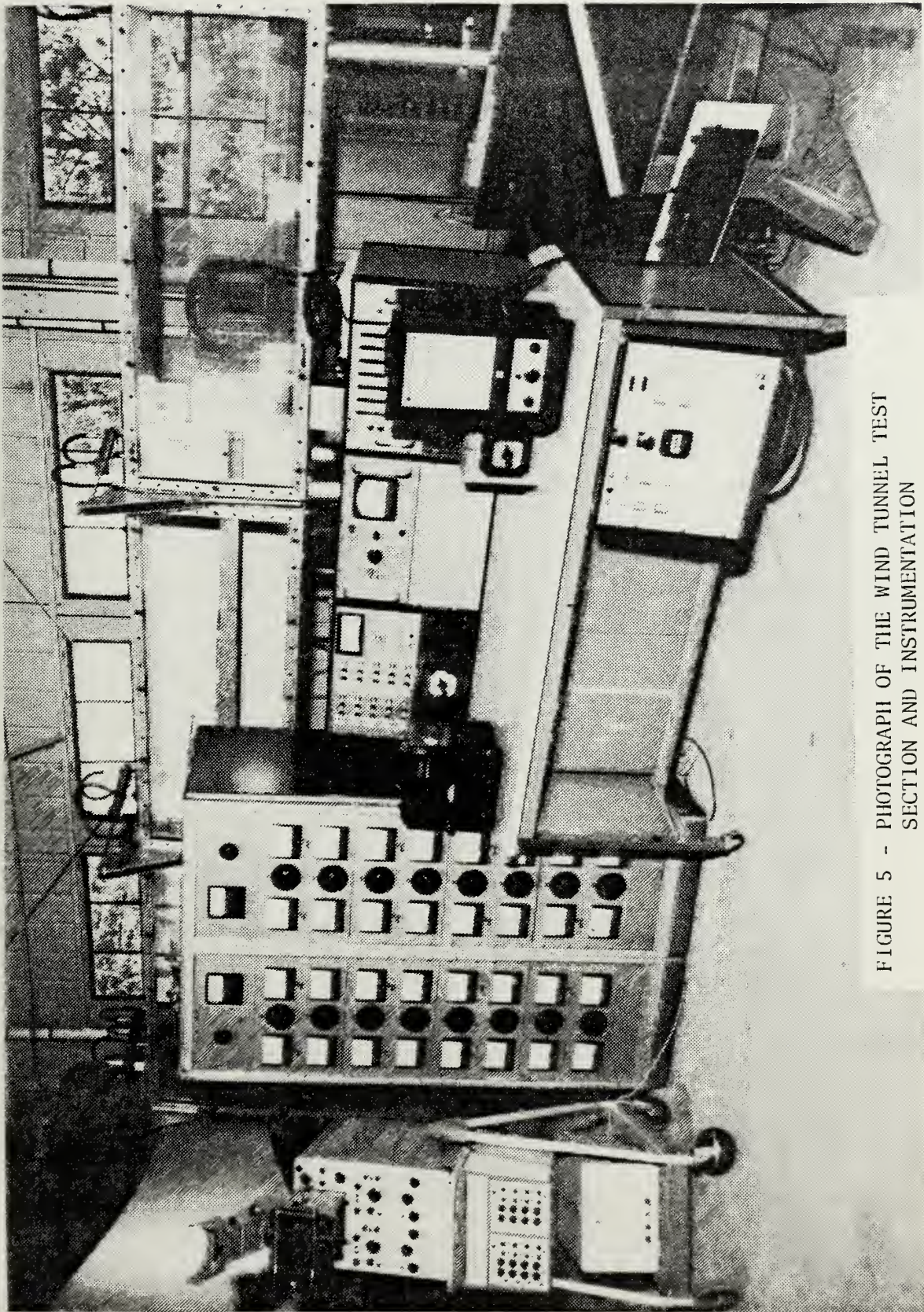


FIGURE 5 - PHOTOGRAPH OF THE WIND TUNNEL TEST
SECTION AND INSTRUMENTATION

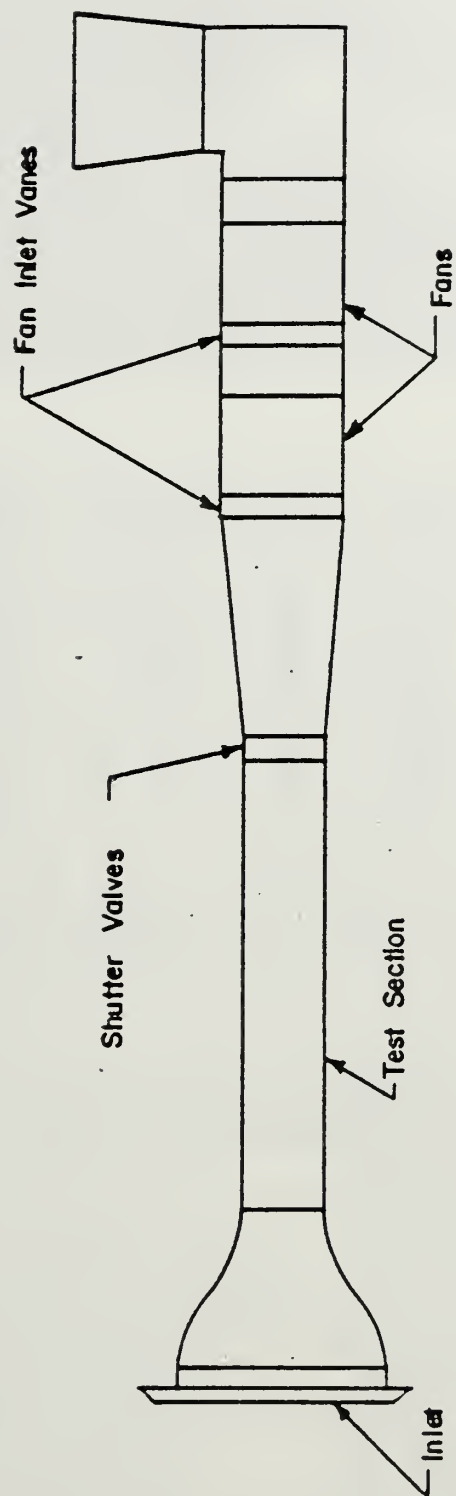


FIGURE 6 - PLAN VIEW OF THE WIND TUNNEL

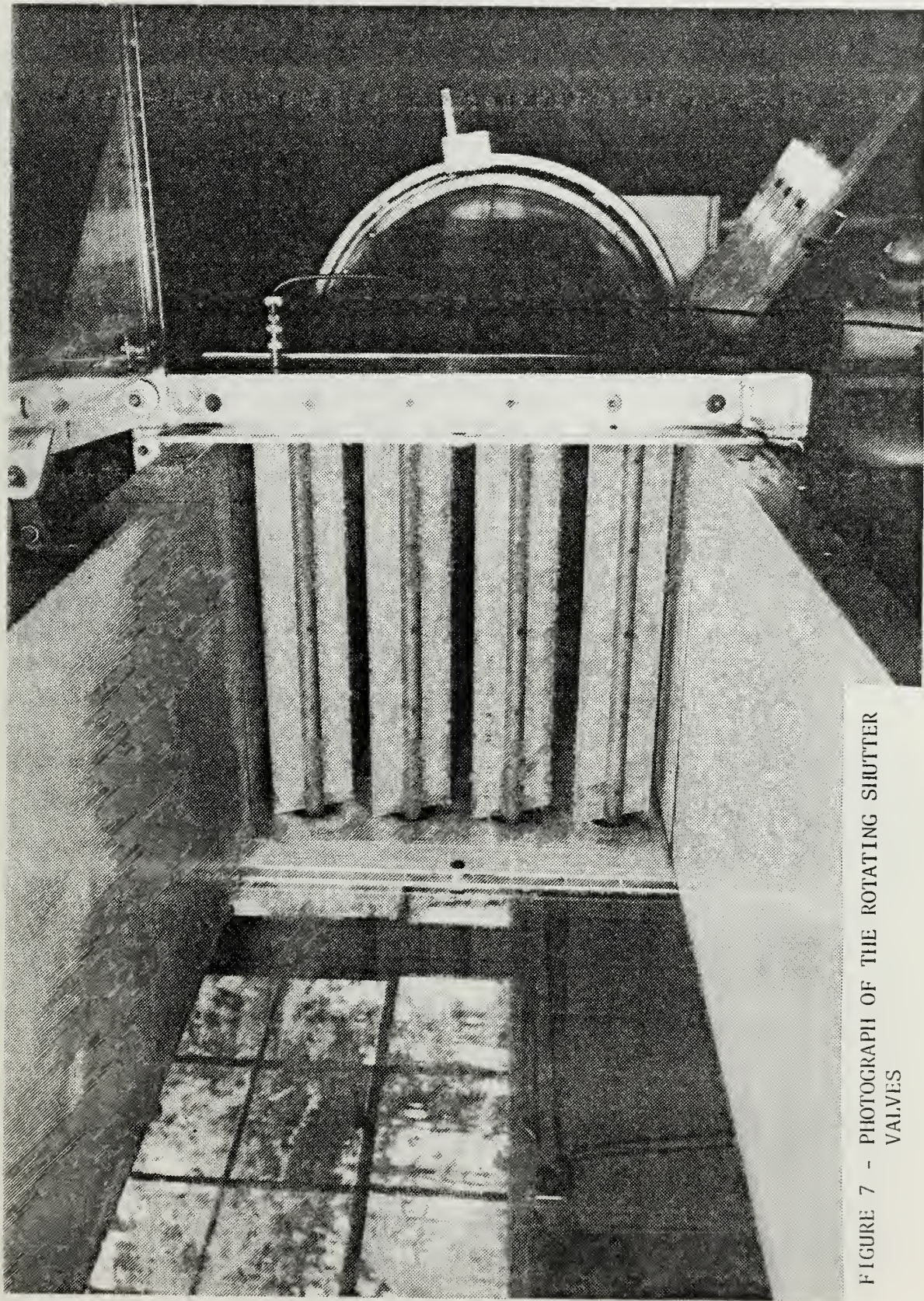
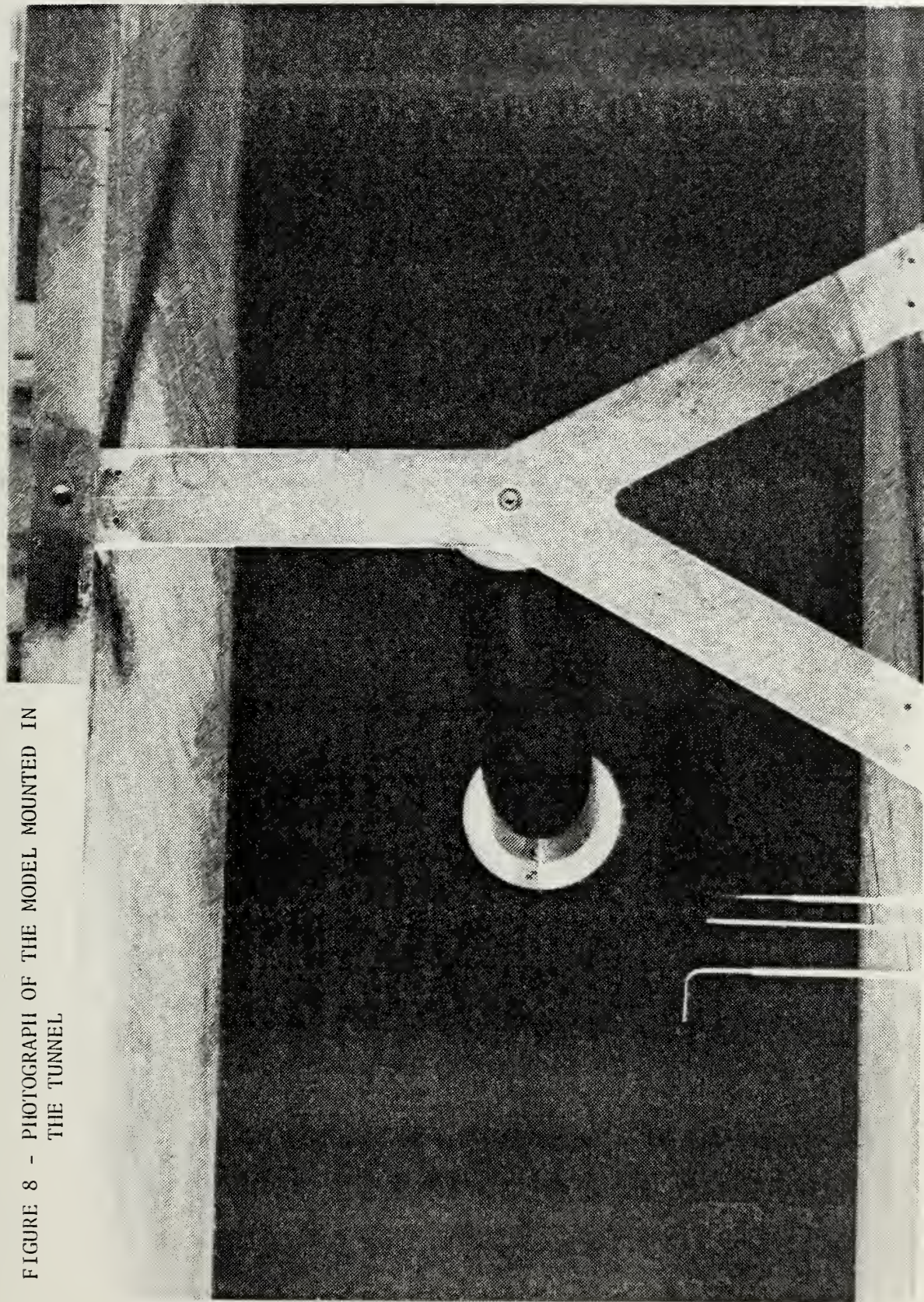
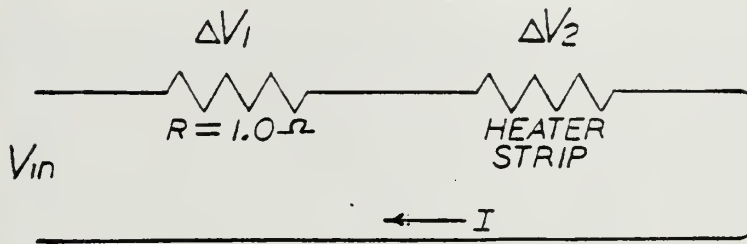


FIGURE 7 - PHOTOGRAPH OF THE ROTATING SHUTTER
VALVES

FIGURE 8 - PHOTOGRAPH OF THE MODEL MOUNTED IN
THE TUNNEL



CALIBRATION CIRCUIT



$$I = \frac{\Delta V_1}{R}$$

$$R_{HTR} = \frac{\Delta V_1 R_1}{\Delta V_2}$$

WORKING CIRCUIT

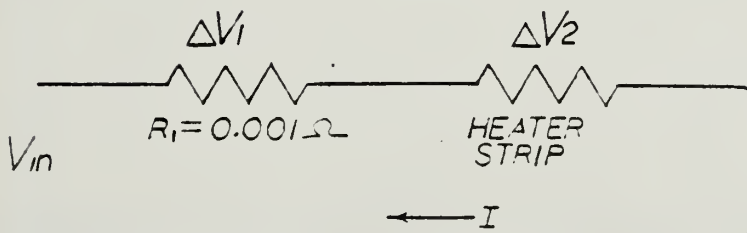


FIGURE 9 - SKETCH OF CALIBRATION AND WORKING CIRCUITS

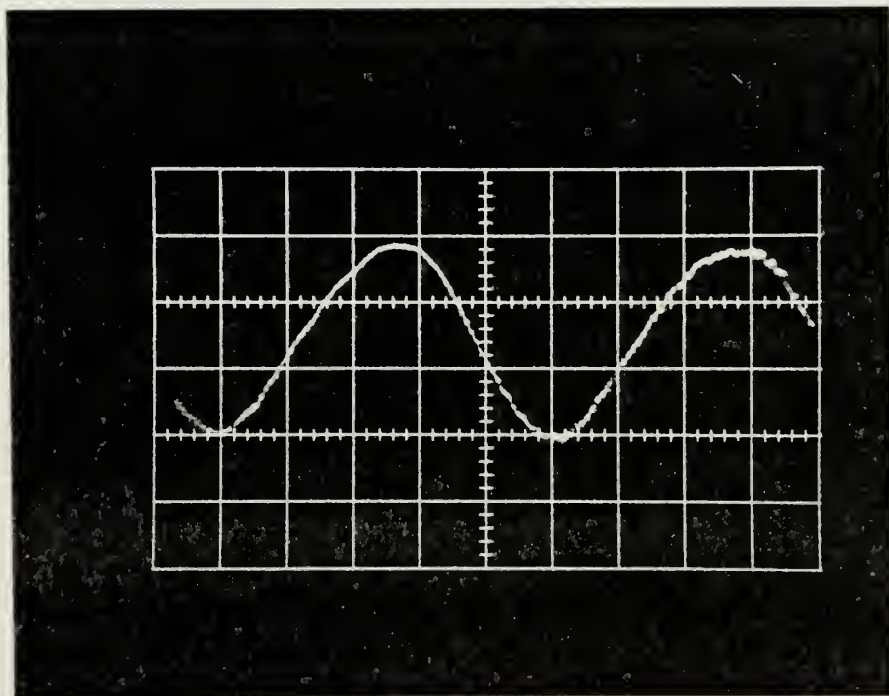
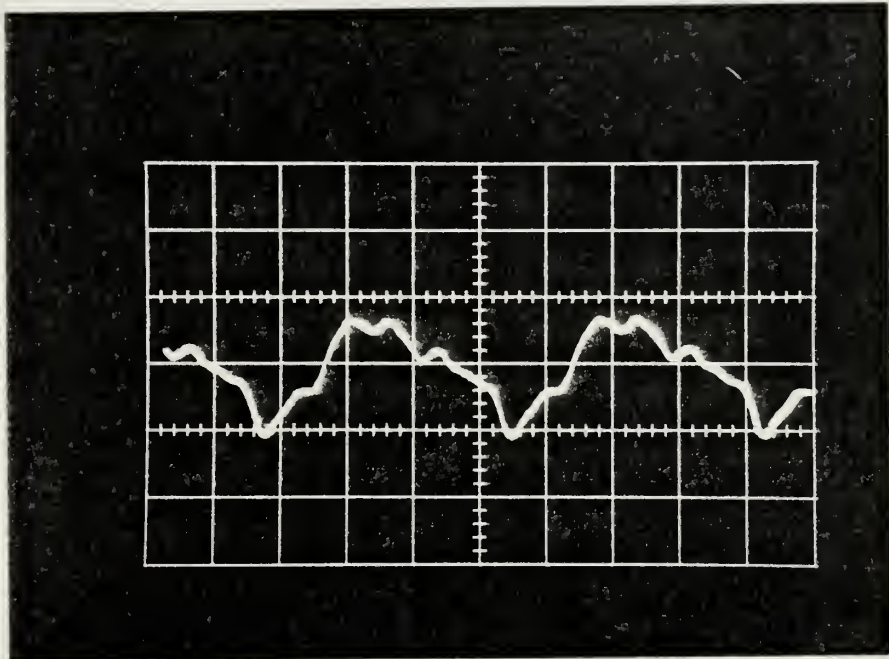
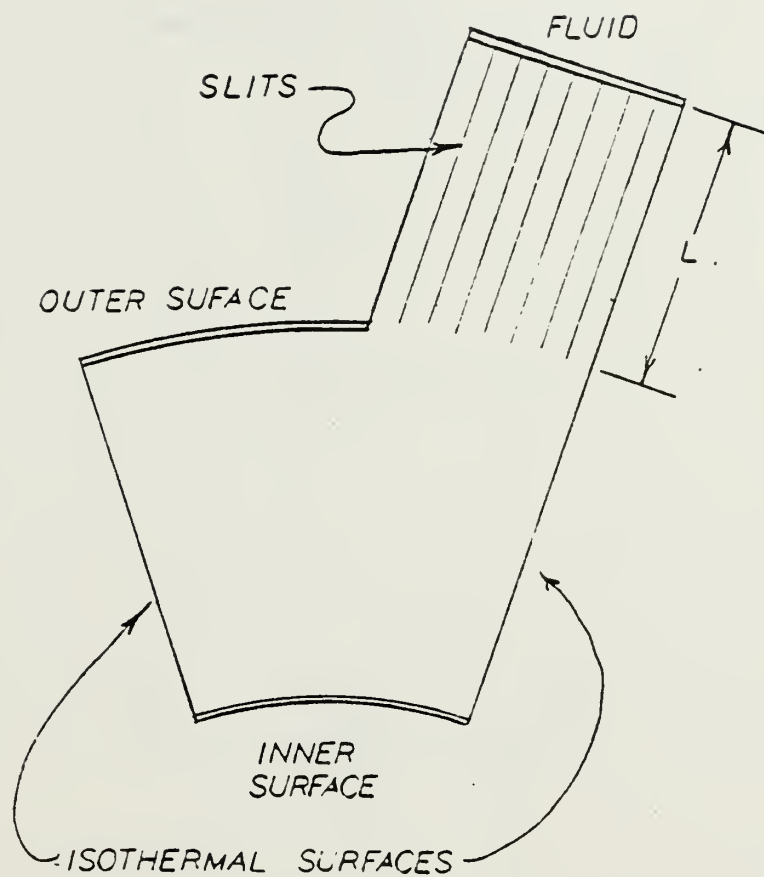


FIGURE 10 - TYPICAL VELOCITY WAVEFORMS



$$L = \frac{k}{h} S$$

$$S = 48$$

FIGURE 11 - SKETCH OF TELEDELTO S PAPER MODEL

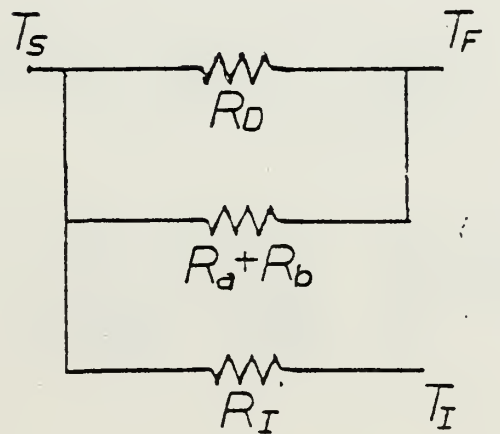
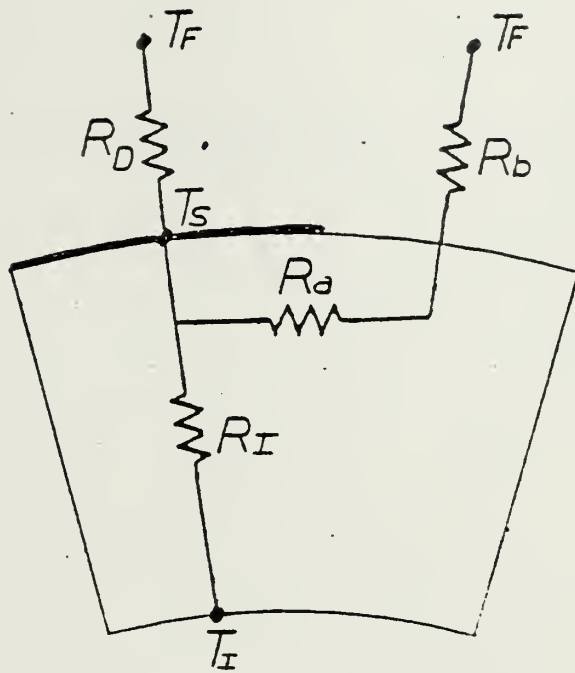
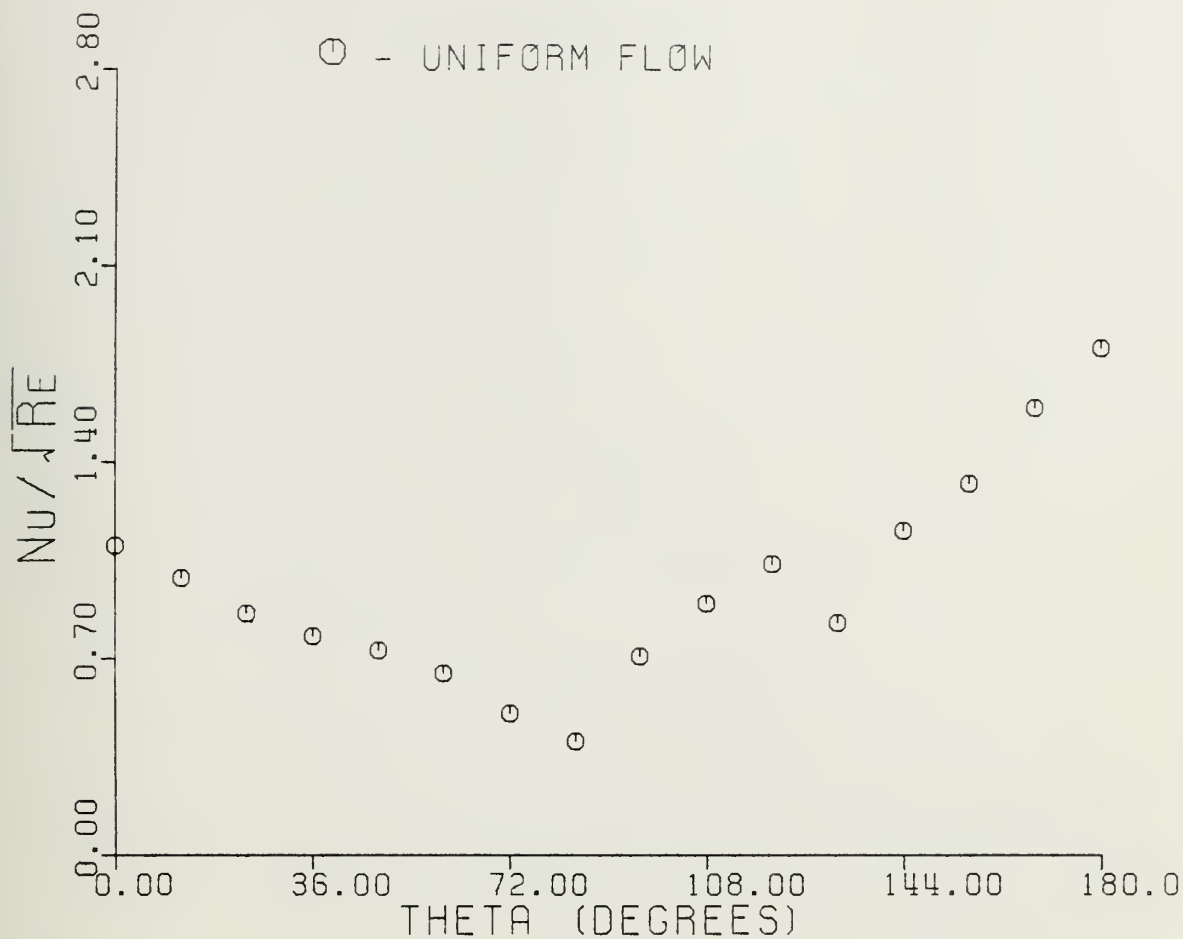


FIGURE 12 - SKETCH OF THE LUMPED RESISTANCE MODEL



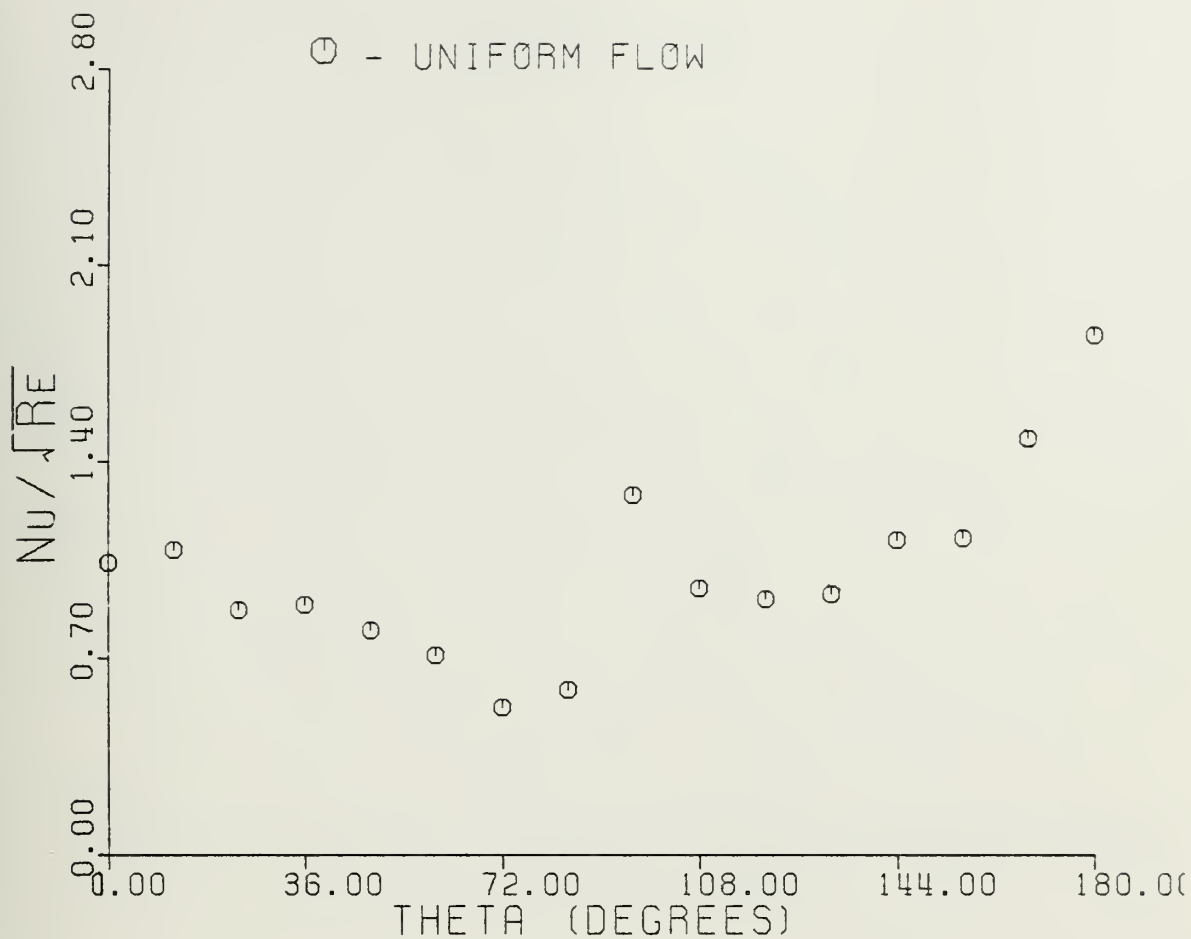
90 DEGREE MODEL
RUN NR 6

REYNOLDS NR = 157029

FREQUENCY NR = 0.0

AMPLITUDE NR = 0.0

FIGURE 13 - LOCAL HEAT TRANSFER COEFFICIENTS IN STEADY FLOW



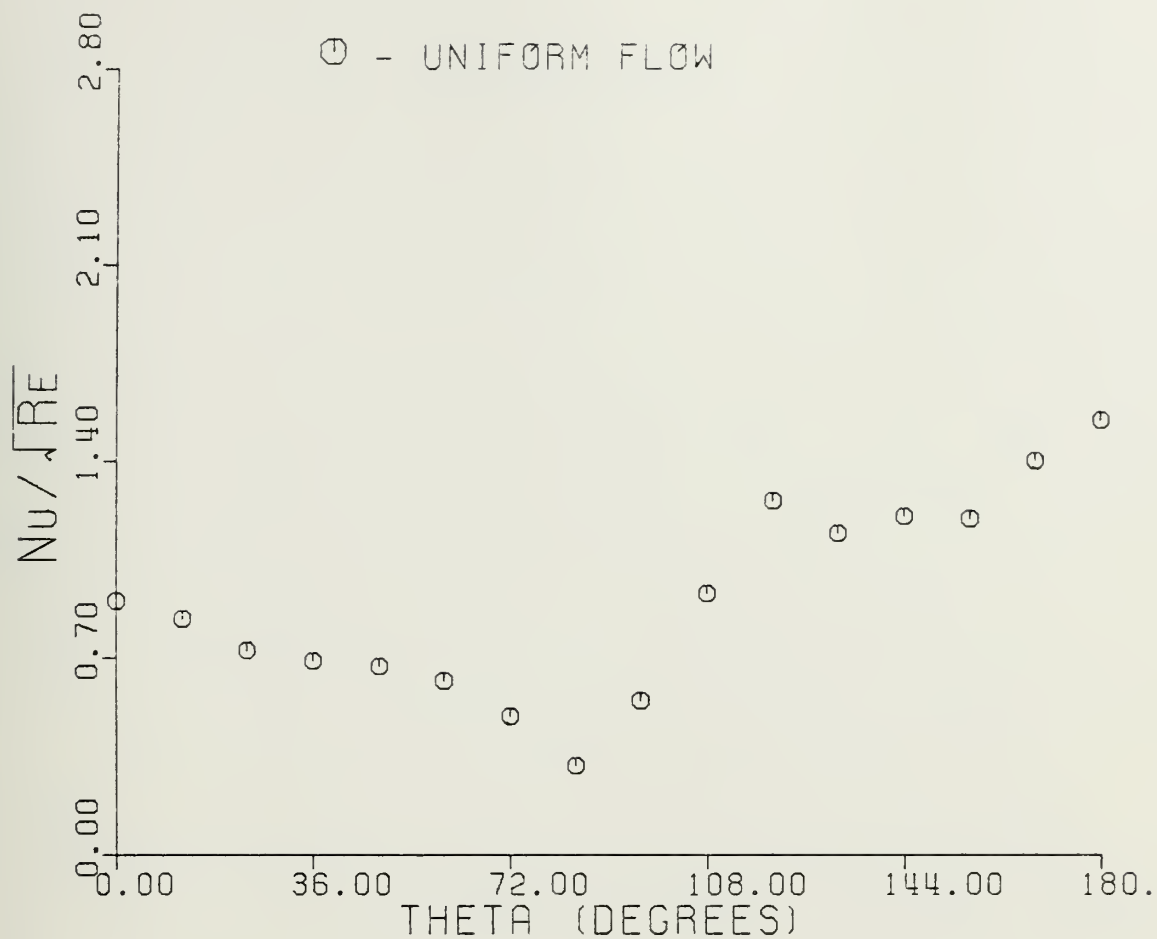
90 DEGREE MODEL
RUN NR 5

REYNOLDS NR = 314058

FREQUENCY NR = 0.0

AMPLITUDE NR = 0.0

FIGURE 14 - LOCAL HEAT TRANSFER COEFFICIENTS IN STEADY FLOW



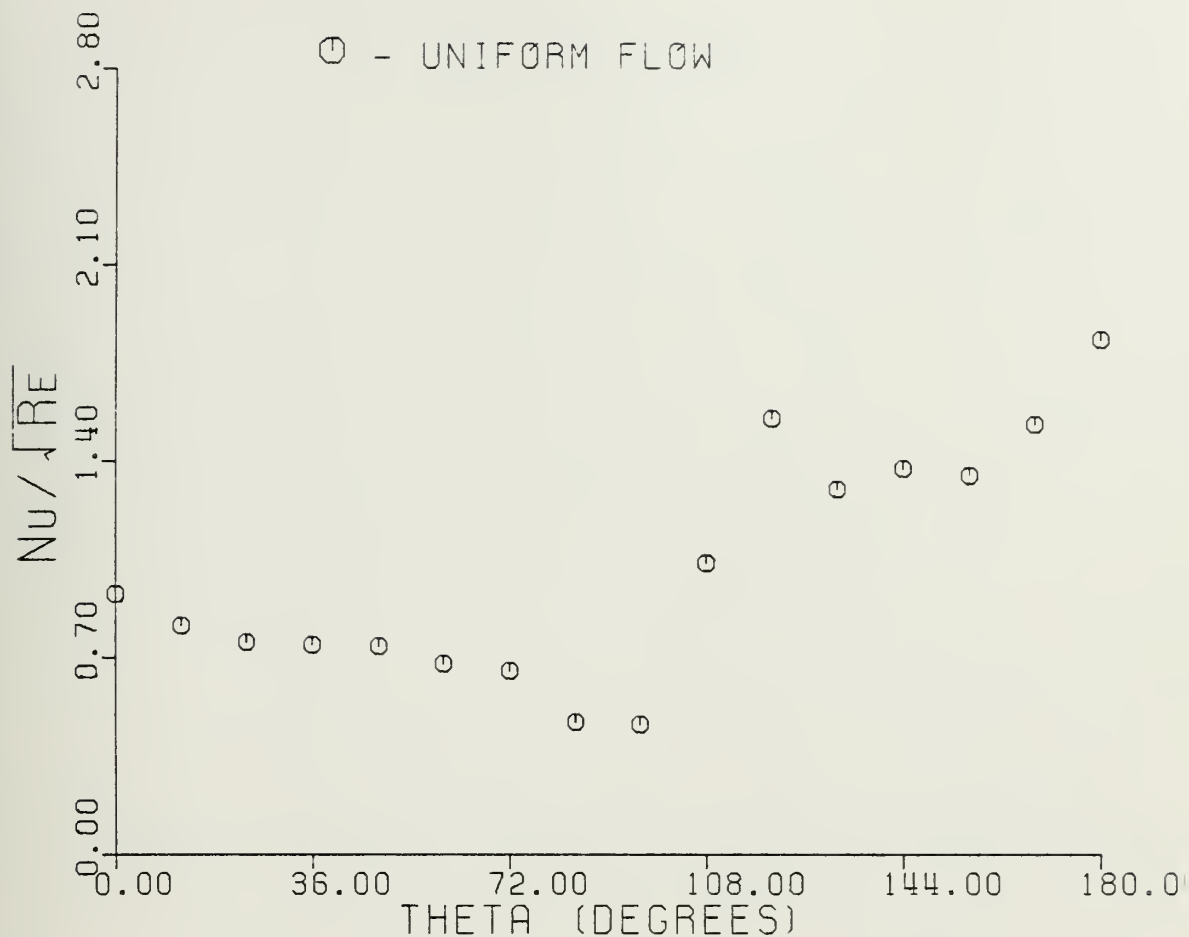
45 DEGREE MODEL
RUN NR 34

REYNOLDS NR = 155314

FREQUENCY NR = 0.0

AMPLITUDE NR = 0.0

FIGURE 15 - LOCAL HEAT TRANSFER COEFFICIENTS IN STEADY FLOW



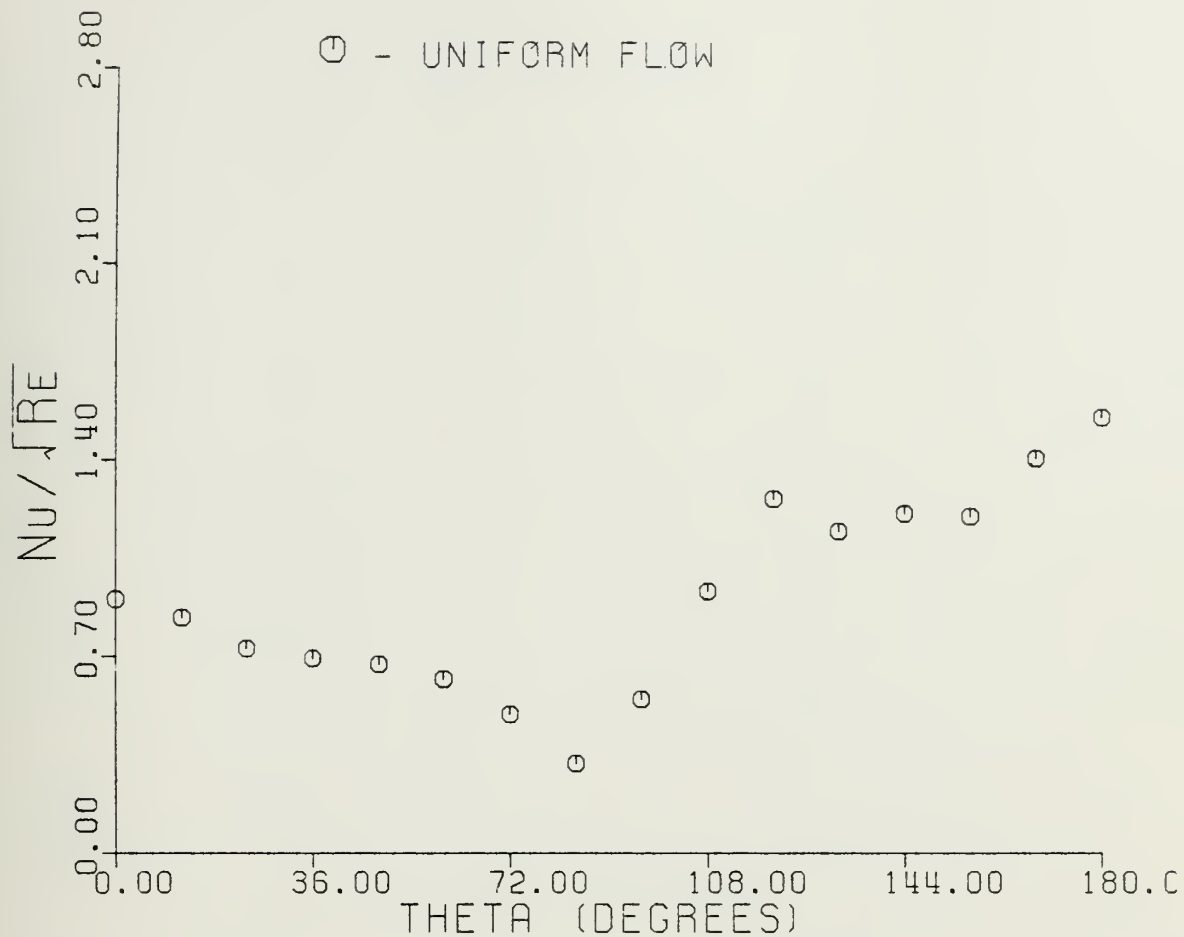
45 DEGREE MODEL
RUN NR 27

REYNOLDS NR = 314058

FREQUENCY NR = 0.0

AMPLITUDE NR = 0.0

FIGURE 16 - LOCAL HEAT TRANSFER COEFFICIENTS IN STEADY FLOW



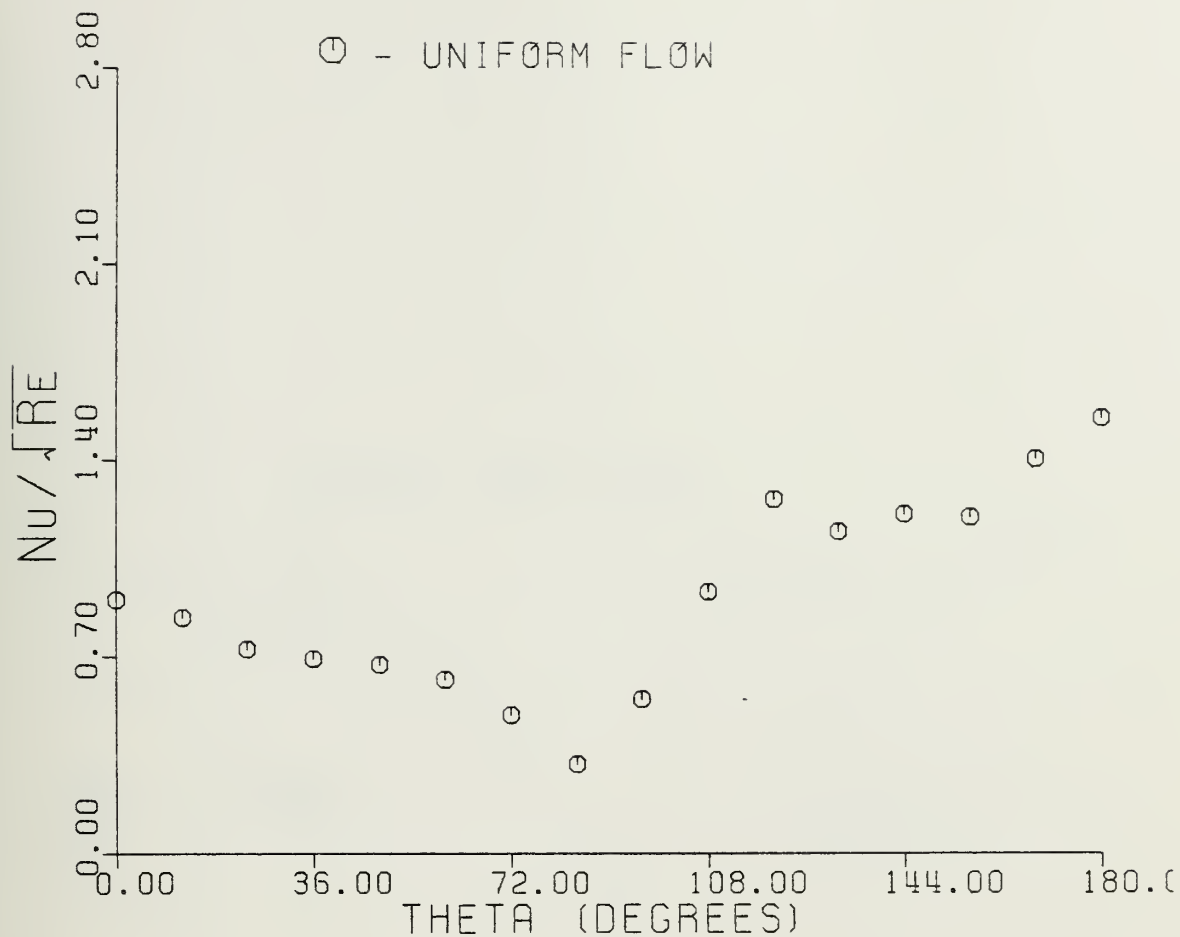
45 DEGREE MODEL
RUN NR 39

REYNOLDS NR = 110648

FREQUENCY NR = 0.0

AMPLITUDE NR = 0.0

FIGURE 17 - LOCAL HEAT TRANSFER COEFFICIENTS IN STEADY FLOW



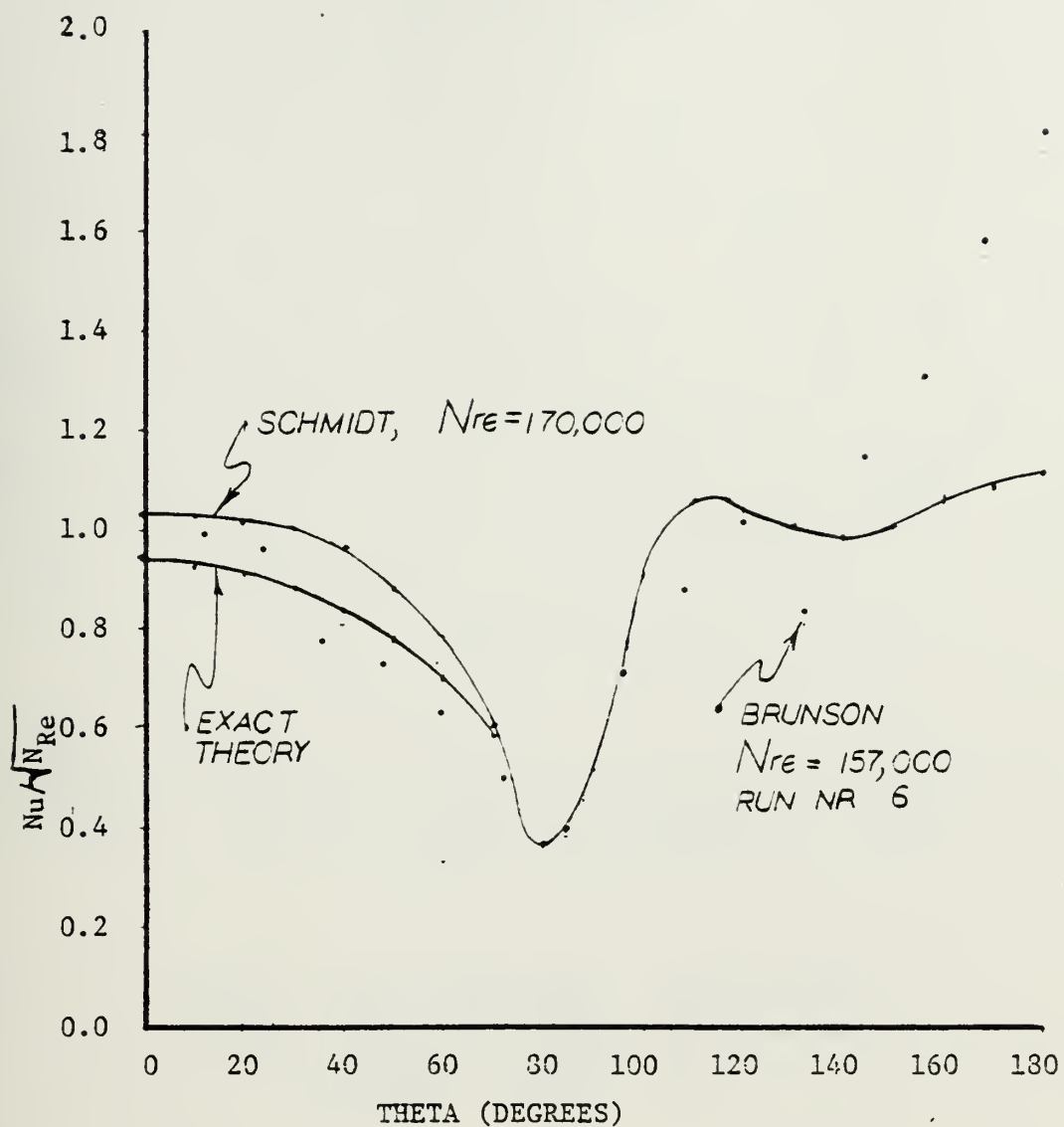
45 DEGREE MODEL
RUN NR 40

REYNOLDS NR = 35630

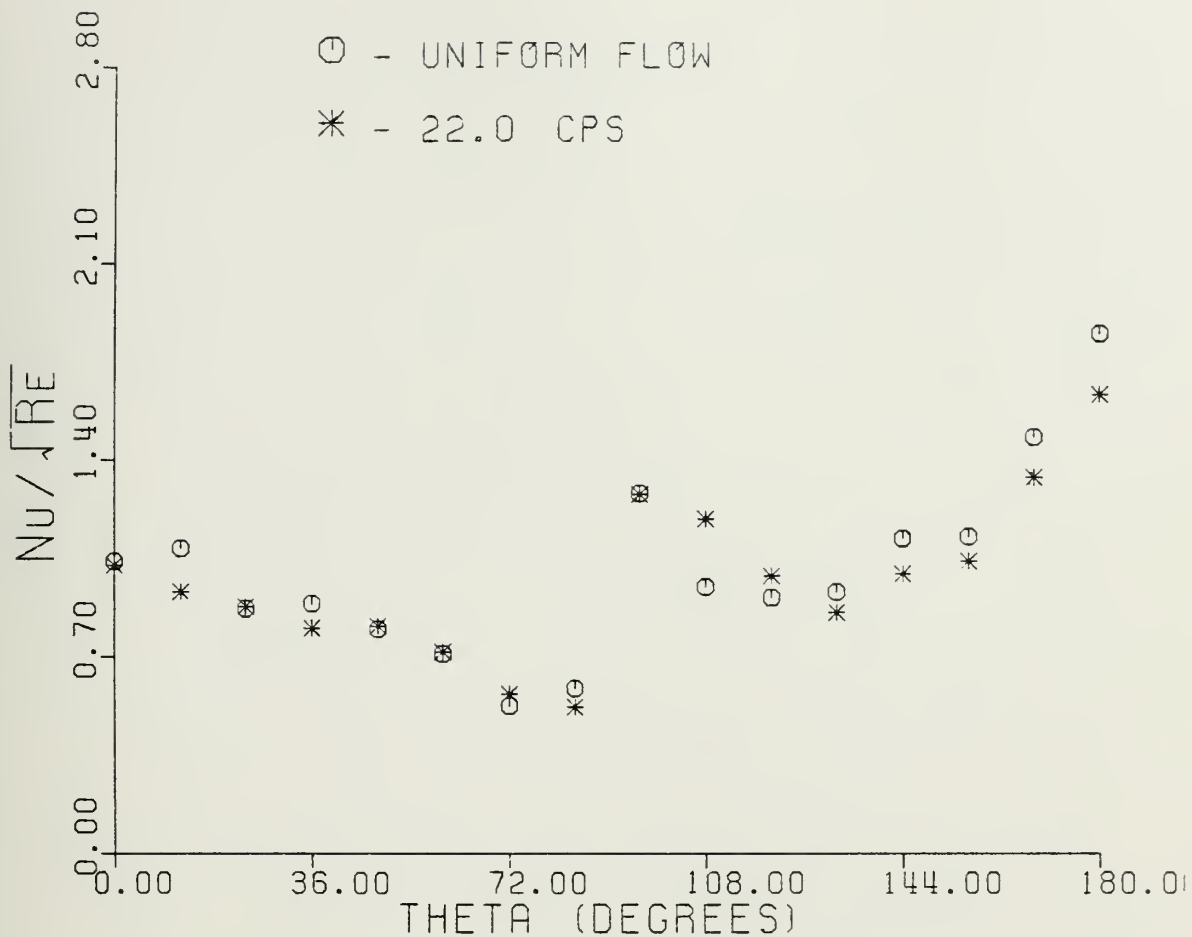
FREQUENCY NR = 0.0

AMPLITUDE NR = 0.0

FIGURE 18 - LOCAL HEAT TRANSFER COEFFICIENTS IN STEADY FLOW



- FIGURE 19 - COMPARISON OF PUBLISHED STEADY
FLOW RESULTS TO EXPERIMENTAL



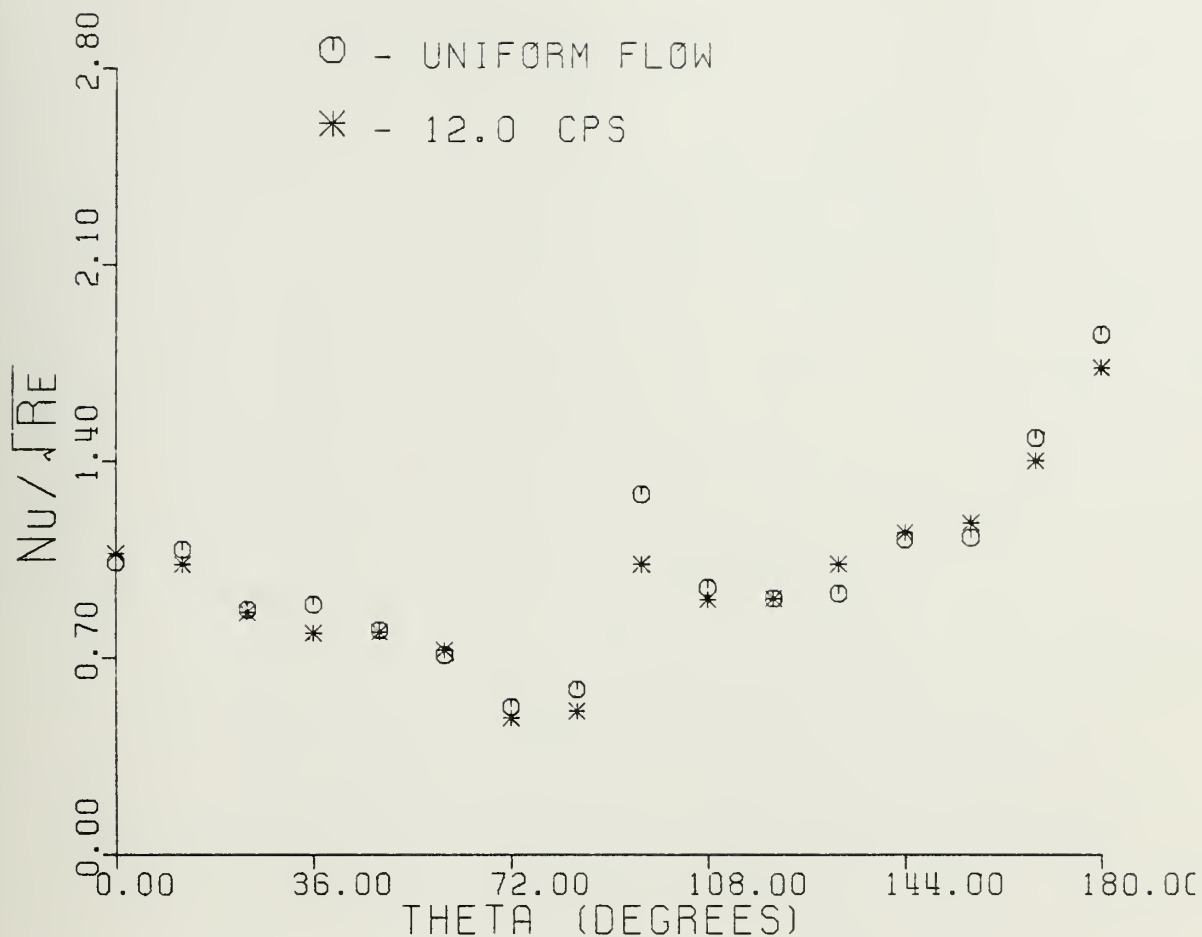
90 DEGREE MODEL RUN NR 9

REYNOLDS NR = 283130

FREQUENCY NR = 1.166×10^{-6}

AMPLITUDE NR = 0.115

FIGURE 20 - LOCAL HEAT TRANSFER COEFFICIENTS IN OSCILLATING FLOW THAT SHOWED UNALTERED RESULTS



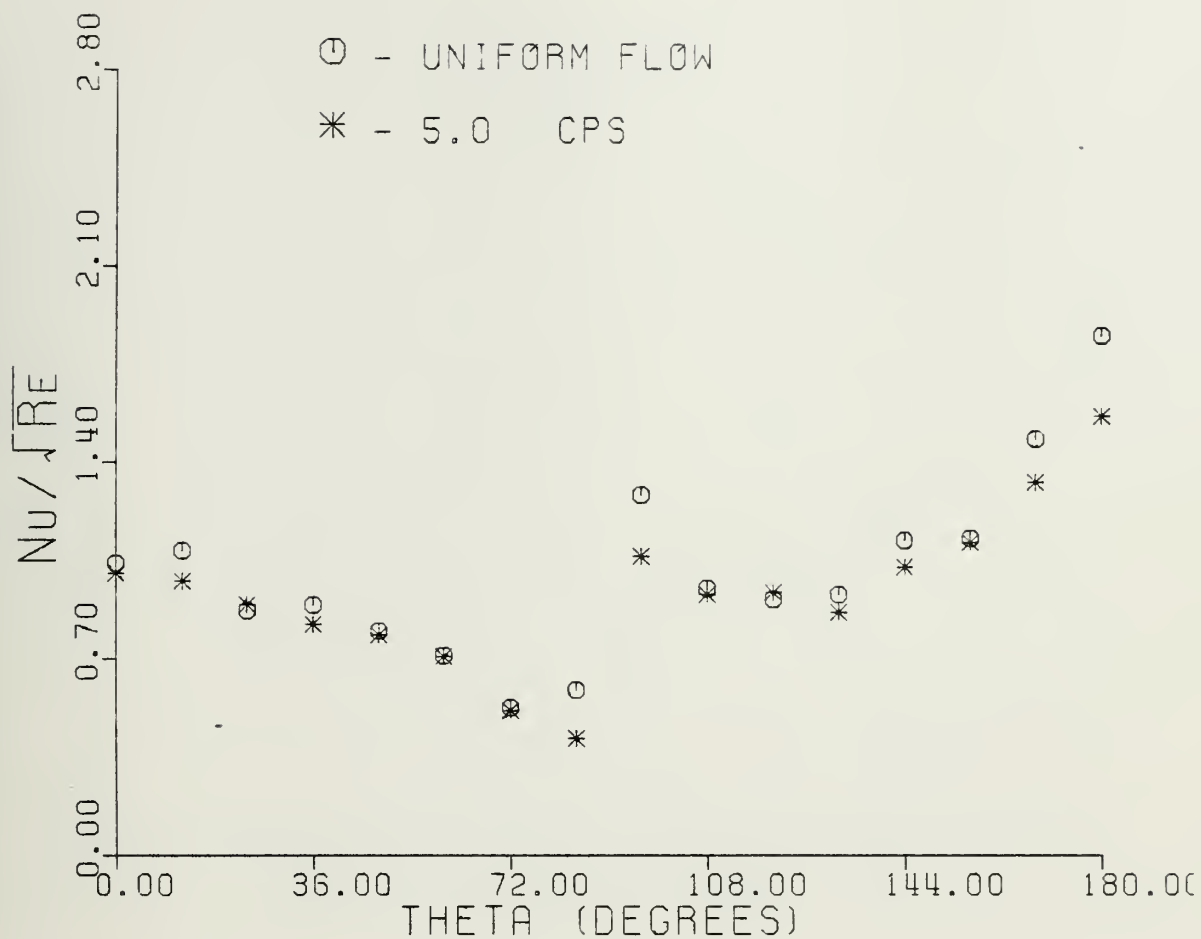
90 DEGREE MODEL RUN NR 18

REYNOLDS NR = 212769

FREQUENCY NR = 1.115×10^{-6}

AMPLITUDE NR = 0.150

FIGURE 21 - LOCAL HEAT TRANSFER COEFFICIENTS IN OSCILLATING FLOW THAT SHOWED UNALTERED RESULTS



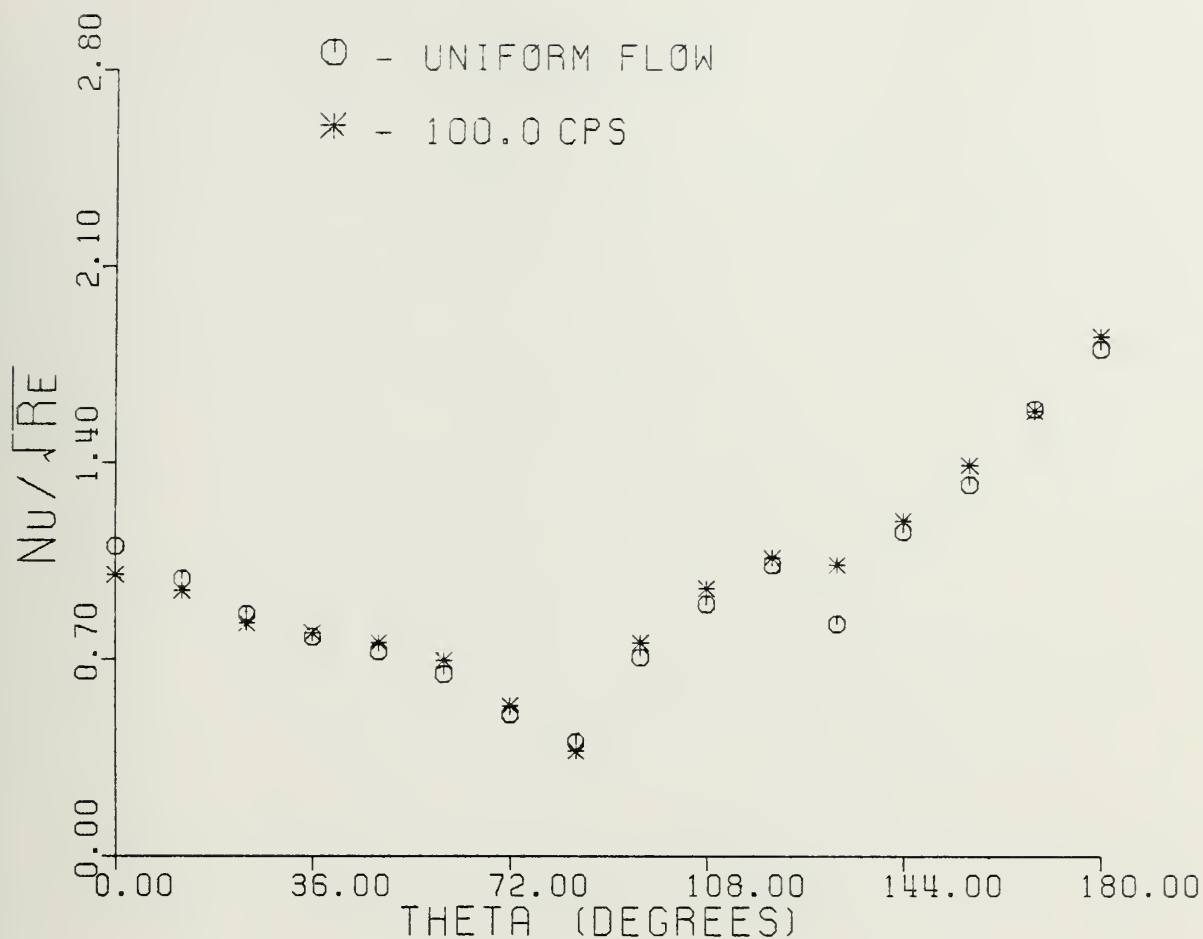
90 DEGREE MODEL RUN NR 8

REYNOLDS NR = 213960

FREQUENCY NR = 0.464×10^{-6}

AMPLITUDE NR = 0.180

FIGURE 22 - LOCAL HEAT TRANSFER COEFFICIENTS IN OSCILLATING FLOW THAT SHOWED UNALTERED RESULTS



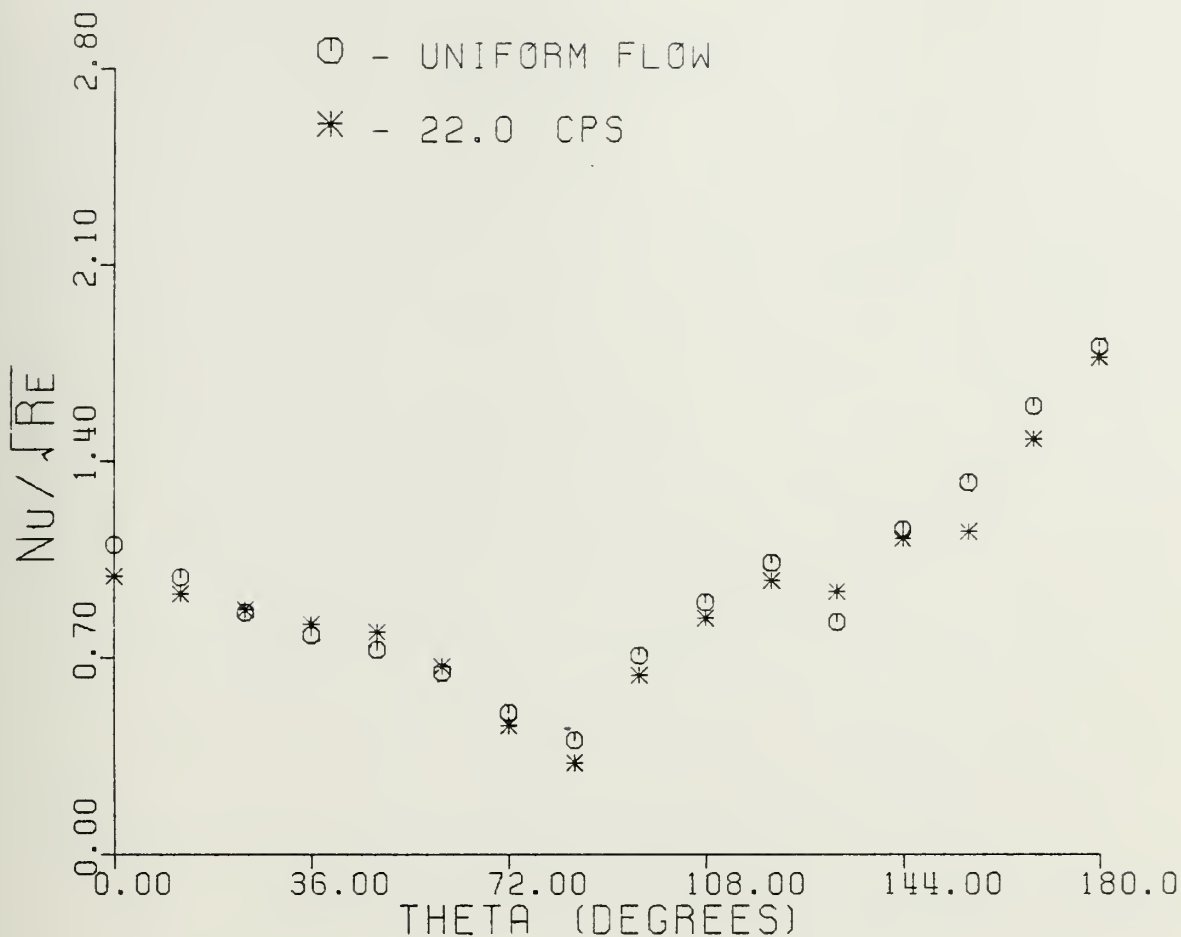
90 DEGREE MODEL RUN NR 12

REYNOLDS NR = 154471

FREQUENCY NR = 17.719×10^{-6}

AMPLITUDE NR = 0.070

FIGURE 23 - LOCAL HEAT TRANSFER COEFFICIENTS IN OSCILLATING FLOW THAT SHOWED UNALTERED RESULTS



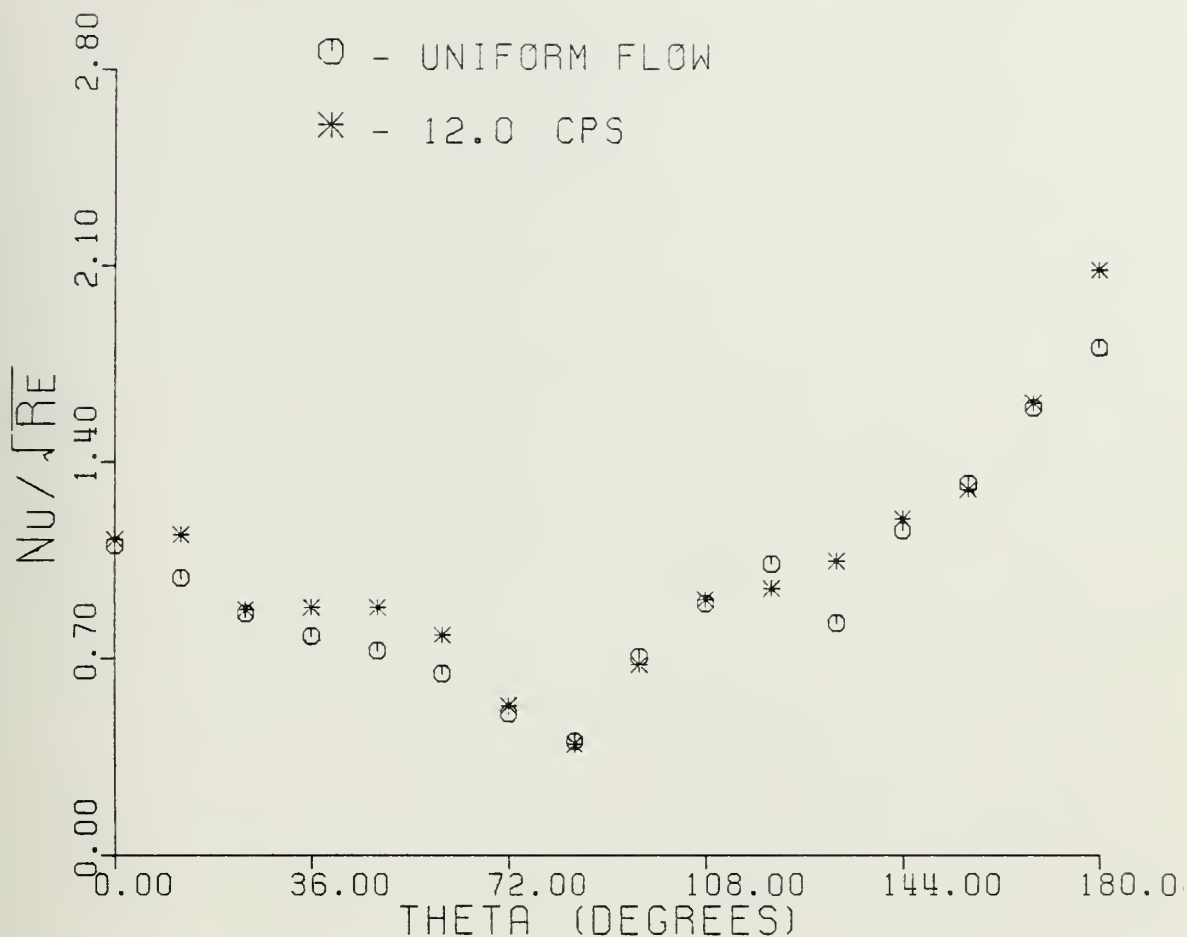
90 DEGREE MODEL RUN NR 10

REYNOLDS NR = 151995

FREQUENCY NR = 3.962×10^{-6}

AMPLITUDE NR = 0.060

FIGURE 24 - LOCAL HEAT TRANSFER COEFFICIENTS IN OSCILLATING FLOW THAT SHOWED UNALTERED RESULTS



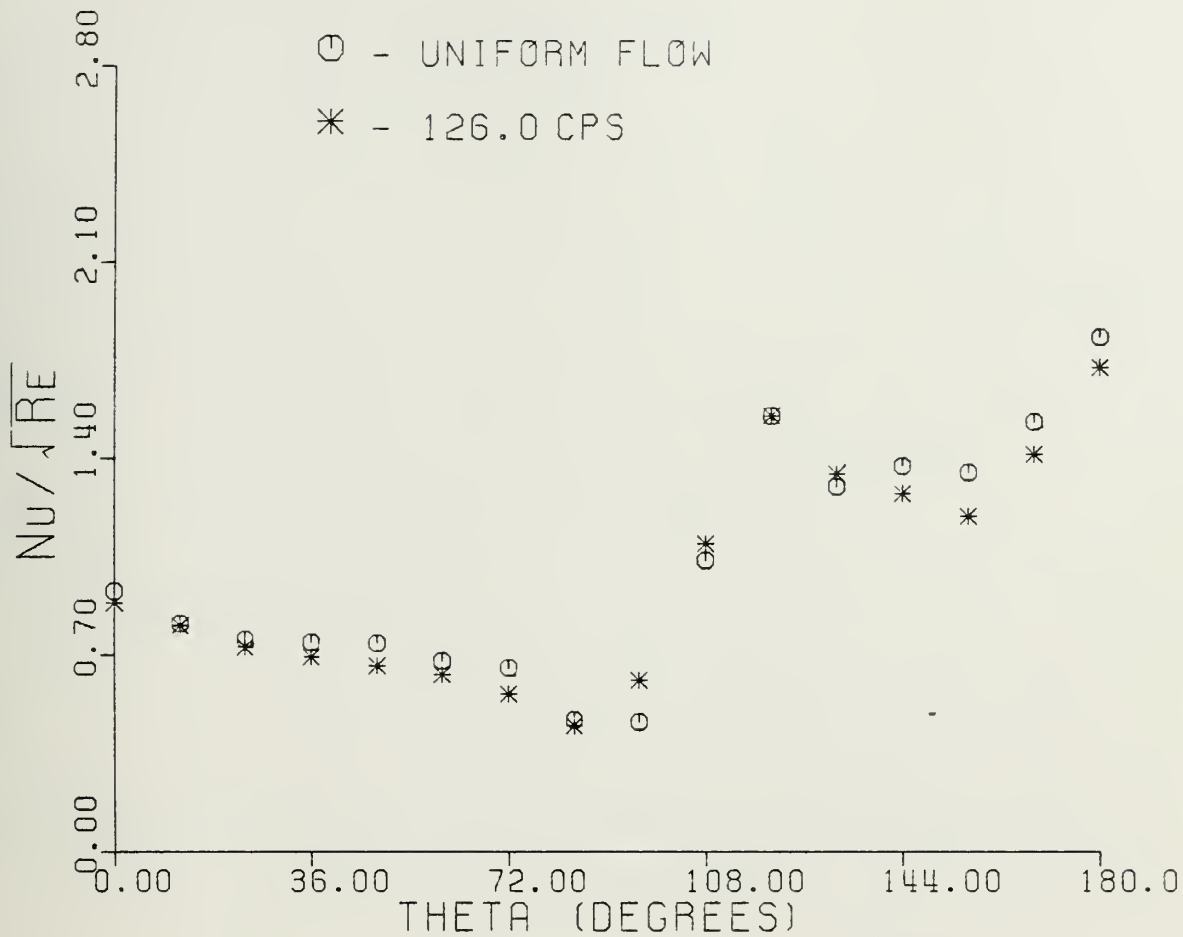
90 DEGREE MODEL RUN NR 19

REYNOLDS NR = 152811

FREQUENCY NR = 2.149×10^{-6}

AMPLITUDE NR = 0.110

FIGURE 25 - LOCAL HEAT TRANSFER COEFFICIENTS IN OSCILLATING FLOW THAT SHOWED UNALTERED RESULTS



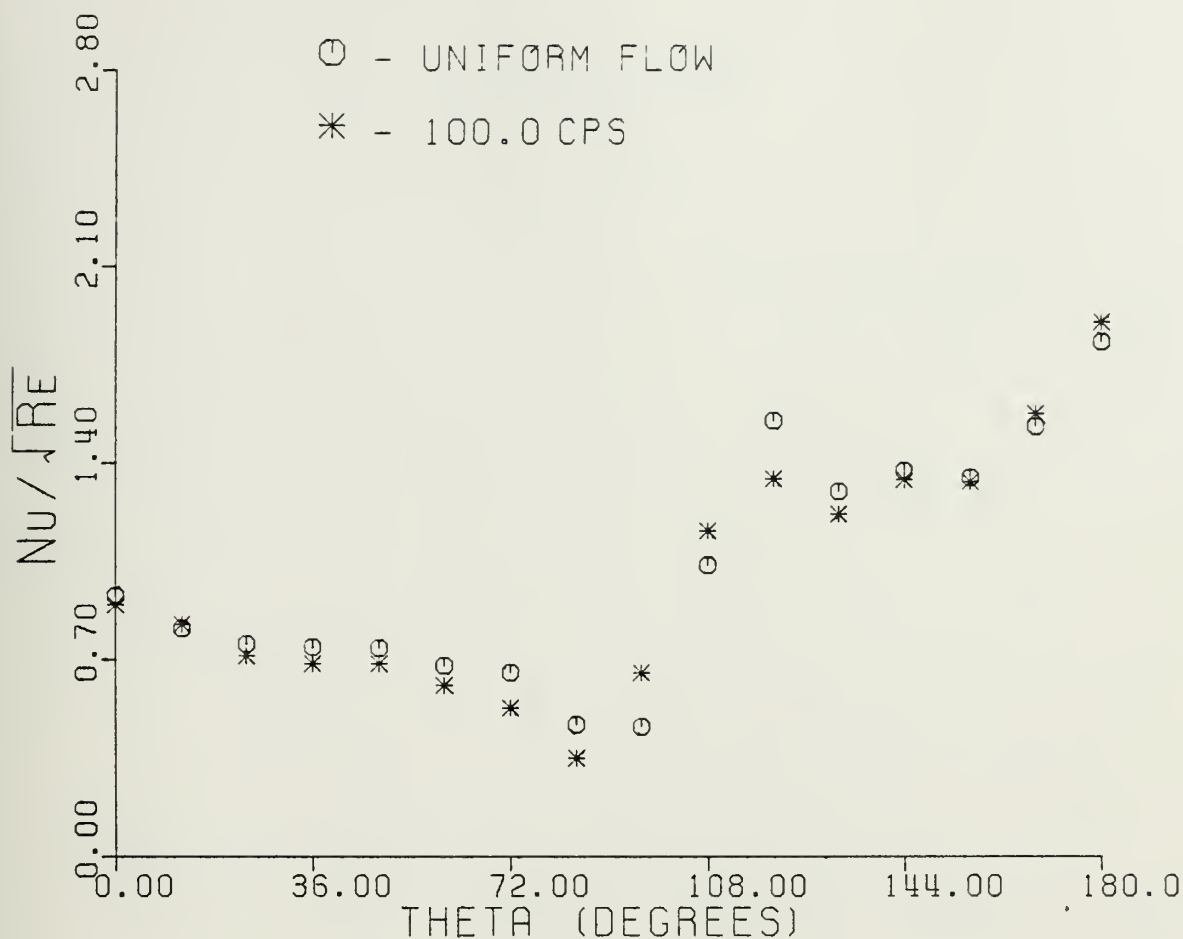
45 DEGREE MODEL RUN NR 30

REYNOLDS NR = 259877

FREQUENCY NR = 8.030×10^{-6}

AMPLITUDE NR = 0.095

FIGURE 26 - LOCAL HEAT TRANSFER COEFFICIENTS IN OSCILLATING FLOW THAT SHOWED UNALTERED RESULTS



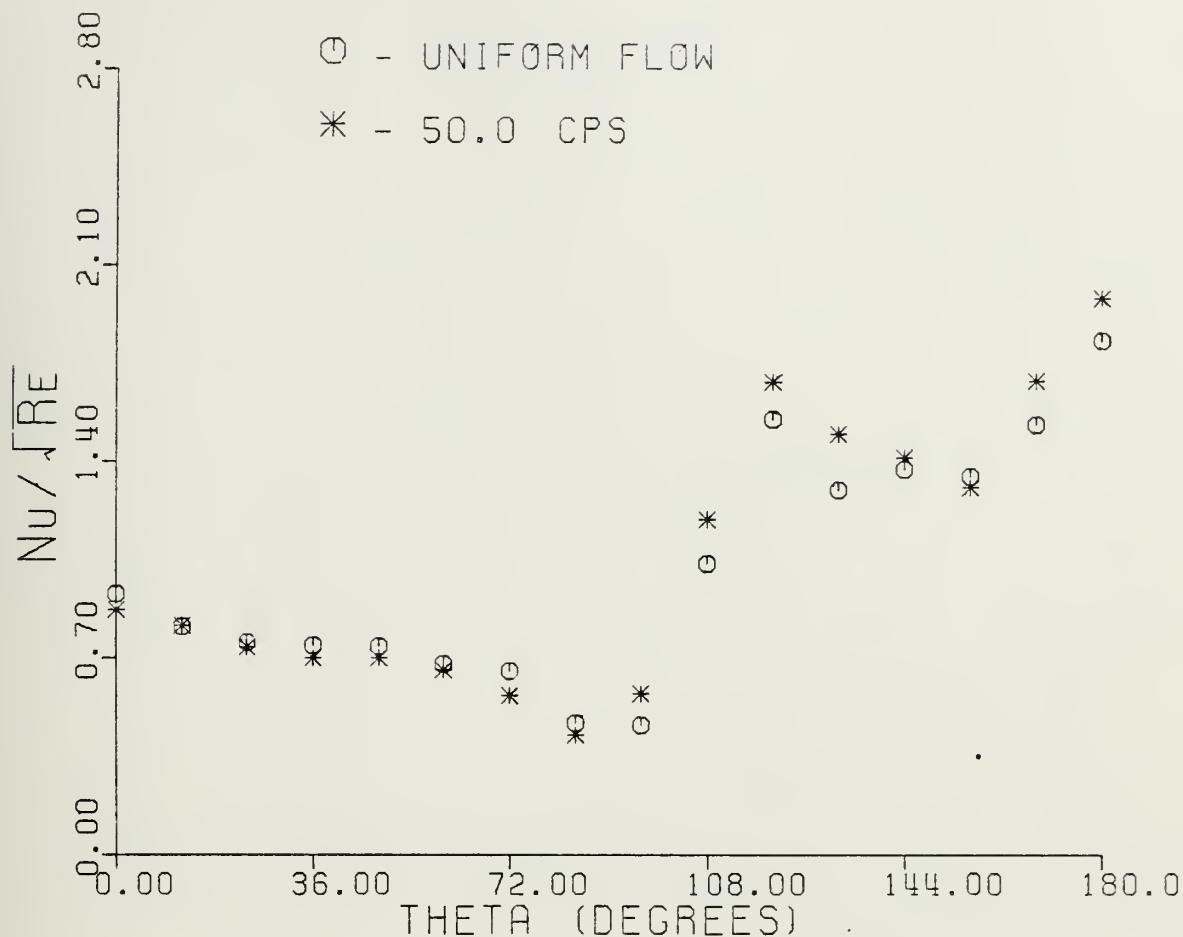
45 DEGREE MODEL
 RUN NR 24

REYNOLDS NR = 217175

FREQUENCY NR = 9.013×10^{-6}

AMPLITUDE NR = 0.049

FIGURE 27 - LOCAL HEAT TRANSFER COEFFICIENTS IN OSCILLATING FLOW THAT SHOWED UNALTERED RESULTS



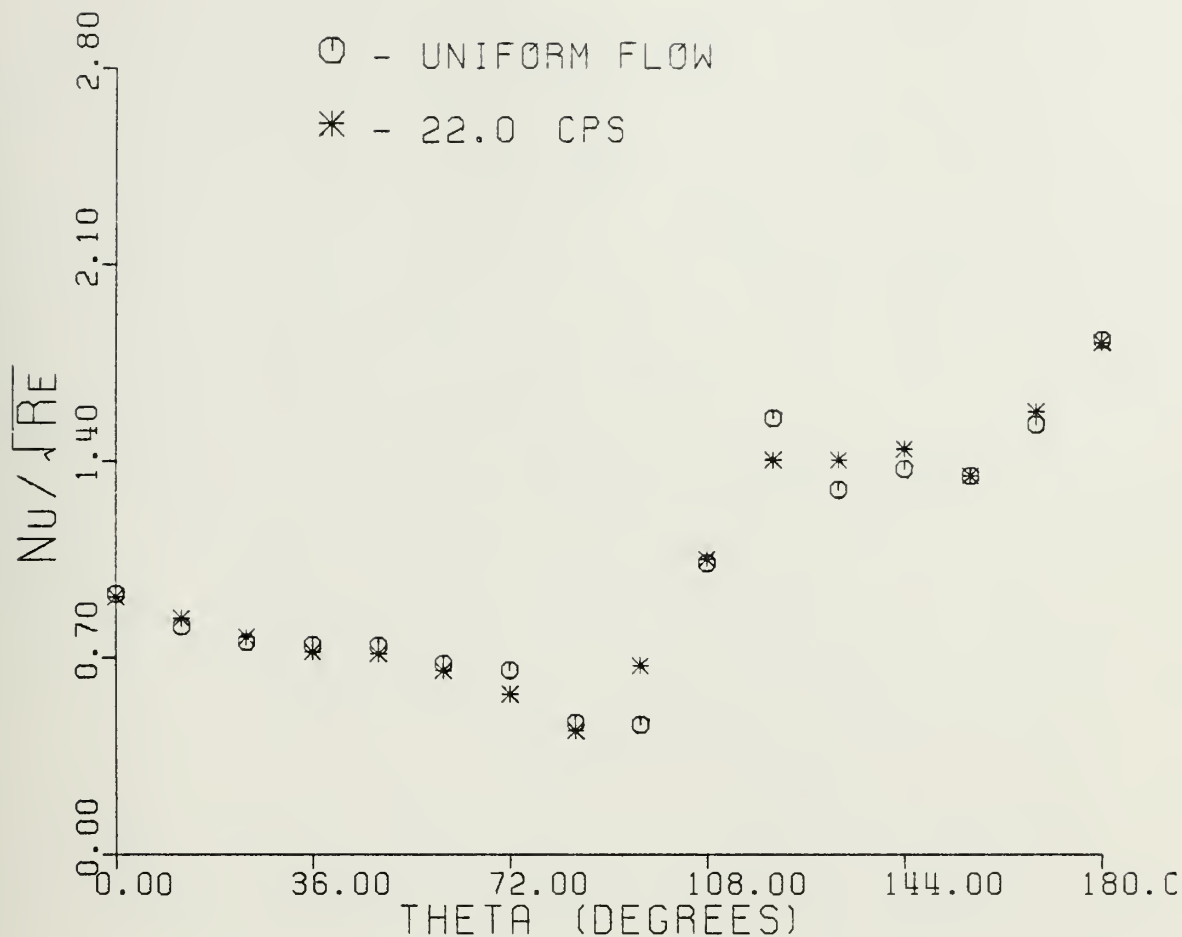
45 DEGREE MODEL RUN NR 29

REYNOLDS NR = 280040

FREQUENCY NR = 2.685×10^{-6}

AMPLITUDE NR = 0.220

FIGURE 28 - LOCAL HEAT TRANSFER COEFFICIENTS IN OSCILLATING FLOW THAT SHOWED UNALTERED RESULTS



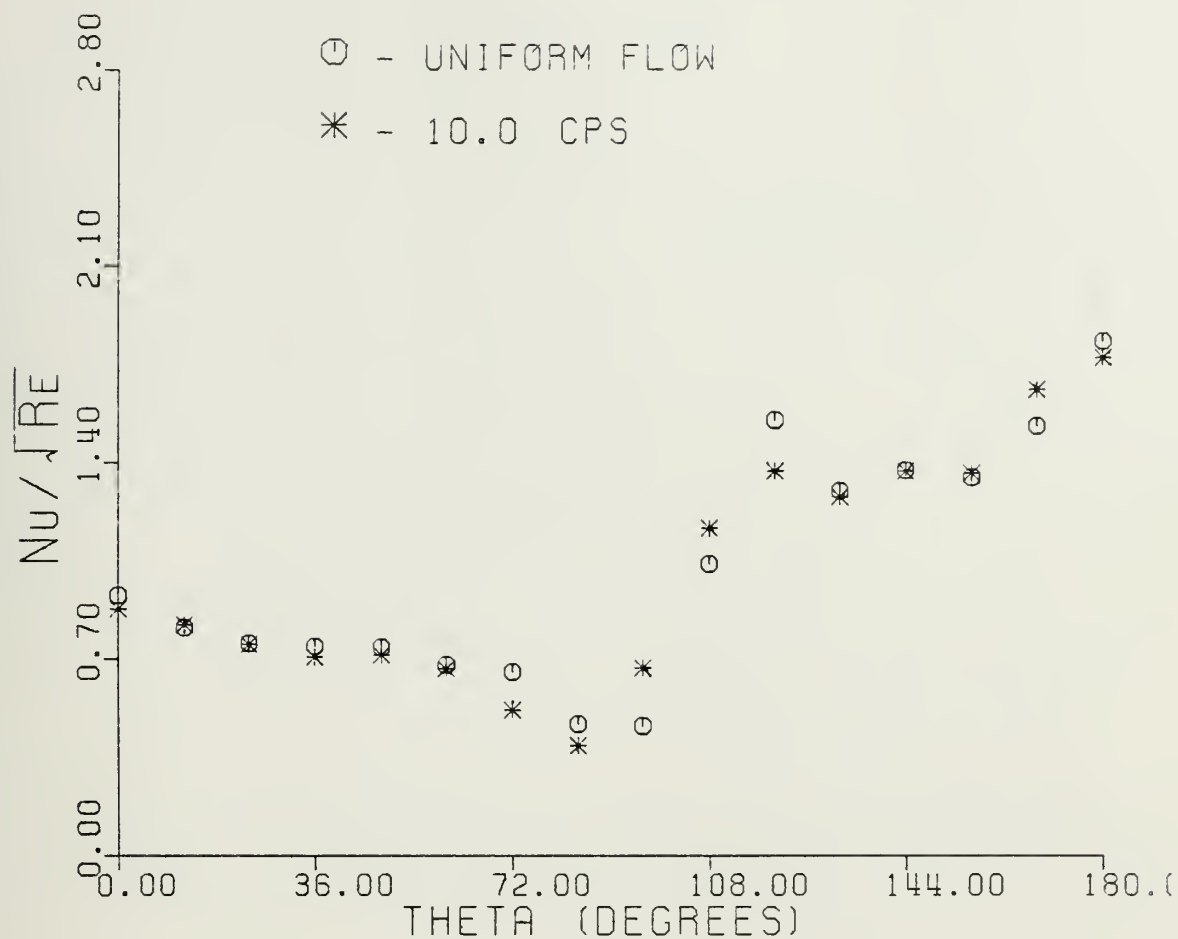
45 DEGREE MODEL
 RUN NR 22

REYNOLDS NR = 254242

FREQUENCY NR = 1.439×10^{-6}

AMPLITUDE NR = 0.055

FIGURE 29 - LOCAL HEAT TRANSFER COEFFICIENTS IN OSCILLATING FLOW THAT SHOWED UNALTERED RESULTS



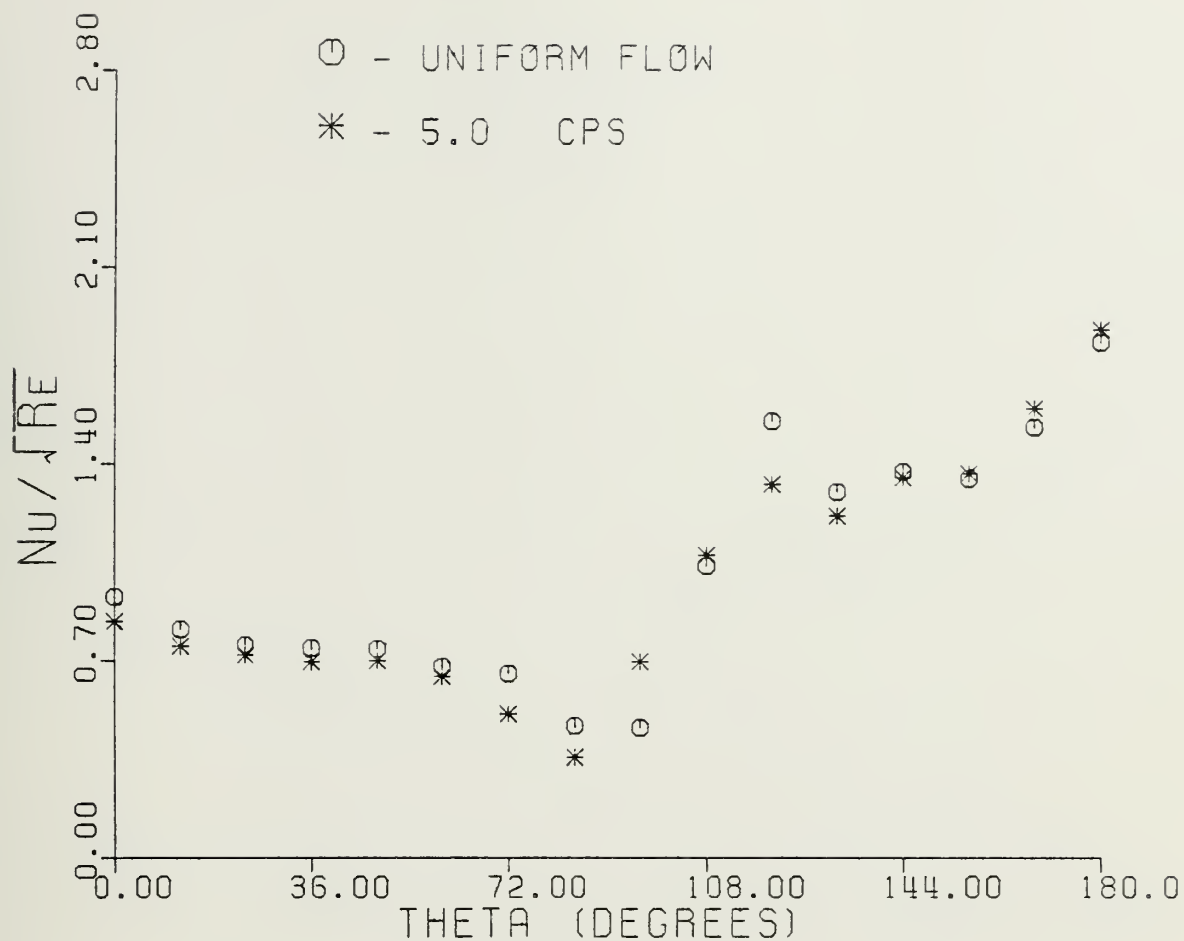
45 DEGREE MODEL
 RUN NR 32

REYNOLDS NR = 203254

FREQUENCY NR = 1.023×10^{-6}

AMPLITUDE NR = 0.115

FIGURE 30 - LOCAL HEAT TRANSFER COEFFICIENTS IN OSCILLATING FLOW THAT SHOWED UNALTERED RESULTS



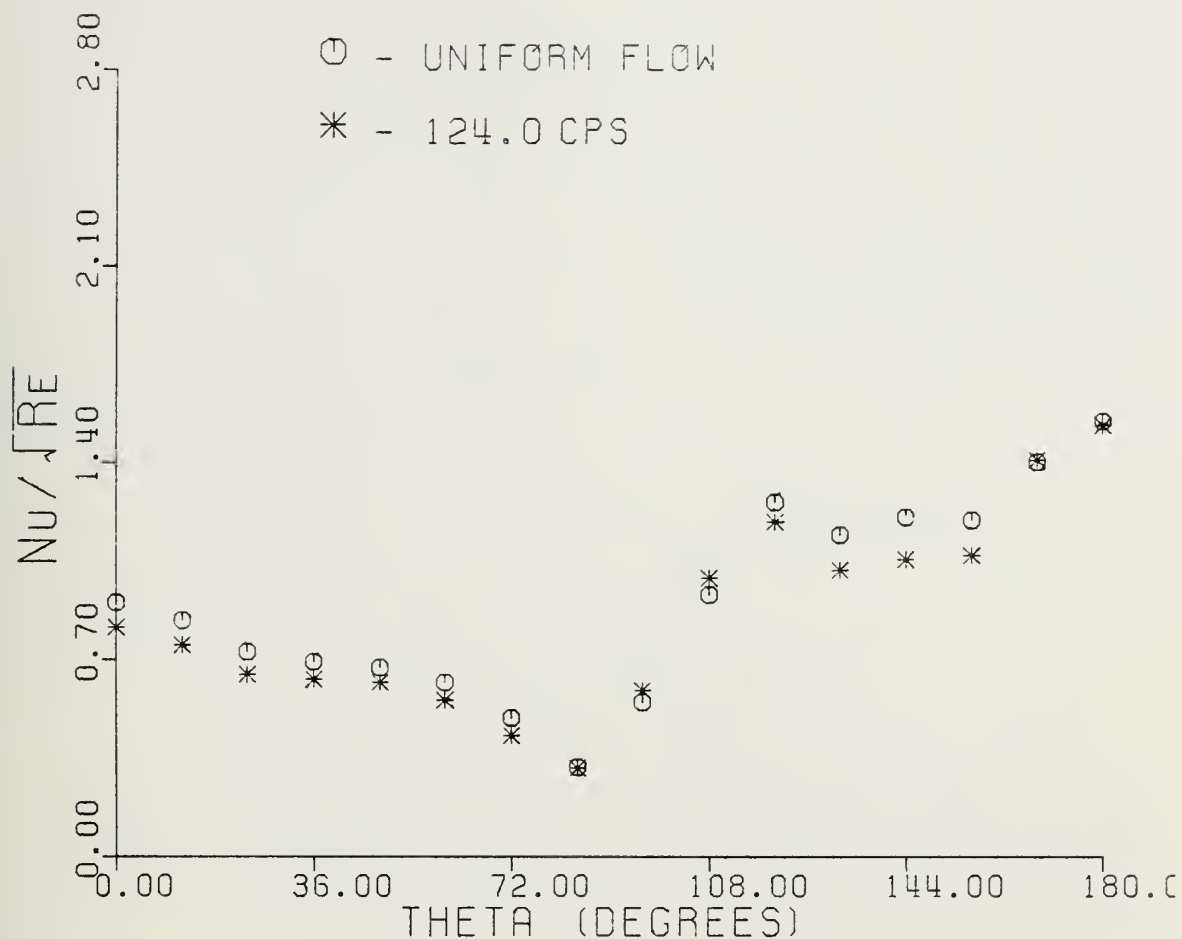
45 DEGREE MODEL RUN NR 26

REYNOLDS NR = 221461

FREQUENCY NR = 0.436×10^{-6}

AMPLITUDE NR = 0.120

FIGURE 31 - LOCAL HEAT TRANSFER COEFFICIENTS IN OSCILLATING FLOW THAT SHOWED UNALTERED RESULTS



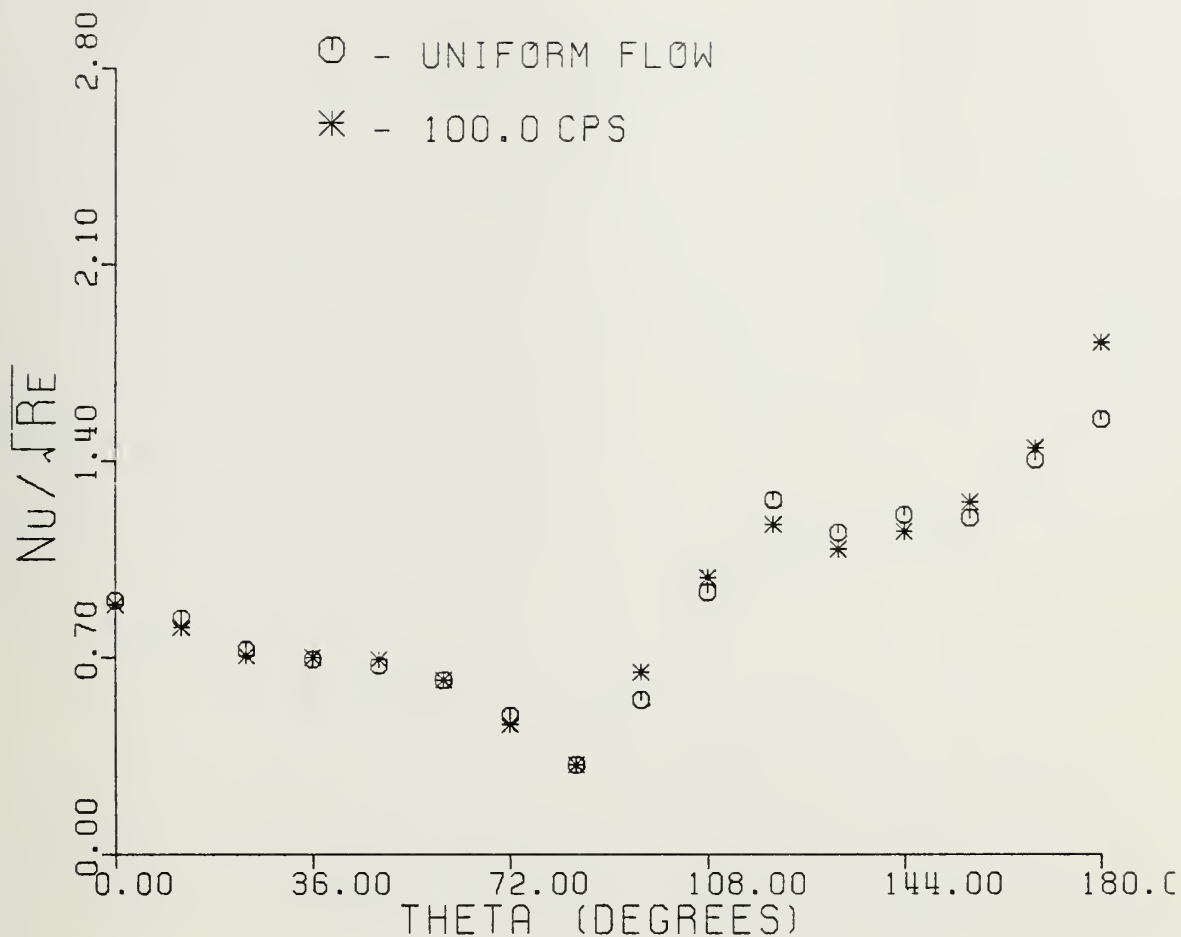
45 DEGREE MODEL RUN NR 31

REYNOLDS NR = 155314

FREQUENCY NR = 21.852×10^{-6}

AMPLITUDE NR = 0.048

FIGURE 32 - LOCAL HEAT TRANSFER COEFFICIENTS IN OSCILLATING FLOW THAT SHOWED UNALTERED RESULTS



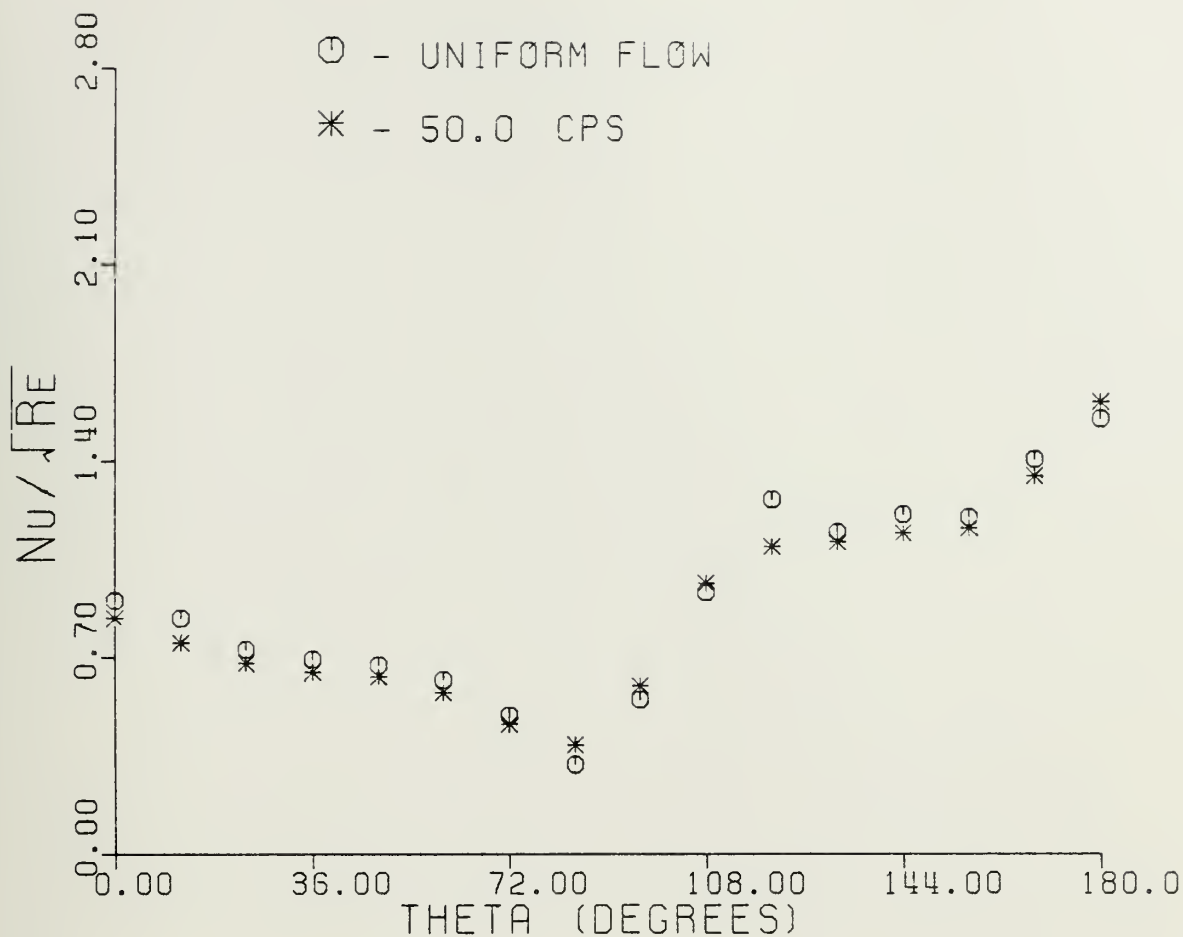
45 DEGREE MODEL
 RUN NR 23

REYNOLDS NR = 154891

FREQUENCY NR = 17.671×10^{-6}

AMPLITUDE NR = 0.045

FIGURE 33 - LOCAL HEAT TRANSFER COEFFICIENTS IN OSCILLATING FLOW THAT SHOWED UNALTERED RESULTS



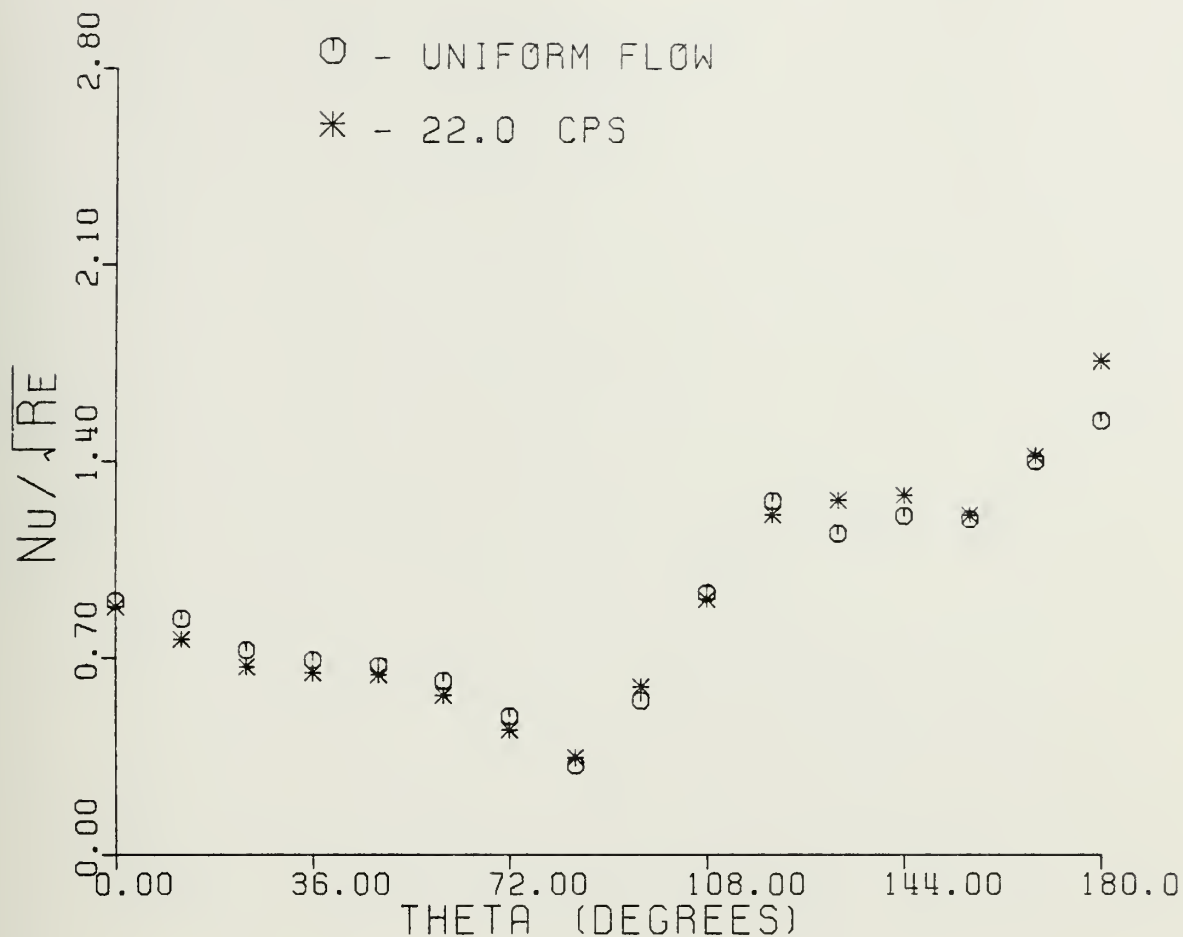
45 DEGREE MODEL RUN NR 28

REYNOLDS NR = 154053

FREQUENCY NR = 8.883×10^{-6}

AMPLITUDE NR = 0.110

FIGURE 34 - LOCAL HEAT TRANSFER COEFFICIENTS IN OSCILLATING FLOW THAT SHOWED UNALTERED RESULTS



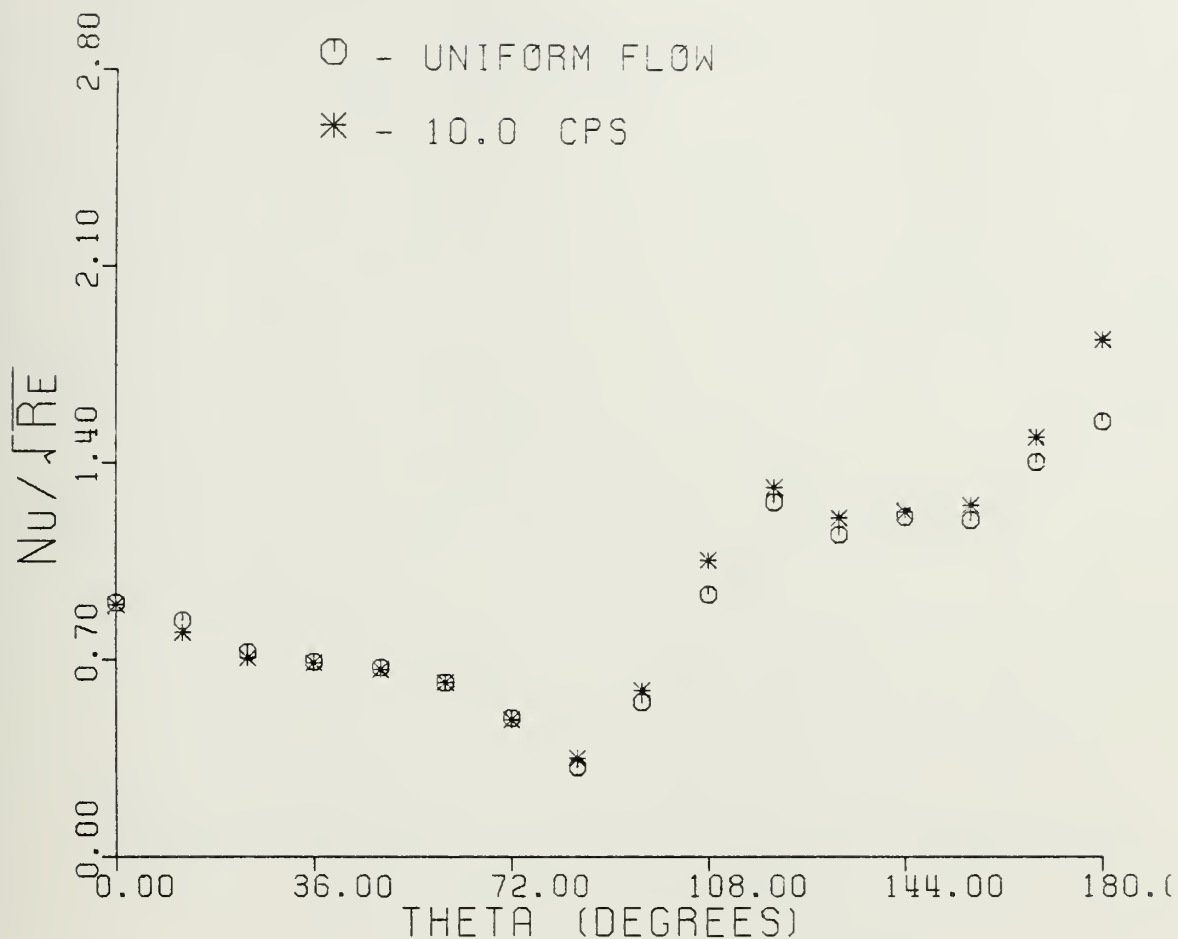
45 DEGREE MODEL RUN NR 21

REYNOLDS NR = 155739

FREQUENCY NR = 3.866×10^{-6}

AMPLITUDE NR = 0.040

FIGURE 35 - LOCAL HEAT TRANSFER COEFFICIENTS IN OSCILLATING FLOW THAT SHOWED UNALTERED RESULTS



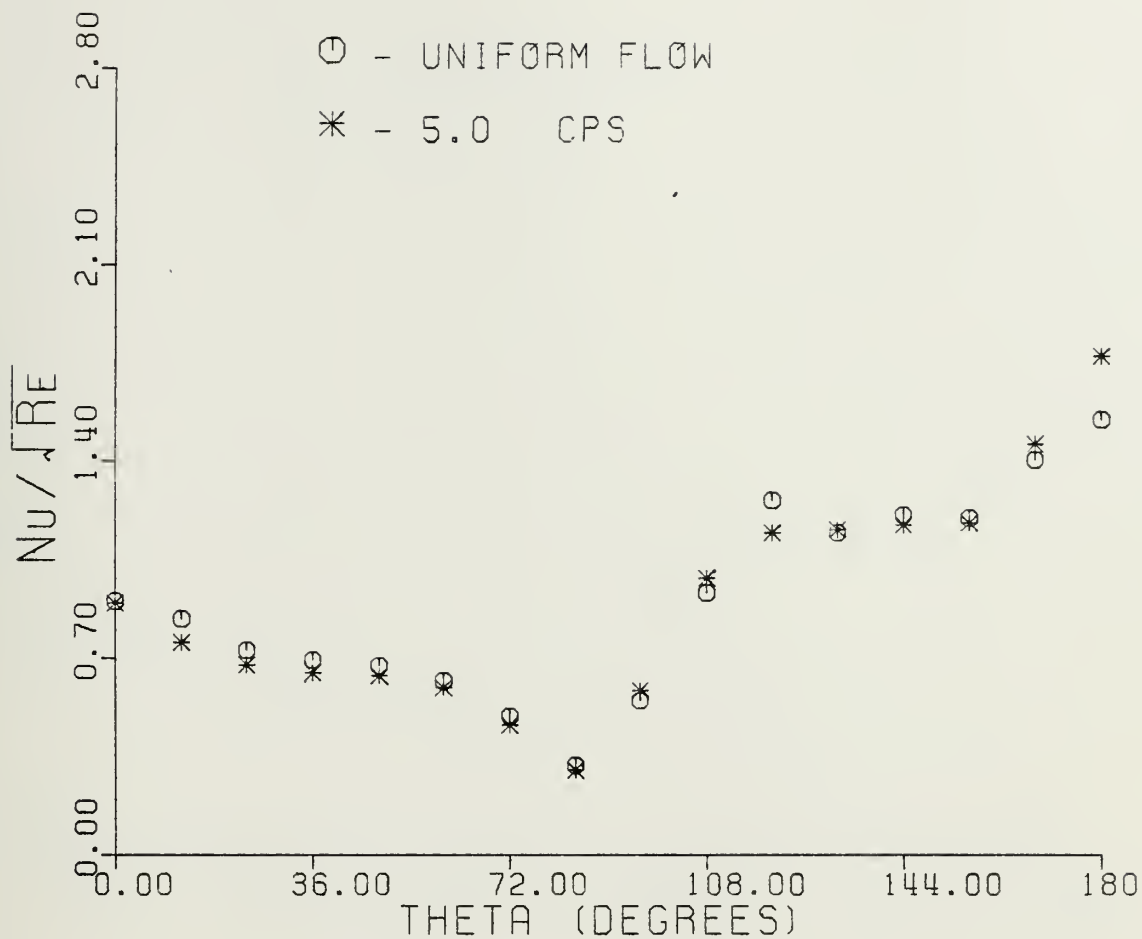
45 DEGREE MODEL RUN NR 33

REYNOLDS NR = 155739

FREQUENCY NR = 1.757×10^{-6}

AMPLITUDE NR = 0.090

FIGURE 36 - LOCAL HEAT TRANSFER COEFFICIENTS IN OSCILLATING FLOW THAT SHOWED UNALTERED RESULTS



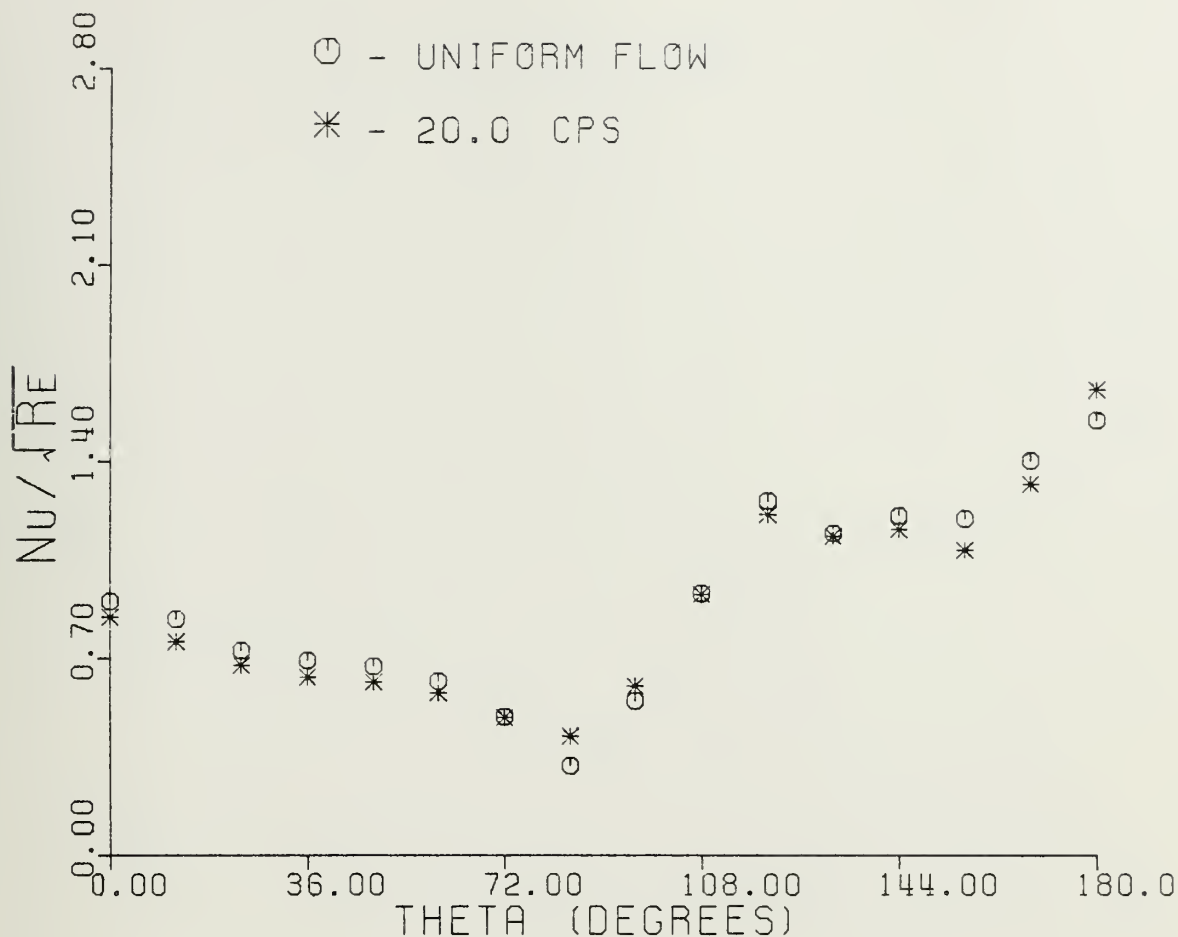
45 DEGREE MODEL RUN NR 25

REYNOLDS NR = 156167

FREQUENCY NR = 0.876×10^{-6}

AMPLITUDE NR = 0.100

FIGURE 37 - LOCAL HEAT TRANSFER COEFFICIENTS IN OSCILLATING FLOW THAT SHOWED UNALTERED RESULTS



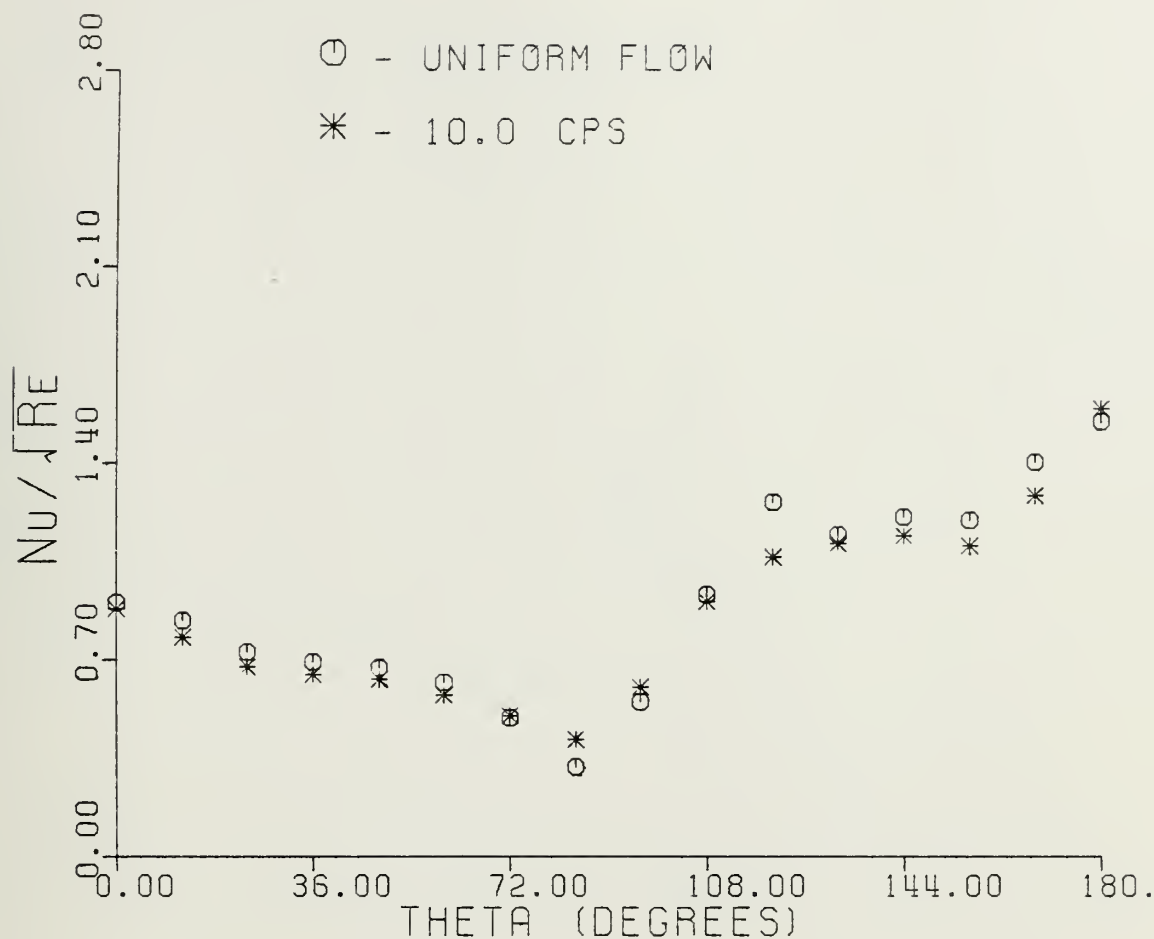
45 DEGREE MODEL
 RUN NR 36

REYNOLDS NR = 149789

FREQUENCY NR = 3.769×10^{-6}

AMPLITUDE NR = 0.240

FIGURE 38 - LOCAL HEAT TRANSFER COEFFICIENTS IN OSCILLATING FLOW THAT SHOWED UNALTERED RESULTS



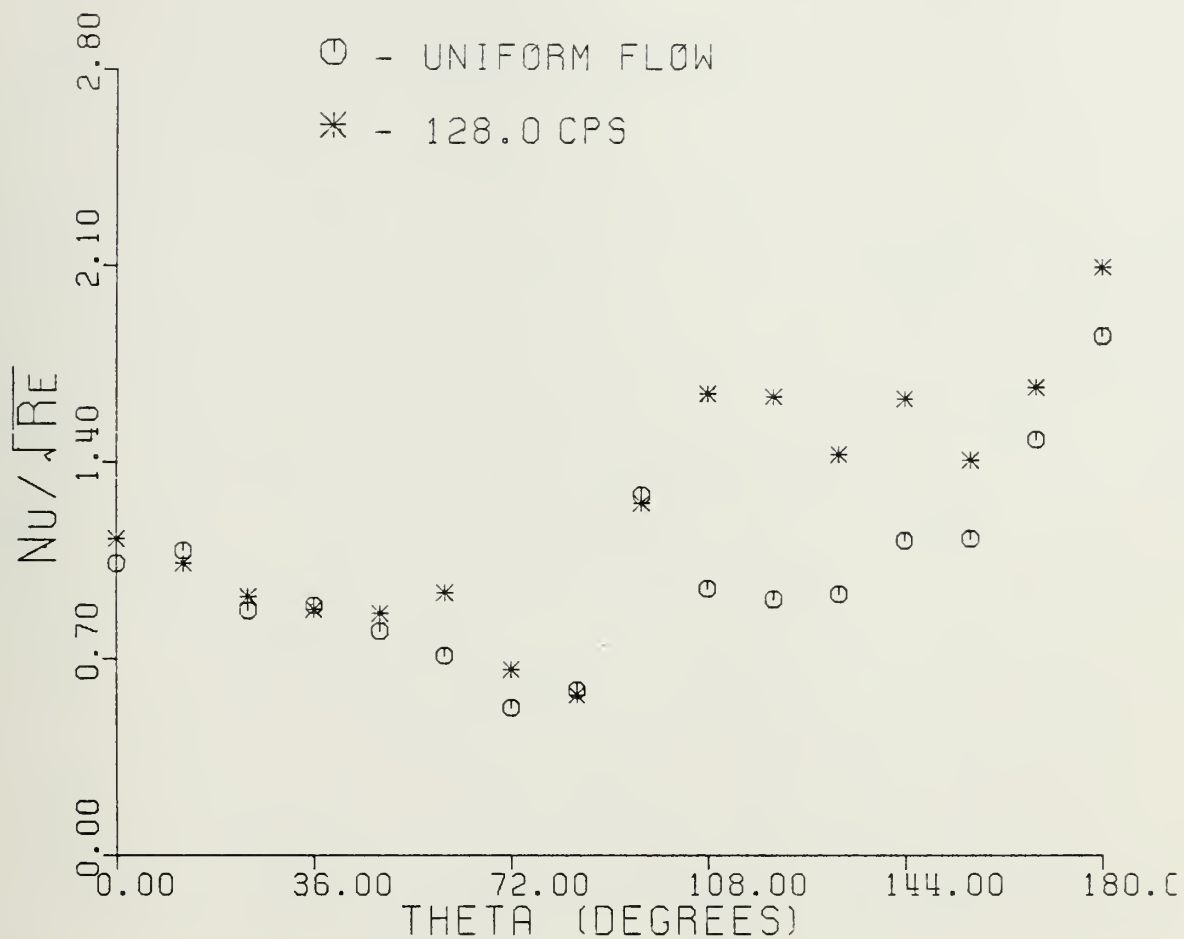
45 DEGREE MODEL
 RUN NR 35

REYNOLDS NR = 110895

FREQUENCY NR = 3.452×10^{-6}

AMPLITUDE NR = 0.440

FIGURE 39 - LOCAL HEAT TRANSFER COEFFICIENTS IN OSCILLATING FLOW THAT SHOWED UNALTERED RESULTS



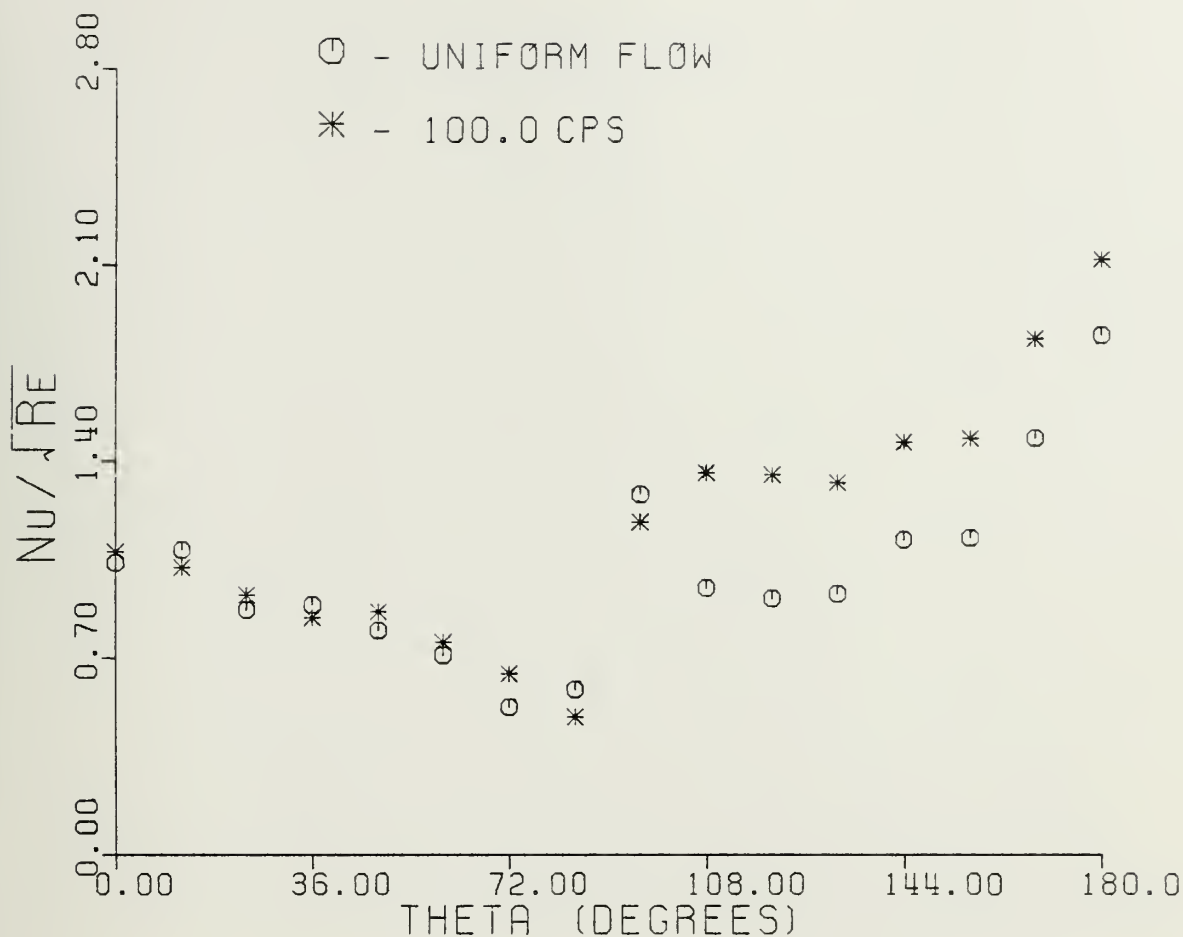
90 DEGREE MODEL RUN NR 17

REYNOLDS NR. = 232762

FREQUENCY NR = 9.725×10^{-6}

AMPLITUDE NR = 0.690

FIGURE 40 - LOCAL HEAT TRANSFER COEFFICIENTS IN OSCILLATING FLOW THAT SHOWED ENHANCED HEAT TRANSFER



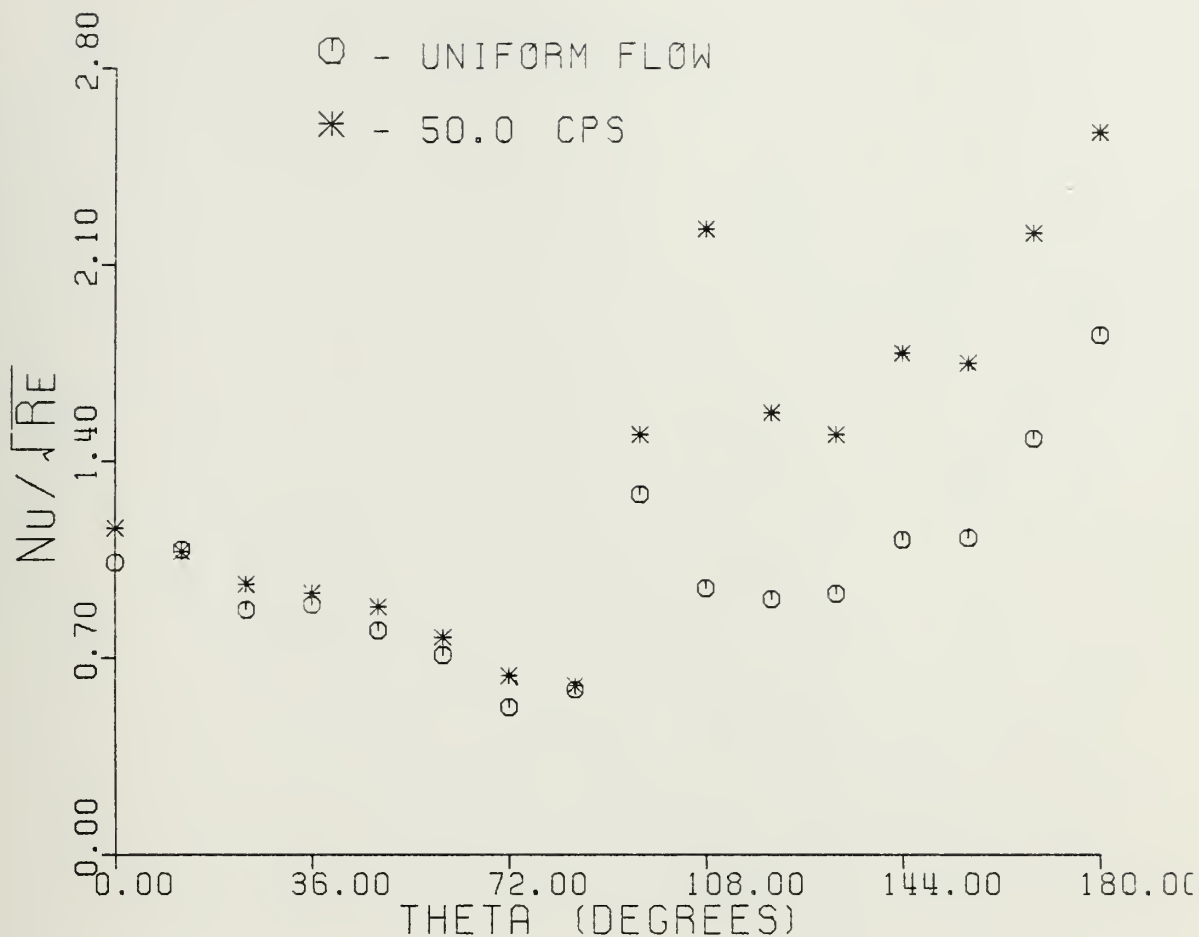
90 DEGREE MODEL RUN NR 15

REYNOLDS NR = 204847

FREQUENCY NR = 9.861×10^{-6}

AMPLITUDE NR = 0.052

FIGURE 41 - LOCAL HEAT TRANSFER COEFFICIENTS IN OSCILLATING FLOW THAT SHOWED ENHANCED HEAT TRANSFER



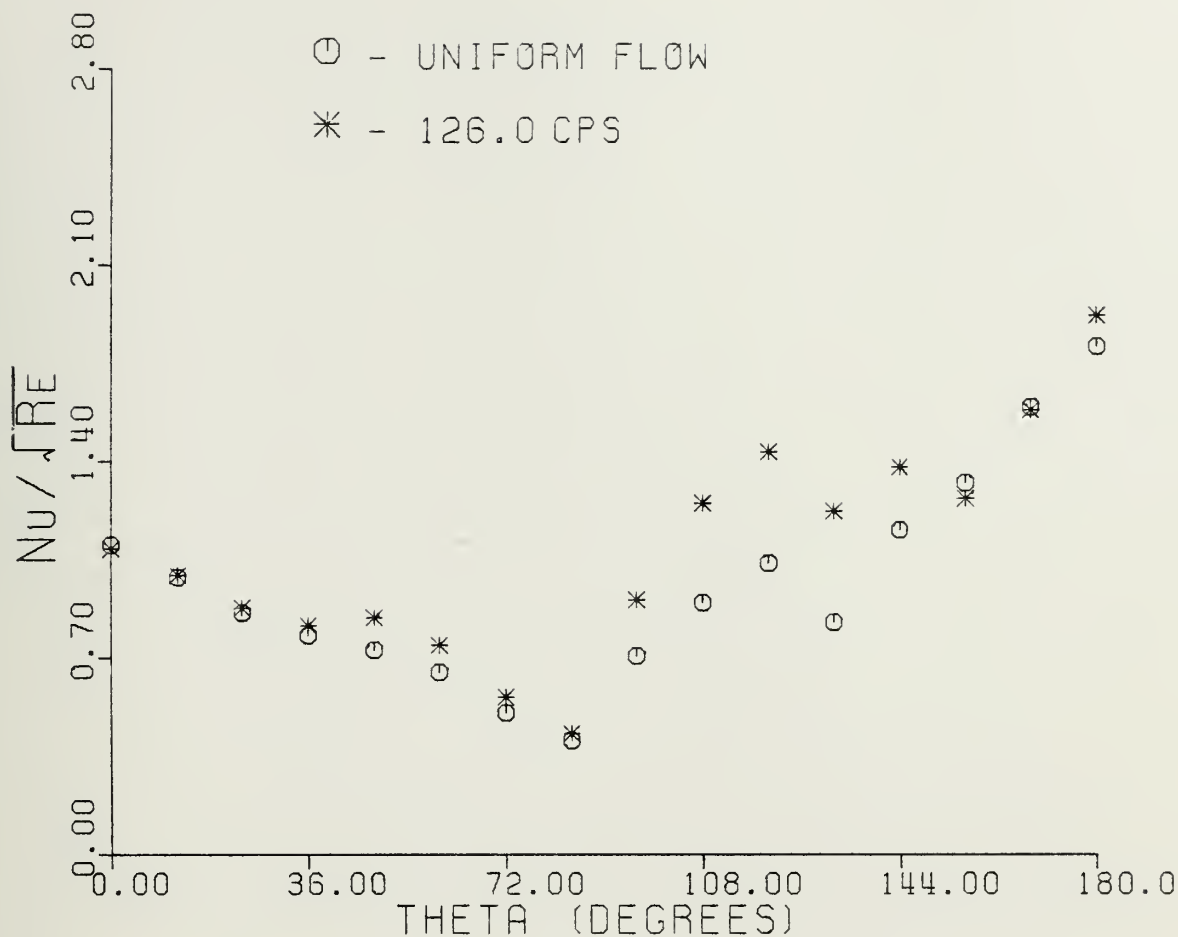
90 DEGREE MODEL RUN NR 20

REYNOLDS NR = 269246

FREQUENCY NR = 2.885×10^{-6}

AMPLITUDE NR = 0.310

FIGURE 42 - LOCAL HEAT TRANSFER COEFFICIENTS IN OSCILLATING FLOW THAT SHOWED ENHANCED HEAT TRANSFER



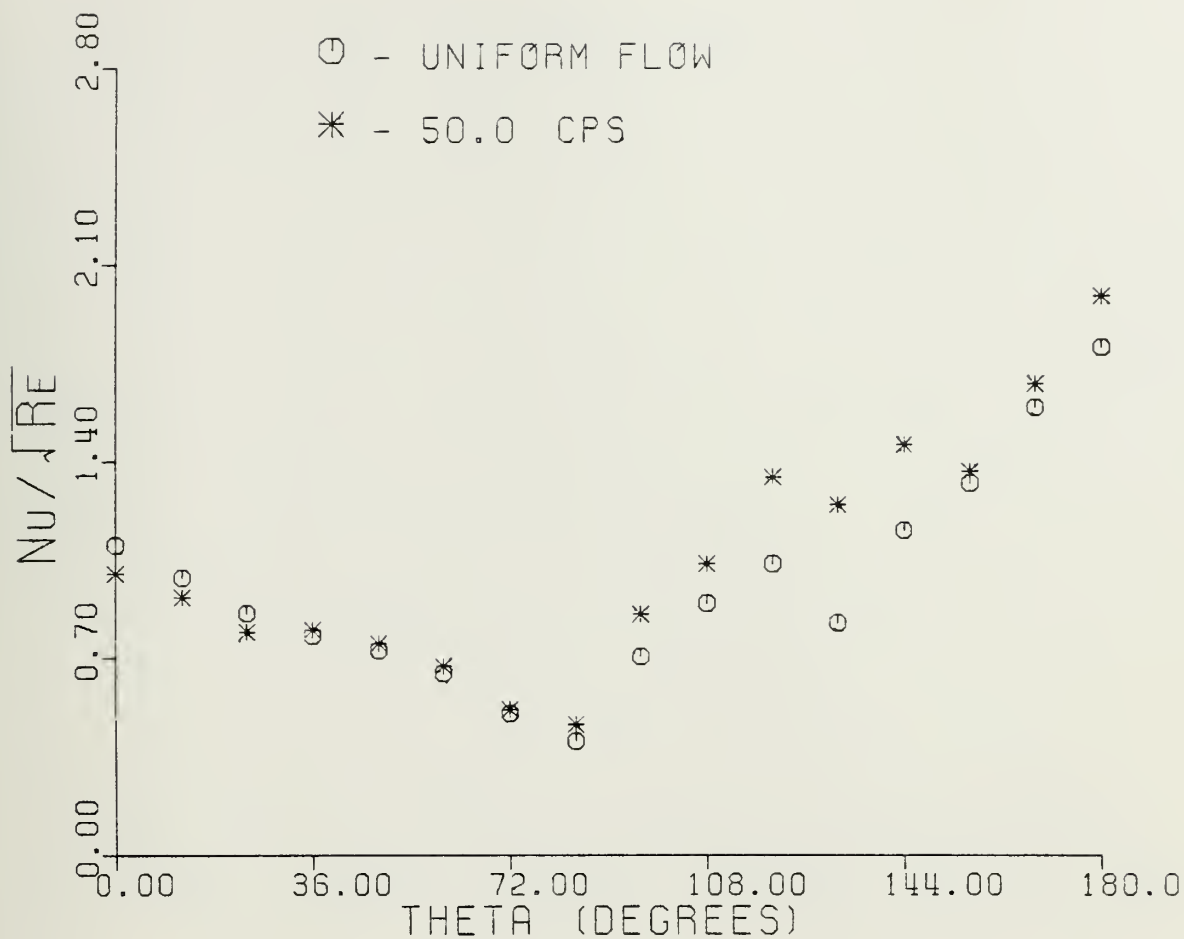
90 DEGREE MODEL RUN NR 16

REYNOLDS NR = 149597

FREQUENCY NR = 23.053×10^{-6}

AMPLITUDE NR = 0.340

FIGURE 43 - LOCAL HEAT TRANSFER COEFFICIENTS IN OSCILLATING FLOW THAT SHOWED ENHANCED HEAT TRANSFER



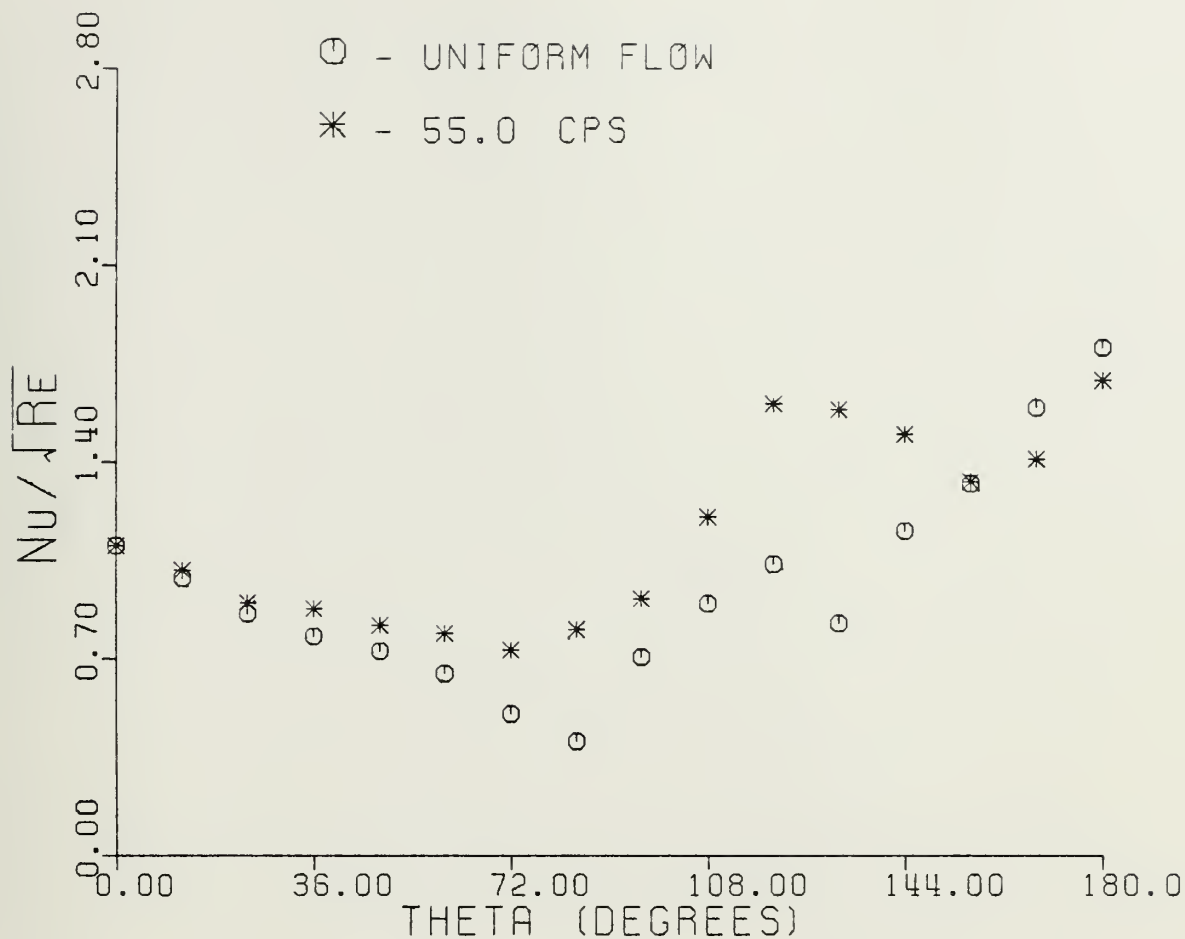
90 DEGREE MODEL RUN NR 11

REYNOLDS NR = 154471

FREQUENCY NR = 8.859×10^{-6}

AMPLITUDE NR = 0.150

FIGURE 44 - LOCAL HEAT TRANSFER COEFFICIENTS IN OSCILLATING FLOW THAT SHOWED ENHANCED HEAT TRANSFER



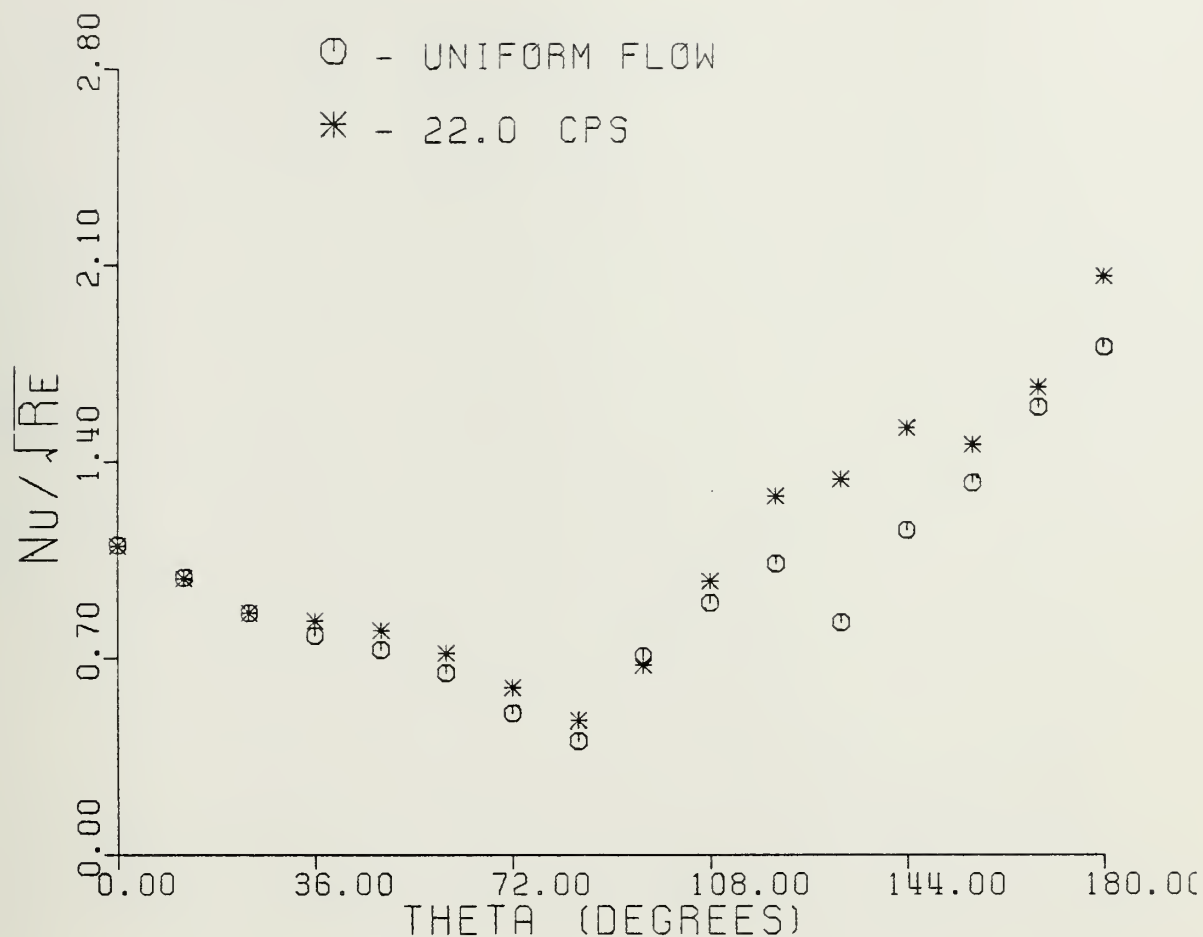
90 DEGREE MODEL RUN NR 42

REYNOLDS NR = 94381

FREQUENCY NR = 25.149×10^{-6}

AMPLITUDE NR = 0.330

FIGURE 45 - LOCAL HEAT TRANSFER COEFFICIENTS IN OSCILLATING FLOW THAT SHOWED ENHANCED HEAT TRANSFER



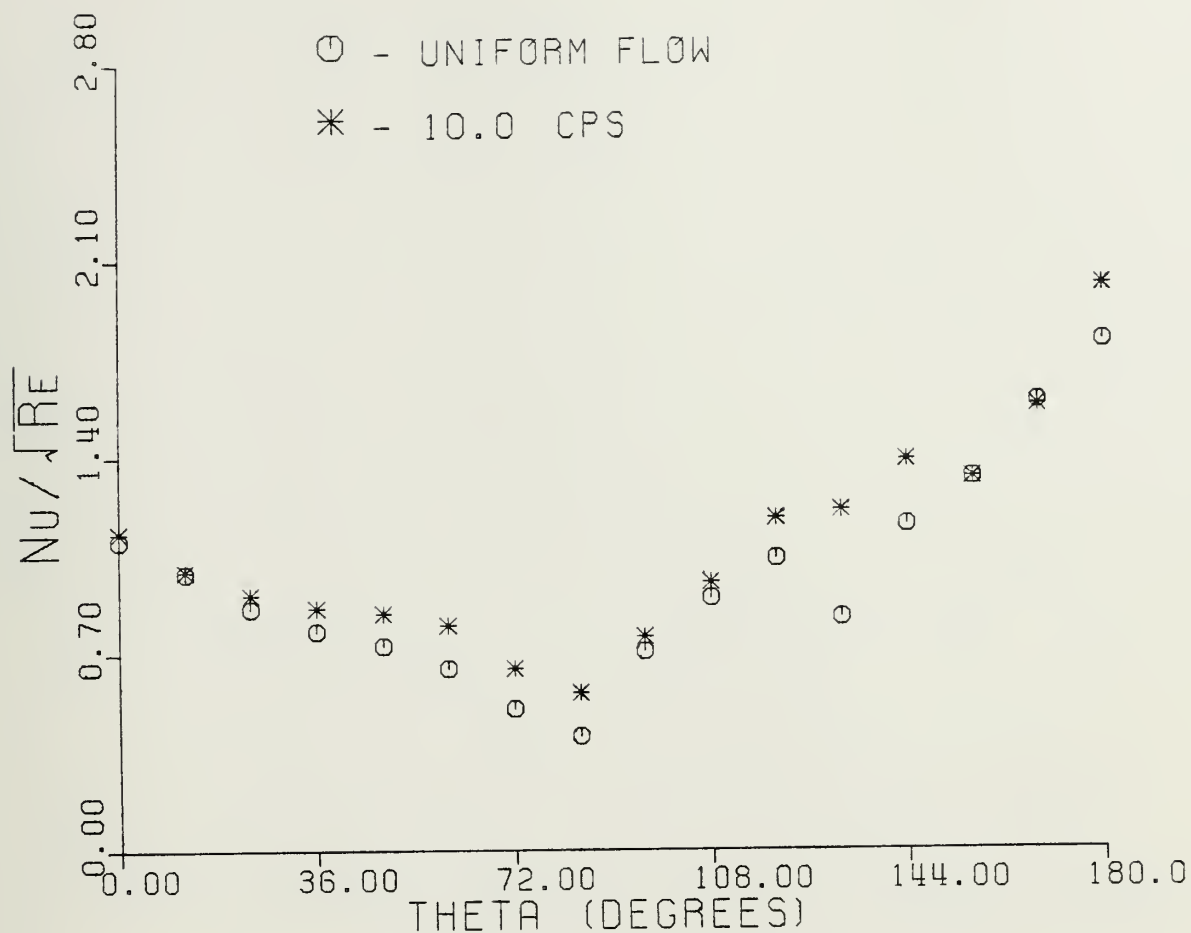
90 DEGREE MODEL RUN NR 41

REYNOLDS NR = 150388

FREQUENCY NR = 4.004×10^{-6}

AMPLITUDE NR = 0.110

FIGURE 46 - LOCAL HEAT TRANSFER COEFFICIENTS IN OSCILLATING FLOW THAT SHOWED ENHANCED HEAT TRANSFER



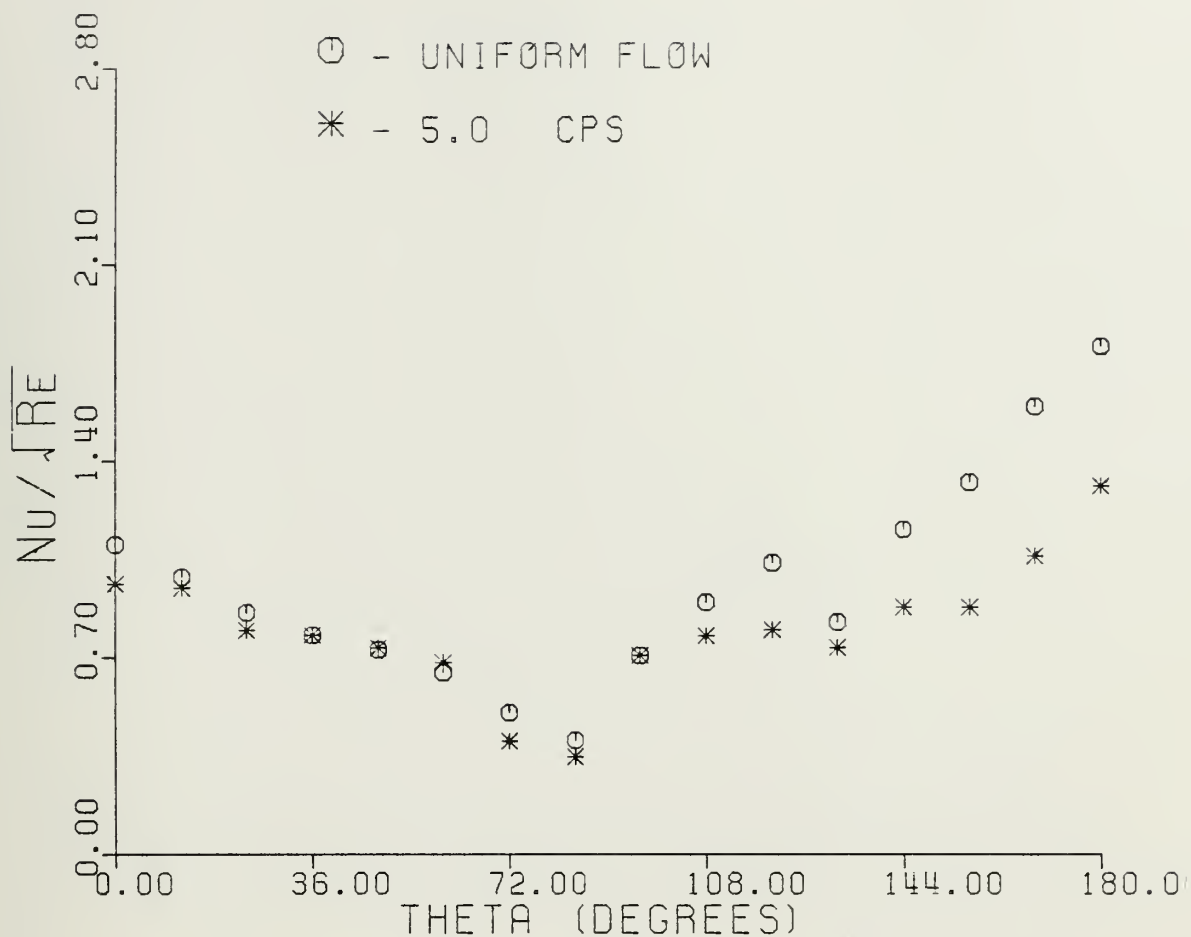
90 DEGREE MODEL
RUN NR 43

REYNOLDS NR = 105536

FREQUENCY NR = 3.638×10^{-6}

AMPLITUDE NR = 0.290

FIGURE 47 - LOCAL HEAT TRANSFER COEFFICIENTS IN OSCILLATING FLOW THAT SHOWED ENHANCED HEAT TRANSFER



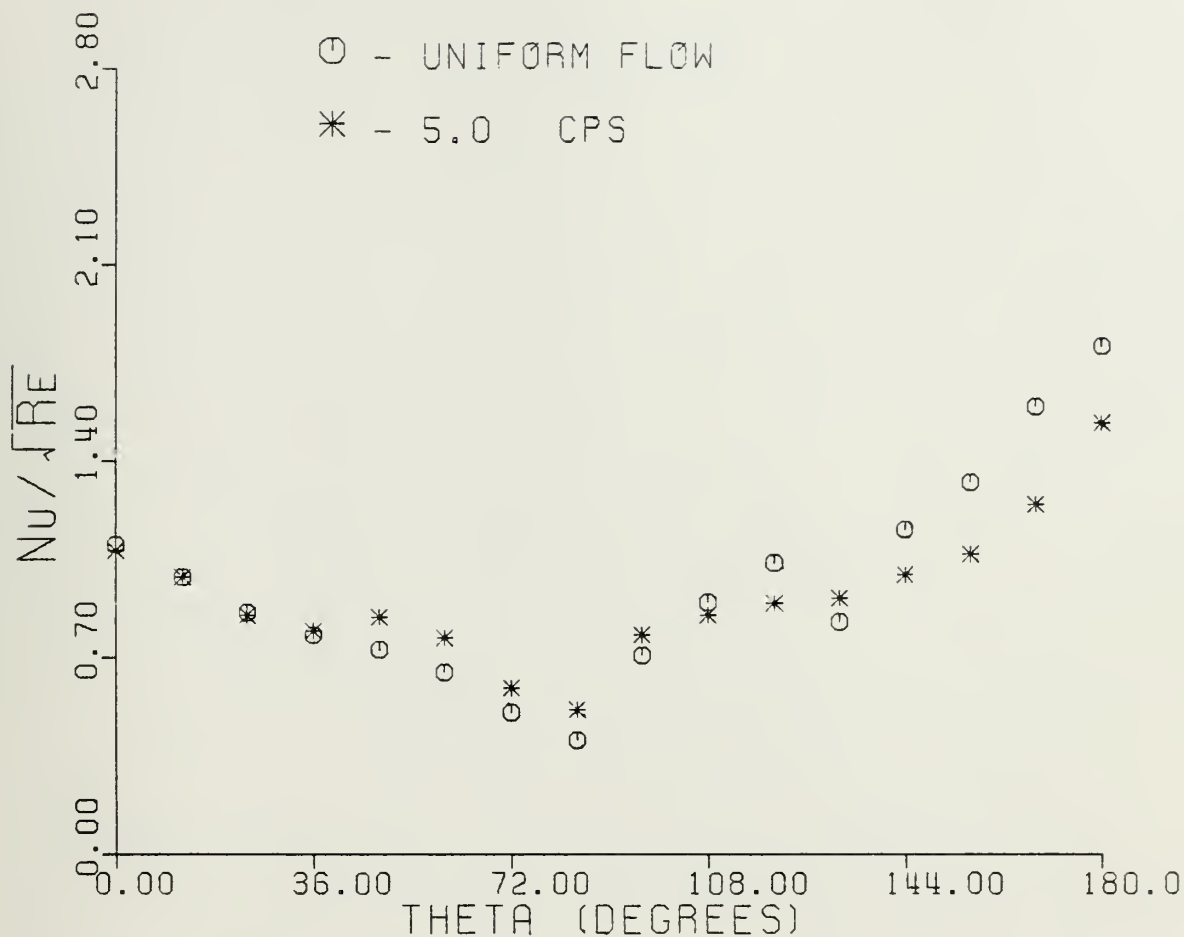
90 DEGREE MODEL RUN NR 13

REYNOLDS NR = 149597

FREQUENCY NR = 0.914×10^{-6}

AMPLITUDE NR = 0.100

FIGURE 48 - LOCAL HEAT TRANSFER COEFFICIENTS IN OSCILLATING FLOW THAT SHOWED DEGRADED HEAT TRANSFER



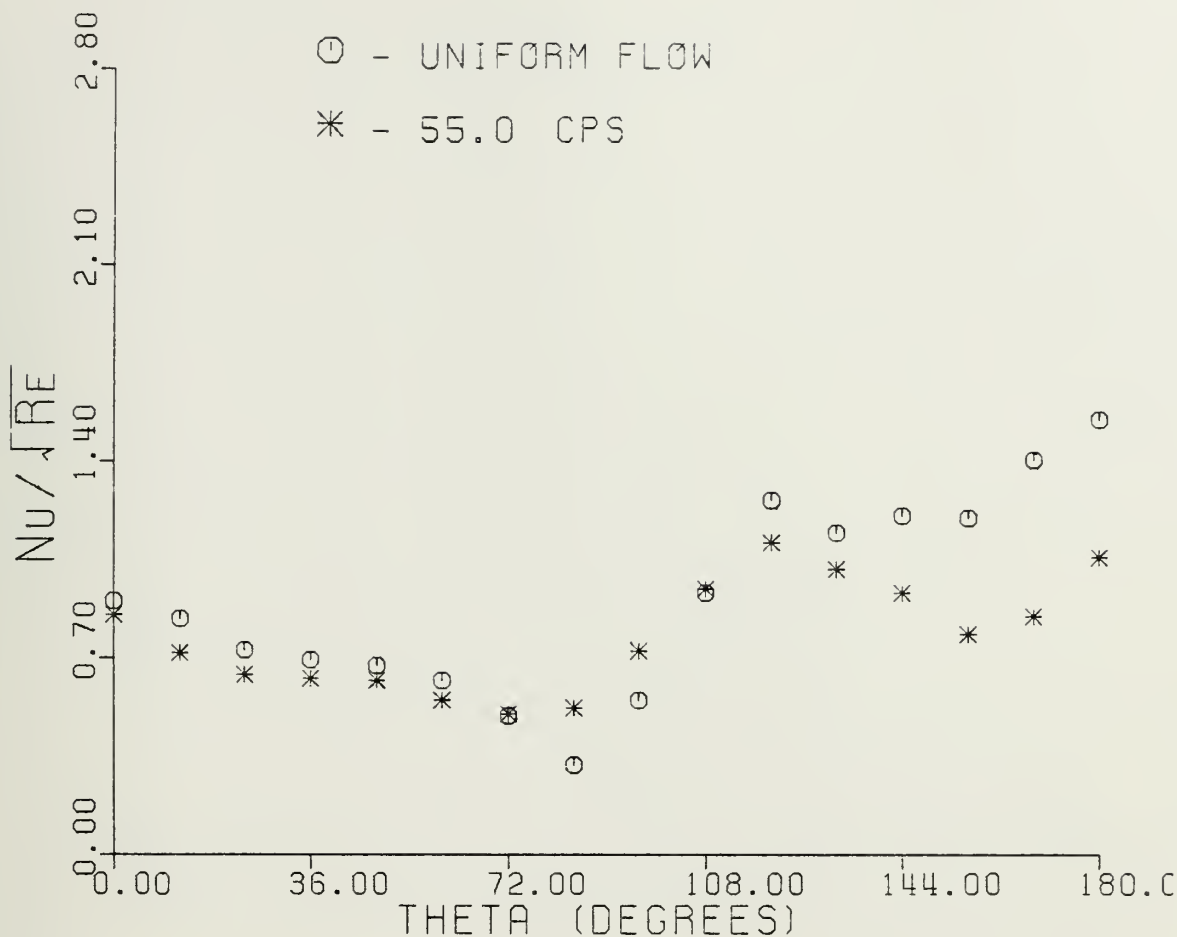
90 DEGREE MODEL RUN NR 7

REYNOLDS NR = 109599

FREQUENCY NR = 1.736×10^{-6}

AMPLITUDE NR = 0.105

FIGURE 49 - LOCAL HEAT TRANSFER COEFFICIENTS IN OSCILLATING FLOW THAT SHOWED DEGRADED HEAT TRANSFER



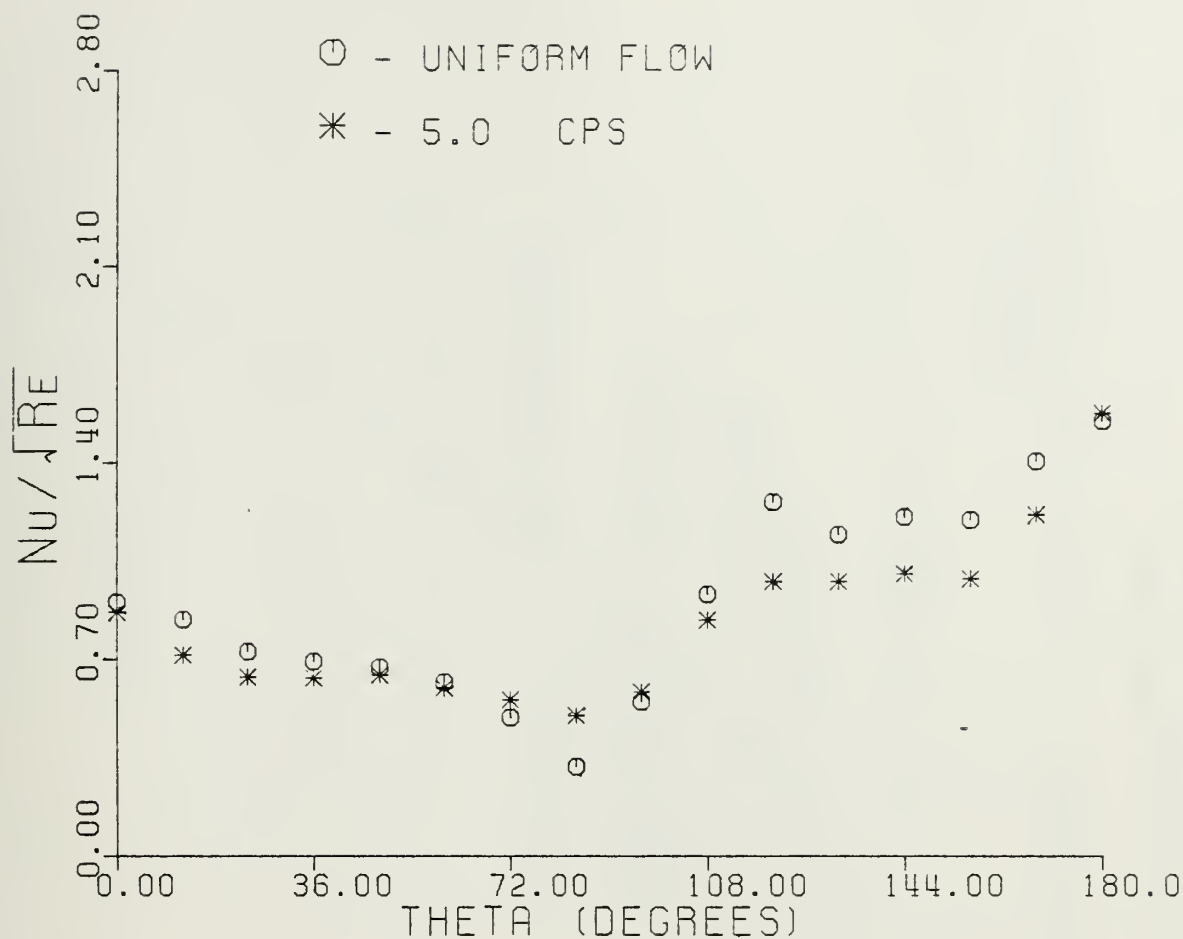
45 DEGREE MODEL RUN NR 38

REYNOLDS NR = 108954

FREQUENCY NR = 20.024×10^{-6}

AMPLITUDE NR = 0.41

FIGURE 50 - LOCAL HEAT TRANSFER COEFFICIENTS IN OSCILLATING FLOW THAT SHOWED DEGRADED HEAT TRANSFER



45 DEGREE MODEL
 RUN NR 37

REYNOLDS NR = 107462

FREQUENCY NR = 1.846×10^{-6}

AMPLITUDE NR = 0.650

FIGURE 51 - LOCAL HEAT TRANSFER COEFFICIENTS IN OSCILLATING FLOW THAT SHOWED DEGRADED HEAT TRANSFER

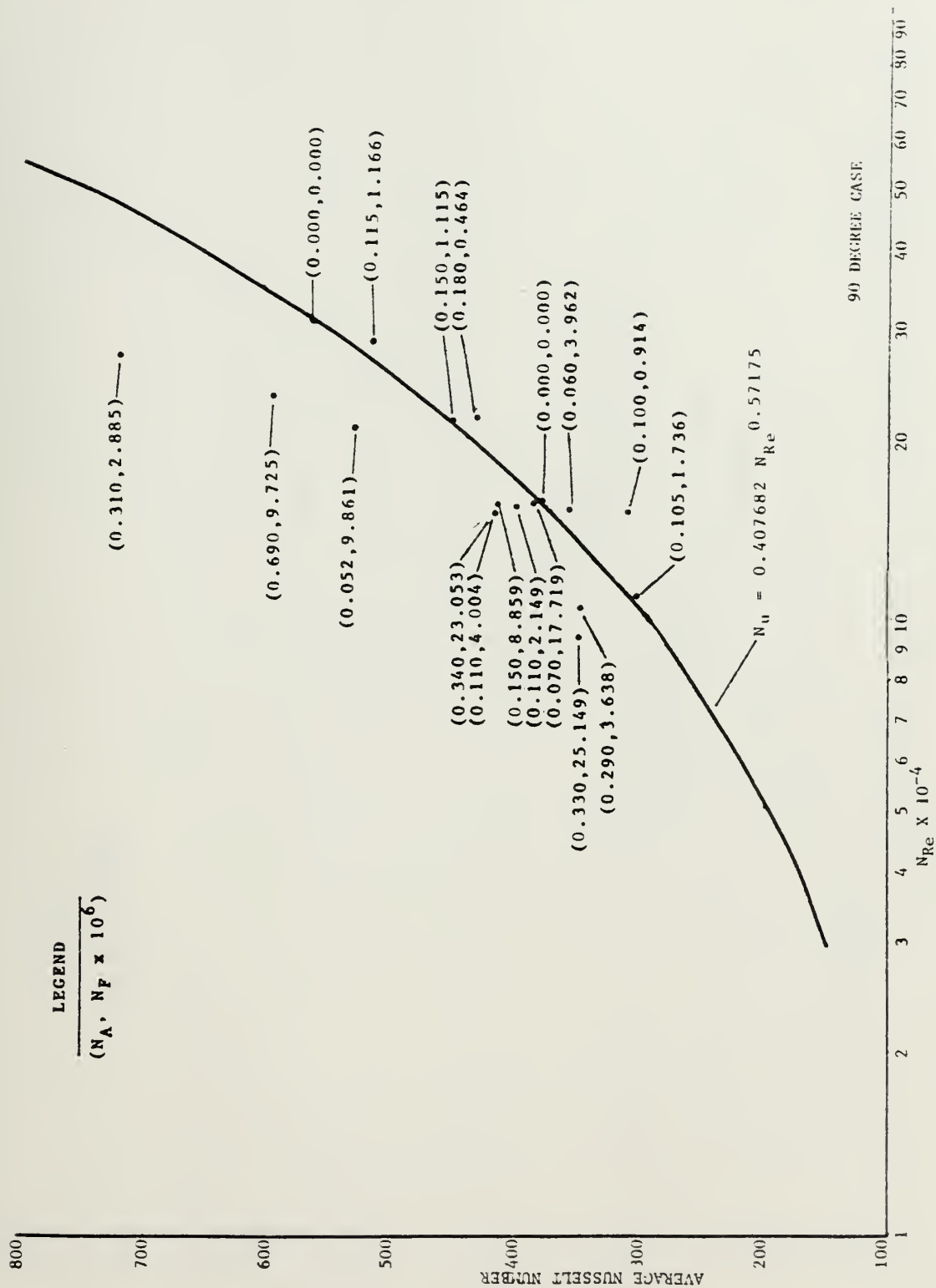


FIGURE 52 - VARIATION OF AVERAGE NUSSLETT NUMBER
 WITH REYNOLDS NUMBER

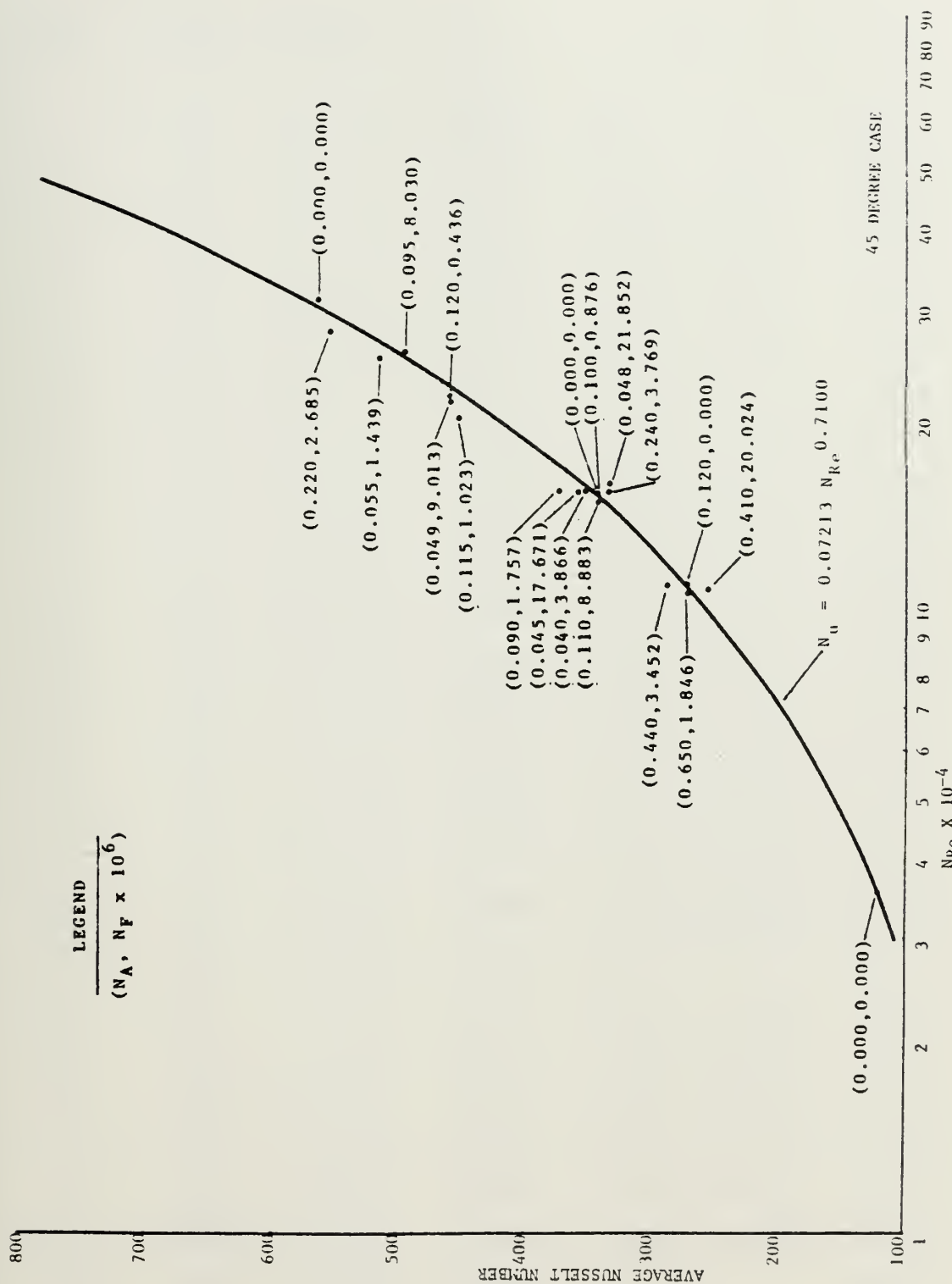


FIGURE 53 - VARIATION OF AVERAGE NUSSULT NUMBER
WITH REYNOLDS NUMBER

TABLE I
SUMMARY OF AVERAGE HEAT TRANSFER RESULTS

Run Number	Yaw Angle	Average Nu	N_{Re}	N_F	N_S	N_A
5	90°	565.49	314057	0.0	0.0	0.0
6	90°	380.50	157028	0.0	0.0	0.0
7	90°	304.32	109598	1.736×10^{-6}	0.190	0.105
8	90°	431.65	213959	0.464×10^{-6}	0.099	0.180
9	90°	517.54	283129	1.166×10^{-6}	0.330	0.115
10	90°	359.58	151994	3.962×10^{-6}	0.602	0.060
11	90°	415.10	154470	8.859×10^{-6}	1.369	0.150
12	90°	387.19	154470	17.719×10^{-6}	2.737	0.070
13	90°	309.30	149596	0.914×10^{-6}	0.137	0.100
15	90°	530.16	204846	9.861×10^{-6}	2.020	0.052
16	90°	418.60	149596	23.053×10^{-6}	3.449	0.340
17	90°	594.91	232762	9.725×10^{-6}	2.264	0.690
18	90°	450.24	212769	1.115×10^{-6}	0.237	0.150
19	90°	400.49	152811	2.149×10^{-6}	0.328	0.110
20	90°	717.90	269246	2.885×10^{-6}	0.777	0.310
21	45°	360.71	155739	3.866×10^{-6}	0.852	0.040
22	45°	515.02	254242	1.439×10^{-6}	0.517	0.055
23	45°	362.85	154891	17.671×10^{-6}	3.871	0.045
24	45°	460.74	217174	9.013×10^{-6}	2.768	0.049
25	45°	356.32	156166	0.876×10^{-6}	0.194	0.100
26	45°	462.35	221461	0.436×10^{-6}	0.137	0.120
27	45°	567.89	314057	0.0	0.0	0.0
28	45°	343.13	154052	8.883×10^{-6}	1.935	0.110
29	45°	556.50	280040	2.685×10^{-6}	1.063	0.220
30	45°	497.50	259876	8.030×10^{-6}	2.951	0.095
31	45°	335.60	155314	21.852×10^{-6}	4.800	0.048
32	45°	453.45	203253	1.023×10^{-6}	0.295	0.115
33	45°	374.23	155739	1.757×10^{-6}	0.381	0.090
34	45°	357.48	155314	0.0	0.0	0.0

TABLE I Continued

Run Number	Yaw Angle	Average Nu	N _{Re}	N _F	N _S	N _A
35	45°	289.59	110894	3.452 x 10 ⁻⁶	0.541	0.440
36	45°	341.41	149788	3.769 x 10 ⁻⁶	0.798	0.240
37	45°	272.71	107462	1.846 x 10 ⁻⁶	0.280	0.650
38	45°	256.67	108953	20.024 x 10 ⁻⁶	3.085	0.410
39	45°	273.36	110647	0.0	0.0	0.0
40	45°	122.07	35630	0.0	0.0	0.0
41	90°	419.91	150387	4.004 x 10 ⁻⁶	0.602	0.110
42	90°	350.94	94381	25.149 x 10 ⁻⁶	2.374	0.330
43	90°	348.06	105535	3.638 x 10 ⁻⁶	0.384	0.290

TABLE II - SUMMARY OF LOCAL HEAT TRANSFER RESULTS

RUN NR	5	- 90 DEGREE MODEL, HIGH FLOW RATE						
STRIP	Q	T	DT	H	NUS	NUSREN		
1	62.214	118.043	59.043	45.372	1035.10547	1.84706		
2	54.442	118.631	59.631	36.370	829.74829	1.48061		
3	47.298	121.180	62.180	27.664	631.13013	1.12620		
4	45.155	118.952	59.992	27.469	626.68481	1.11826		
5	40.269	119.968	60.968	22.767	519.40723	0.92684		
6	38.686	118.801	59.801	22.370	510.34399	0.91066		
7	39.668	118.810	59.810	23.270	530.87598	0.94730		
8	48.536	118.576	59.576	31.470	717.96289	1.28114		
9	24.077	120.635	61.635	14.466	330.01563	0.58888		
10	26.592	119.914	60.914	12.867	293.55200	0.52382		
11	23.121	119.655	60.655	17.468	398.50977	0.71111		
12	36.312	119.976	60.976	19.567	446.40186	0.79657		
13	39.172	119.710	60.710	21.868	498.88818	0.89022		
14	38.794	119.734	60.734	21.368	487.48022	0.86987		
15	44.083	118.211	59.211	26.671	608.47583	1.08577		
16	44.263	119.832	60.832	25.567	583.29346	1.04084		

REYNOLDS NR = 314057.68750
VELOCITY = 153.04166
FREQUENCY = 0.0
FREQUENCY NR = 0.0

STROUHAL NR = 0.0
AMPLITUDE NR = 0.0
BLADES = 6.0 INCHES

TABLE II - CONTINUED

RUN NR	6	- 90 DEGREE MODEL, LOW FLOW RATE			
STRIP	Q	T	DT	H	NUS
1	51.710	121.650	62.650	31.363	715.51660
2	46.466	120.643	61.643	27.665	631.15918
3	39.637	119.218	60.218	22.969	524.00977
4	36.652	120.479	61.479	20.066	457.78198
5	31.750	126.412	67.412	14.352	327.42163
6	33.382	120.568	61.568	17.966	409.86768
7	29.053	119.382	60.382	15.568	355.17822
8	23.758	119.113	60.113	12.269	279.90674
9	15.333	118.307	59.307	7.071	161.31740
10	18.723	119.067	60.067	8.769	200.06038
11	23.544	120.391	61.391	11.266	257.02417
12	27.296	122.844	63.844	12.660	288.83154
13	28.056	121.246	62.246	13.564	309.45020
14	29.595	119.722	60.722	14.968	341.47168
15	33.126	120.001	61.001	17.167	391.64697
16	35.476	119.185	60.185	19.169	437.31865

REYNOLDS NR = 157028.81250
 VELOCITY = 76.52080 FT/S
 FREQUENCY = 0.0 CPS
 STROUHAL NR = 0.0
 AMPLITUDE NR = 0.0
 BLADES = 6.0 INCHES

TABLE II - CONTINUED

RUN NR	I	- 90 DEGREE	MODEL, LOW FLOW RATE						
STRIP	Q	T	DT	H	NUS	NUSREN			
1	38.261	122.722	58.222	22.448	507.27075	1.53228			
2	31.566	120.536	56.036	18.254	412.47998	1.24595			
3	27.813	120.115	55.615	15.655	353.75049	1.06855			
4	27.105	121.713	57.213	14.551	328.80786	0.99321			
5	24.729	120.993	56.493	13.353	301.72998	0.91141			
6	23.476	119.892	55.392	13.055	295.00977	0.89112			
7	22.584	120.422	55.922	12.454	281.42310	0.85008			
8	20.386	119.430	54.930	11.456	258.87891	0.78198			
9	14.254	118.099	53.599	7.559	170.82118	0.51599			
10	16.256	118.341	53.841	8.659	195.66519	0.59103			
11	20.028	117.800	53.300	11.260	254.44662	0.76859			
12	22.722	119.718	55.218	12.356	279.20093	0.84336			
13	22.873	121.221	56.721	11.652	263.30249	0.79534			
14	23.621	119.827	55.327	12.455	281.45493	0.85017			
15	26.170	119.308	54.808	14.457	326.67700	0.98677			
16	29.414	121.466	56.966	15.851	358.19727	1.08198			

REYNOLDS NR = 109598.56250
 VELOCITY = 55.02930 FT/S
 FREQUENCY = 5.00 CPS
 FREQUENCY NR = 1.736×10^{-6}
 STRUCTURAL NR = 0.190
 AMPLITUDE NR = 0.105
 BLADES = 6.0 INCHES

TABLE II - CONTINUED

RUN NR	8	- 90 DEGREE MODEL, HIGH FLOW RATE							
STRIP	Q	T	DT	H	NUS	NUSREN			
1	54.670	126.321	65.321	31.748	721.77002	1.56039			
2	45.257	122.014	61.014	26.958	612.87720	1.32497			
3	38.560	120.341	59.341	22.662	515.20850	1.11382			
4	36.059	119.513	58.513	20.864	474.33032	1.02545			
5	32.016	120.227	59.227	17.562	399.26758	0.86317			
6	38.257	127.419	66.419	19.045	432.98071	0.93606			
7	34.845	122.828	61.828	18.856	428.68286	0.92677			
8	34.087	116.871	55.871	21.570	490.38550	1.06016			
9	19.085	122.571	61.571	8.457	192.25676	0.41564			
10	21.459	120.099	59.099	10.462	237.85901	0.51423			
11	27.201	119.694	58.694	14.363	326.54565	0.70596			
12	29.015	118.660	57.660	15.966	362.97607	0.78472			
13	30.492	118.919	57.919	16.765	381.14990	0.82401			
14	32.004	118.100	57.100	18.167	413.02271	0.89291			
15	33.420	116.649	55.649	19.870	451.74854	0.97663			
16	35.651	118.639	57.639	20.466	465.28320	1.00589			

REYNOLDS NR = 213959.62500
 VELOCITY = 105.41451 FT/S
 FREQUENCY = 5.00 CPS
 FREQUENCY NR = 0.464×10^{-6}
 STROUHAL NR = 0.059
 AMPLITUDE NR = 0.180
 BLADES = 4.0 INCHES

TABLE II - CONTINUED

RUN NR	S	- 90 DEGREE MODEL, HIGH FLOW RATE							
STRIP	Q	T	DT	H	NUS	NUSREN			
1	54.762	119.255	58.255	38.164	867.65356	1.63062			
2	45.532	116.519	55.519	31.271	710.93018	1.33609			
3	38.969	117.457	56.457	24.369	554.01123	1.04118			
4	37.643	117.664	56.664	23.268	528.99219	0.99416			
5	32.215	115.348	54.348	20.074	456.36450	0.85767			
6	38.173	119.167	58.167	23.065	524.36499	0.98546			
7	35.081	108.744	47.744	27.889	634.04224	1.19159			
8	34.842	106.545	45.545	29.894	675.62573	1.27725			
9	19.108	110.152	49.152	12.186	277.03491	0.52065			
10	21.528	111.628	50.628	13.282	301.96558	0.56750			
11	26.789	113.093	52.093	16.779	381.45923	0.71690			
12	28.258	111.337	50.337	18.883	425.29468	0.80679			
13	29.510	113.046	52.046	18.779	426.93091	0.80235			
14	32.576	114.406	53.406	20.576	467.78149	0.87912			
15	33.308	113.183	52.183	21.779	495.12793	0.93052			
16	35.941	113.431	52.431	23.978	545.13086	1.02449			

REYNOLDS NR = 283129.50000
 VELOCITY = 139.49338 FT/S
 FREQUENCY = 22.00 CPS
 STROUHAL NR = 0.330
 AMPLITUDE NR = 0.115
 BLADES = 4.0 INCHES
 FREQUENCY NR = 1.166×10^{-6}

TABLE II - CONTINUED

RUN NR	10	-	90	DEGREE	MODEL,	LOW	FLOW	RATE		
STRIP	Q	T	DT	H	NUS	NUSREN				
1	52.894	130.538	65.538	30.529	689.26196	1.76795				
2	47.515	131.698	66.698	25.526	576.30981	1.47823				
3	38.655	130.369	65.369	19.829	447.69043	1.14832				
4	38.155	130.755	65.755	19.428	438.63794	1.12510				
5	32.577	129.784	64.784	16.130	364.18530	0.93413				
6	35.860	134.338	69.338	16.819	379.73877	0.97403				
7	29.093	129.235	64.235	14.532	328.09106	0.84155				
8	25.215	133.767	68.767	11.021	248.82037	0.63822				
9	15.420	133.912	68.912	5.620	126.89305	0.32548				
10	19.624	132.225	67.225	7.924	178.91470	0.45891				
11	25.768	131.406	66.406	11.526	260.23926	0.66751				
12	29.072	130.428	65.428	13.629	307.70605	0.78926				
13	30.167	130.382	65.382	14.129	318.99731	0.81823				
14	31.921	130.625	65.625	15.028	339.30396	0.87031				
15	34.438	131.739	66.739	16.026	361.81982	0.92806				
16	36.625	132.291	67.291	17.124	386.62524	0.99169				

REYNOLDS NR = 151994.75000
 VELOCITY = 76.52080 FT/S
 FREQUENCY = 22.00 CPS
 FREQUENCY NR = 3.962×10^{-6}
 STROUHAL NR = 0.602
 AMPLITUDE NR = 0.060
 BLADES = 4.0 INCHES

TABLE II - CONTINUED

RUN NR	11	- 90 DEGREE MODEL, LOW FLOW RATE						
STRIP	Q	T	DT	H	NUS	NUSREN		
1	53.470	123.059	61.059	34.453	781.92090	1.98948		
2	46.042	121.251	59.251	29.057	659.46460	1.67791		
3	39.424	120.777	58.777	23.659	536.93604	1.36615		
4	39.057	118.246	56.246	25.265	573.38354	1.45889		
5	34.449	117.847	55.847	21.566	489.43286	1.24529		
6	36.760	118.679	56.679	23.264	527.97046	1.34334		
7	29.437	117.755	55.755	17.966	407.73486	1.03742		
8	25.293	117.956	55.956	14.865	337.36963	0.85839		
9	15.528	117.935	55.935	8.065	183.04361	0.46573		
10	18.809	121.628	59.628	8.957	203.27144	0.51719		
11	24.182	123.333	61.333	11.653	264.45630	0.67287		
12	25.915	122.078	60.078	13.056	296.29736	0.75388		
13	27.420	122.267	60.267	13.855	314.44336	0.80005		
14	28.189	123.232	61.232	13.753	312.12183	0.79415		
15	31.039	122.712	60.712	15.854	359.80957	0.91548		
16	31.652	119.810	57.810	17.361	394.00830	1.00249		

REYNOLDS NR = 154470.75000
 VELOCITY = 76.52080 FT/S
 FREQUENCY = 50.00 CPS

FREQUENCY NR = 8.859 x 10⁻⁶

STROUHAL NR = 1.369
 AMPLITUDE NR = 0.150
 BLADES = 4.0 INCHES

TABLE II - CONTINUED

RUN NR	12	-	90	DEGREE	MODEL,	LOW	FLOW	RATE		
STRIP	Q	T	DT	H	NUS	NLSREN				
1	53.188	125.471	63.471	32.047	727.32202	1.85056				
2	46.647	124.221	62.221	27.450	622.99194	1.58511				
3	44.234	126.590	64.590	24.145	547.96948	1.39423				
4	39.688	126.059	64.059	20.646	468.56519	1.19219				
5	33.255	122.900	60.900	17.954	407.45898	1.03672				
6	32.644	121.614	59.614	18.357	416.60645	1.05999				
7	29.206	120.516	58.516	16.459	373.54468	0.95043				
8	24.382	120.749	58.749	13.159	298.63843	0.75984				
9	14.343	121.511	59.511	6.457	146.53973	0.37285				
10	18.846	120.515	58.515	9.259	210.13976	0.53467				
11	24.124	122.000	60.000	12.056	273.60645	0.69615				
12	25.559	121.985	59.989	13.156	298.57178	0.75967				
13	27.527	122.605	60.605	13.754	312.15552	0.79423				
14	28.411	122.131	60.131	14.355	325.79834	0.82895				
15	31.554	122.293	60.293	16.355	371.17993	0.94441				
16	31.576	120.282	58.282	17.360	393.98291	1.00243				

REYNOLDS NR = 154470.75000
 VELOCITY = 76.52080 FT/S
 FREQUENCY = 100.00 CPS
 FREQUENCY NR = 17.719×10^{-6}
 SIRCUAL NR = 2.737
 AMPLITUDE NR = 0.070
 BLADES = 4.0 INCHES

TABLE II - CONTINUED

RUN NR	13	- 90 DEGREE MODEL, LOW FLOW RATE							
STRIP	Q	T	DT	H	NUS	NUSREN			
1	36.717	123.421	55.421	22.539	506.25439	1.30890			
2	31.691	123.758	55.758	18.238	409.65259	1.05914			
3	26.731	121.538	53.938	15.143	340.12085	0.87937			
4	26.781	122.595	54.595	15.141	340.08545	0.87928			
5	22.514	121.831	53.831	12.643	283.97339	0.73420			
6	21.985	117.778	49.778	13.752	308.89697	0.79864			
7	21.617	118.684	50.684	13.350	299.86426	0.77529			
8	21.078	120.992	52.992	12.145	272.78160	0.70528			
9	12.154	120.380	52.380	5.946	133.56023	0.34532			
10	14.819	122.833	54.833	6.940	155.88998	0.40305			
11	20.581	120.048	52.048	11.747	263.85352	0.68218			
12	22.625	121.160	53.160	12.644	284.00928	0.73430			
13	22.876	119.323	51.323	13.449	302.07642	0.78101			
14	23.602	119.370	51.370	13.749	308.81226	0.75842			
15	26.787	119.244	51.244	16.349	367.21826	0.94943			
16	27.141	118.990	50.990	16.550	371.72412	0.96108			

REYNOLDS NR = 149596.87500
 VELOCITY = 76.52080 FT/S
 FREQUENCY = 5.00 CPS
 FREQUENCY NR = 0.914×10^{-6}
 STROUHAL NR = 0.137
 AMPLITUDE NR = 0.100
 BLADES = 4.0 INCHES

TABLE II - CONTINUED

RUN NR	15	- 90 DEGREE	MODEL, HIGH FLOW RATE						
STRIP	Q	T	DT	H	NUS	NUSREN			
1	53.216	118.990	52.990	42.554	959.11255	2.11912			
2	49.036	119.729	53.729	36.852	830.60254	1.83518			
3	40.504	117.661	51.661	29.757	670.63750	1.48185			
4	38.135	115.366	49.366	29.463	664.04736	1.46718			
5	37.343	118.006	52.006	26.556	598.54541	1.32246			
6	39.197	119.932	53.932	27.152	611.96582	1.35211			
7	38.378	118.968	52.968	27.254	614.27100	1.35720			
8	36.227	121.314	55.314	23.748	535.26001	1.18263			
9	18.111	120.515	54.515	9.850	222.01488	0.49053			
10	24.417	123.786	57.786	12.943	291.70898	0.64452			
11	25.031	119.022	53.022	15.154	341.54980	0.75464			
12	28.525	119.942	53.942	17.352	391.08594	0.86409			
13	27.514	118.729	52.729	16.955	382.13477	0.84431			
14	29.330	118.244	52.244	18.556	418.22266	0.92404			
15	32.701	119.490	53.490	20.553	463.23389	1.02349			
16	33.256	118.180	52.180	21.656	488.09644	1.07843			

REYNOLDS NR = 204846.93750
 VELOCITY = .
 FREQUENCY = 103.67995
 STROUFAL NR = 2.020
 AMPLITUDE NR = 0.052
 BLADES = 4.0 INCHES

FREQUENCY NR = 9.861 x 10⁻⁶
 FT/S
 CPS

TABLE II - CONTINUED

RUN NR	16	-	90	DEGREE	MODEL,	LOW	FLOW	RATE		
STRIP	Q	T	DT	H	NUS	NUSREN				
1	48.339	125.107	57.107	33.035	742.00757	1.91843				
2	41.523	124.832	56.832	27.236	611.74658	1.58165				
3	36.014	125.275	57.275	21.835	490.43164	1.26799				
4	37.540	125.312	57.312	23.734	533.10596	1.37833				
5	33.400	123.582	55.582	21.039	472.55396	1.22177				
6	36.546	123.154	55.154	24.640	553.43774	1.43089				
7	34.017	124.330	56.330	21.537	483.74414	1.25070				
8	26.409	124.744	56.744	15.636	351.20044	0.90802				
9	14.075	123.925	55.929	7.438	167.06168	0.43193				
10	18.324	124.967	56.967	9.635	216.42055	0.55955				
11	22.762	123.844	55.844	12.838	288.35718	0.74554				
12	25.866	124.809	56.809	14.536	326.48950	0.84413				
13	24.823	123.401	55.401	14.039	315.33472	0.81529				
14	27.058	124.410	56.410	15.137	339.98779	0.87903				
15	30.506	125.210	57.210	17.135	384.86694	0.99506				
16	32.545	124.943	56.943	18.735	420.81958	1.08801				

REYNOLDS NR = 149596.87500
 VELOCITY = 76.52080 FT/S
 FREQUENCY = 126.00 CPS
 FREQUENCY NR = 23.053 x 10⁻⁶
 STROUHAL NR = 3.449
 AMPLITUDE NR = 0.340
 BLADES = 4.0 INCHES

TABLE II - CONTINUED

KUN NR	17	- 90 DEGREE MODEL, HIGH FLOW RATE						
STRIP	Q	T	DT	H	NUS	NUSREN		
1	53.008	118.118	51.118	44.854	1009.20923	2.09182		
2	45.415	117.938	50.938	35.754	804.46899	1.66745		
3	39.591	117.106	50.106	30.156	678.51367	1.40638		
4	42.265	115.656	48.656	34.860	784.34009	1.62573		
5	36.626	113.620	46.620	30.564	687.69751	1.42541		
6	41.494	115.124	48.124	34.961	786.61792	1.63045		
7	39.816	113.275	46.275	35.165	791.21558	1.63998		
8	33.972	115.038	48.038	26.861	604.37280	1.25270		
9	18.455	115.204	48.204	12.261	275.86499	0.57179		
10	20.553	115.123	48.123	14.161	318.61938	0.66041		
11	24.926	110.936	43.936	20.071	451.58862	0.93602		
12	27.555	117.911	50.911	18.454	415.22095	0.86064		
13	21.089	115.620	48.620	18.760	422.09253	0.87489		
14	29.578	117.602	50.602	19.755	444.48730	0.92130		
15	32.705	117.891	50.891	22.254	500.72192	1.03786		
16	33.430	116.036	49.036	24.159	543.57056	1.12668		

REYNOLDS NR = 232762.25000
 VELOCITY = 118.43491
 FREQUENCY = 128.00

FT/S
 CPS

STROUHAL NR = 2.264
 AMPLITUDE NR = 0.690
 BLADES = 4.0 INCHES

FREQUENCY NR = 9.725×10^{-6}

TABLE II - CONTINUED

RUN NR	18	-	90	DEGREE	MODEL,	HIGH	FLOW	RATE		
SIRIP	Q	T	DT	H	NUS	NUSREN				
1	64.125	134.826	71.826	35.223	757.99707	1.73000				
2	53.009	131.741	68.741	28.530	646.37329	1.40129				
3	45.824	130.359	67.359	24.033	544.49805	1.18043				
4	44.283	129.869	66.869	23.335	528.66602	1.14611				
5	38.564	126.421	63.421	21.043	476.74585	1.03355				
6	35.662	127.768	64.768	18.540	420.03247	0.91060				
7	36.076	129.176	66.176	18.436	417.68994	0.90552				
8	39.061	128.324	65.324	21.038	476.64185	1.03333				
9	22.845	128.577	65.577	10.438	236.47633	0.51266				
10	22.625	129.167	66.167	9.936	225.11609	0.48804				
11	30.024	127.336	64.336	14.841	336.22974	0.72892				
12	33.171	128.743	65.743	16.137	365.60547	0.79261				
13	34.422	130.605	67.605	16.033	363.23755	0.78747				
14	36.481	129.958	66.958	17.534	397.25708	0.86123				
15	42.840	131.522	68.522	21.031	476.46655	1.03295				
16	41.763	127.899	64.899	21.839	494.79004	1.07267				

REYNOLDS NR = 212769.18750
 VELOCITY = 105.97266
 FREQUENCY = 12.00

FI/S
 CPS

STROUHAL NR = 0.237
 AMPLITUDE NR = 0.150
 BLADES = 4.0 INCHES

FREQUENCY NR = 1.115×10^{-6}

TABLE II - CONTINUED

RUN NR	19	- 90 DEGREE MODEL, LOW FLOW RATE							
STRIP	Q	T	DT	H	NUS	NUSREN			
1	62.428	133.275	69.275	36.024	814.74561	2.08422			
2	52.548	133.663	69.663	27.823	629.26733	1.60975			
3	44.757	133.117	69.117	22.524	509.42920	1.30318			
4	43.676	135.805	71.805	20.718	468.57007	1.19866			
5	40.564	138.531	74.531	18.111	409.61499	1.04785			
6	35.507	135.090	71.090	16.420	371.35791	0.94998			
7	34.823	135.931	71.931	15.718	355.47974	0.90936			
8	28.009	136.879	72.879	11.715	264.96045	0.67780			
9	18.836	137.904	73.904	6.813	154.08162	0.39416			
10	22.129	133.294	69.294	9.224	208.61774	0.53367			
11	29.402	131.935	67.935	13.527	305.94434	0.78264			
12	32.685	132.422	68.422	15.226	344.36572	0.88093			
13	34.035	134.117	70.117	15.222	344.27197	0.88069			
14	36.228	137.710	73.710	15.113	341.81079	0.87440			
15	42.048	134.584	70.584	19.721	446.02100	1.14098			
16	41.783	134.357	70.357	19.421	439.24634	1.12365			

REYNOLDS NR = 152811.25000
 VELOCITY = 76.52080 FT/S
 FREQUENCY = 12.00 CPS

STRUCTURAL NR = 0.328
 AMPLITUDE NR = 0.110
 BLADES = 4.0 INCHES

FREQUENCY NR = 2.149×10^{-6}

TABLE II - CONTINUED

RUN NR	20	- 90 DEGREE MODEL, HIGH FLOW RATE							
STRIP	Q	T	DT	H	NUS	NLSREN			
1	62.295	114.462	50.462	58.969	1333.68311	2.57026			
2	53.776	111.880	47.880	50.775	1148.36255	2.21312			
3	45.254	110.958	46.958	40.177	908.67505	1.75119			
4	45.207	110.452	46.452	40.978	926.79443	1.78611			
5	42.145	112.768	48.768	34.273	775.14111	1.49385			
6	41.376	110.539	46.539	36.078	815.96826	1.57253			
7	48.226	107.283	43.283	51.086	1155.38818	2.22666			
8	38.561	109.183	45.183	34.281	775.32886	1.49421			
9	20.187	110.287	46.287	13.779	311.62964	0.60057			
10	21.836	111.368	47.368	14.576	329.66650	0.63533			
11	28.101	115.709	51.709	17.766	401.81055	0.77437			
12	30.193	114.392	50.392	20.269	458.42188	0.88347			
13	32.001	115.053	51.053	21.368	483.26563	0.93135			
14	23.236	115.536	51.536	22.067	499.07178	0.96181			
15	36.871	116.560	52.560	24.764	560.08252	1.07939			
16	37.885	115.215	51.215	26.667	603.12549	1.16234			

REYNOLDS NR = 269246.25000
 VELOCITY = 134.82610 FT/S
 FREQUENCY = 50.00 CPS
 FREQUENCY NR = 2.885×10^{-6}
 STROUHAL NR = 0.777
 AMPLITUDE NR = 0.310
 BLADES = 4.0 INCHES

TABLE II - CONTINUED

RUN NR	21	- 45 DEGREE MODEL, LOW FLOW RATE							
STRIP	Q	T	DT	H	NUS	NUSREN			
1	63.046	139.042	78.542	30.518	694.41479	1.75962			
2	51.172	135.301	74.801	24.627	560.37280	1.41997			
3	47.167	137.914	77.414	21.021	478.31104	1.21202			
4	47.427	136.059	75.559	22.225	505.71948	1.28148			
5	48.460	138.634	78.134	21.919	498.74951	1.26381			
6	45.870	137.673	77.173	21.021	478.32446	1.21206			
7	38.659	141.333	80.833	15.812	359.79614	0.91171			
8	29.948	146.849	86.349	10.398	236.60916	0.59956			
9	18.081	142.902	82.402	6.008	136.71429	0.34643			
10	21.937	141.173	80.673	7.713	175.49452	0.44470			
11	26.416	139.681	79.181	9.816	223.36282	0.56599			
12	30.429	141.557	81.097	11.111	252.83563	0.64068			
13	31.504	142.406	81.906	11.209	255.06540	0.64633			
14	32.539	141.749	81.249	11.611	264.20410	0.66948			
15	36.317	141.948	81.448	13.311	302.87549	0.76748			
16	39.853	140.900	80.400	15.313	348.44336	0.88294			

REYNOLDS NR = 155739.25000
 VELOCITY = 76.52080
 FREQUENCY = 22.00

STROUHAL NR = 0.852
 AMPLITUDE NR = 0.040
 BLADES = 4.0 INCHES

FREQUENCY NR = 3.866×10^{-6}

TABLE II - CONTINUED

RUN NR	22	- 45	DEGREE	MODEL,	HIGH FLOW	RATE			
STRIP	Q	T	DT	H	NUS	NUSREN			
1	62.531	126.574	64.574	40.445	917.90137	1.82042			
2	51.782	121.344	59.344	34.957	793.36084	1.57343			
3	47.407	122.436	60.436	29.955	679.82617	1.34826			
4	47.572	120.644	58.644	32.059	727.58276	1.44297			
5	48.785	122.577	60.977	31.153	707.03149	1.40222			
6	49.036	123.349	61.349	31.152	707.01147	1.40218			
7	38.828	122.351	60.351	23.355	530.04297	1.05120			
8	28.071	123.380	61.380	14.952	339.34790	0.67301			
9	18.218	119.270	57.270	9.762	221.55412	0.43940			
10	22.545	118.982	56.982	12.663	287.38550	0.56996			
11	26.535	120.887	58.887	14.558	330.40405	0.65527			
12	28.875	121.305	59.305	15.857	359.88550	0.71374			
13	29.715	122.003	60.003	16.056	364.38672	0.72267			
14	30.508	121.097	59.097	17.158	389.40039	0.77228			
15	34.197	122.826	60.826	18.654	423.35010	0.83961			
16	38.356	125.570	63.570	20.347	461.78320	0.91583			

REYNOLDS NR = 254242.06250
 VELOCITY = 125.94490
 FREQUENCY = 22.00

FT/S
 CPS

SURCUHAL NR = 0.517
 AMPLITUDE NR = 0.055
 BLADES = 4.0 INCHES

FREQUENCY NR = 1.439×10^{-6}

TABLE II - CONTINUED

RUN NR	23	- 45 DEGREE	MODEL, LOW FLOW RATE						
STRIP	Q	I	DT	H	NUS	NUSREN			
1	59.829	134.643	73.143	31.526	716.11792	1.81958			
2	52.025	136.306	74.806	25.022	568.37842	1.44419			
3	48.647	138.303	76.803	21.717	493.30762	1.25344			
4	45.497	139.328	77.828	19.915	452.36328	1.14941			
5	44.212	140.647	79.147	18.812	427.30298	1.08573			
6	45.389	139.145	77.645	20.315	461.45996	1.17252			
7	39.327	139.181	77.681	17.015	386.49854	0.98205			
8	28.546	140.104	78.604	11.213	254.70082	0.64717			
9	16.944	142.319	80.819	5.507	125.10112	0.31787			
10	22.776	141.357	79.897	8.010	181.94038	0.46229			
11	26.724	136.457	74.557	10.722	243.54755	0.61883			
12	29.477	136.370	74.870	12.022	273.08179	0.69387			
13	30.534	137.165	75.665	12.120	275.30884	0.69953			
14	31.090	137.053	75.553	12.220	277.58643	0.70532			
15	34.183	135.961	74.461	14.023	318.53418	0.80936			
16	36.568	135.791	74.291	15.424	350.34424	0.89019			

REYNOLDS NR = 154891.31250
 VELOCITY = 76.52080 FT/S
 FREQUENCY = 100.00 CPS

STRUHAL NR = 3.871
 AMPLITUDE NR = 0.045
 BLADES = 4.0 INCHES

FREQUENCY NR = 17.671×10^{-6}

TABLE II - CONTINUED

RUN NR	24	- 45	DEGREE	MODEL,	HIGH	FLOW	RATE	
STRIP	G	T	DT	H	NUS	NUSREN		
1	57.502	122.115	61.115	38.958	885.68726	1.90053		
2	50.771	122.580	61.580	32.257	733.34033	1.57362		
3	46.634	124.507	63.507	27.352	621.83643	1.33435		
4	44.107	121.580	60.580	27.459	624.26782	1.33957		
5	43.052	124.349	63.349	24.952	567.28174	1.21729		
6	43.405	121.048	60.048	27.560	626.56982	1.34451		
7	37.688	119.837	58.837	23.763	540.24341	1.15927		
8	27.130	126.565	65.565	13.447	305.71338	0.65601		
9	16.039	126.085	65.089	7.148	162.51114	0.34872		
10	21.492	123.060	62.060	10.855	246.79349	0.52958		
11	25.492	125.334	64.334	12.450	283.04565	0.60737		
12	28.030	124.686	63.686	14.052	319.45630	0.68550		
13	28.568	125.593	64.593	14.049	319.40698	0.68539		
14	29.874	125.035	64.035	14.651	333.07813	0.71473		
15	32.761	123.858	62.858	16.953	385.43091	0.82707		
16	35.383	124.305	63.305	18.352	417.23560	0.89532		

REYNOLDS NR = 217174.81250
 VELOCITY = 106.99857 FT/S
 FREQUENCY = 100.00 CPS

STRUTURAL NR = 2.768
 AMPLITUDE NR = 0.049
 BLADES = 4.0 INCHES

FREQUENCY NR = 9.013×10^{-6}

TABLE II - CONTINUED

KUN NR	25	- 45	DEGREE	MODEL,	LOW	FLOW	RATE	
STRIP	Q	T	DT	H	NUS	NLSREN		
1	54.111	127.254	67.254	30.748	700.25244	1.77199		
2	46.887	127.089	67.089	25.348	577.28052	1.46081		
3	40.105	127.166	67.166	20.448	465.68237	1.17841		
4	39.240	126.657	66.657	20.349	463.43286	1.17271		
5	37.625	125.207	65.207	20.052	456.67944	1.15563		
6	39.012	128.342	68.342	19.845	451.95361	1.14367		
7	33.222	126.255	66.255	17.050	388.29980	0.98259		
8	22.525	128.741	68.741	10.144	231.02235	0.58460		
9	13.636	129.953	69.953	5.241	119.36212	0.30205		
10	19.537	129.695	69.695	8.042	183.14417	0.46345		
11	23.724	128.716	68.716	10.344	235.57857	0.59613		
12	25.046	128.031	68.031	11.046	251.55800	0.63657		
13	25.623	127.574	67.574	11.247	256.13770	0.64816		
14	26.943	127.708	67.708	11.747	267.51758	0.67695		
15	29.707	128.005	68.005	13.146	299.38525	0.75759		
16	36.558	132.764	72.764	15.534	353.78149	0.89524		

REYNOLDS NR = 156166.75000
 VELOCITY = 76.52080
 FREQUENCY = 5.00

STROUHAL NR = 0.194
 AMPLITUDE NR = 0.100
 BLADES = 4.0 INCHES

FREQUENCY NR = 0.876×10^{-6}

TABLE II - CONTINUED

RUN NR	26	- 45	DEGREE	MODEL,	HIGH FLOW RATE			
STRIP	Q	T	DT	H	NUS	NUSREN		
1	58.197	121.188	61.688	38.763	883.56885	1.87755		
2	52.020	121.207	61.707	32.963	751.36230	1.59662		
3	45.420	119.832	60.332	28.166	642.02490	1.36428		
4	46.241	121.614	62.114	27.862	635.09058	1.34954		
5	42.227	120.999	61.499	25.064	571.30054	1.21399		
6	45.969	122.540	63.040	27.360	623.64380	1.32522		
7	37.259	119.776	60.276	22.166	505.26367	1.07367		
8	25.376	117.870	58.370	14.371	327.57178	0.69608		
9	15.154	119.235	59.735	7.368	167.94046	0.35687		
10	21.229	120.347	60.847	10.565	240.82187	0.51174		
11	25.502	120.727	61.227	13.264	302.34521	0.64247		
12	26.919	118.873	59.373	14.469	329.79761	0.70081		
13	27.168	119.016	59.516	14.368	327.51050	0.69595		
14	28.264	119.206	59.706	14.868	338.89746	0.72014		
15	30.244	120.410	60.910	15.565	354.78857	0.75391		
16	34.921	123.605	64.105	17.357	395.64551	0.84073		

REYNOLDS NR = 221461.06250
 VELOCITY = 108.21678
 FREQUENCY = 5.00

FREQUENCY NR = 0.436×10^{-6}

STROUHAL NR = 0.137
 AMPLITUDE NR = 0.120
 BLADES = 4.0 INCHES

TABLE 11 - CONTINUED

RUN NR	27	- 45 DEGREE MODEL, HIGH FLOW RATE							
STRIP	Q	T	DT	H	NUS	NUSREN			
1	61.017	117.604	58.604	44.973	1026.00317	1.83081			
2	53.532	117.350	58.350	37.573	857.19360	1.52959			
3	45.804	113.355	54.355	33.083	754.74268	1.34677			
4	46.281	113.450	54.450	33.682	768.42651	1.37119			
5	42.713	111.502	52.502	31.887	727.46387	1.29810			
6	46.186	109.448	50.448	38.092	869.01807	1.55069			
7	38.250	114.590	55.590	25.480	581.29126	1.03726			
8	21.021	115.666	56.666	11.377	259.55811	0.46316			
9	16.721	106.523	47.523	11.498	262.31982	0.46809			
10	23.233	107.907	48.907	16.095	367.19189	0.65522			
11	25.591	110.279	51.279	16.690	380.75610	0.67943			
12	26.582	109.352	50.352	18.192	415.02563	0.74058			
13	27.402	109.410	50.410	18.292	417.30371	0.74464			
14	28.153	109.746	50.746	18.591	424.13062	0.75682			
15	30.255	110.445	51.445	19.989	456.03296	0.81375			
16	35.279	112.844	53.844	22.784	519.78613	0.92751			

REYNOLDS NR = 314057.68750
 VELOCITY = 153.04166 FT/S
 FREQUENCY = 0.0 CPS
 STROUHAL NR = 0.0
 AMPLITUDE NR = 0.0
 BLADES = 4.0 INCHES

FREQUENCY NR = 0.0

TABLE II - CONTINUED

RUN NR	28	45	DEGREE	MODEL, LOW FLOW RATE					
STRIP	Q	T	DT	H	NUS	NUSREN			
1	50.029	129.213	66.713	27.837	631.22534	1.60824			
2	43.815	129.326	66.826	23.237	526.91162	1.34247			
3	38.676	128.543	66.043	20.039	454.39307	1.15770			
4	39.787	131.340	68.840	19.732	447.43677	1.13998			
5	38.319	130.647	68.147	19.234	436.13721	1.11119			
6	38.866	132.656	70.156	18.929	429.22388	1.09358			
7	34.474	131.881	69.381	16.631	377.11304	0.96081			
8	21.557	128.136	65.636	10.340	234.46313	0.59737			
9	16.494	131.959	69.459	6.731	152.62151	0.38885			
10	20.749	135.268	72.768	8.023	181.91660	0.46349			
11	23.513	133.226	70.726	9.928	225.11319	0.57354			
12	25.576	131.934	69.434	10.931	247.86005	0.63150			
13	26.645	132.309	69.809	11.230	254.64203	0.64878			
14	27.990	132.358	69.858	11.730	265.97705	0.67766			
15	30.081	131.490	68.990	13.032	295.50293	0.75288			
16	32.543	131.805	69.305	14.531	329.49878	0.83950			

REYNOLDS NR = 154052.50000

VELOCITY = 76.52080 FT/S

FREQUENCY = 50.00 CPS

STROUHAL NR = 1.935
AMPLITUDE NR = 0.110
BLADES = 4.0 INCHESFREQUENCY NR = 8.883 x 10⁻⁶

TABLE II - CONTINUED

RUN NR	29	- 45	DEGREE	MODEL,	HIGH	FLOW	RATE		
STRIP	Q	T	DT	H	NUS	NUSREN			
1	48.510	108.902	46.152	46.285	1049.07324	1.98242			
2	43.279	108.663	45.913	39.385	892.69263	1.68691			
3	37.563	110.810	48.060	30.580	693.12231	1.30978			
4	39.053	109.845	47.099	32.982	747.57007	1.41267			
5	38.053	107.169	44.419	34.989	793.04126	1.49860			
6	40.884	106.877	44.127	39.289	890.51880	1.68280			
7	34.252	110.035	47.285	27.882	631.96558	1.19422			
8	21.223	114.472	51.722	13.372	303.08008	0.57273			
9	16.159	113.423	50.673	9.974	226.07230	0.42721			
10	20.393	112.639	49.889	13.276	300.91040	0.56863			
11	23.579	113.288	50.538	15.375	348.47388	0.65851			
12	25.451	114.098	51.348	16.373	371.09692	0.70126			
13	26.258	114.962	52.212	16.371	371.05127	0.70117			
14	27.705	115.328	52.578	17.270	391.43091	0.73968			
15	29.961	115.209	52.459	19.070	432.23535	0.81679			
16	32.552	116.476	53.726	20.367	461.63379	0.87234			

REYNOLDS NR = 280040.25000
 VELOCITY = 139.28961
 FREQUENCY = 50.00

STROUHAL NR = 1.063
 AMPLITUDE NR = 0.220
 BLADES = 4.0 INCHES

FREQUENCY NR = 2.685 x 10⁻⁶

TABLE II - CONTINUED

RUN NR	30	- 45	DEGREE	MODEL,	HIGH	FLOW	RATE			
STRIP	Q	T	DT	H	NUS	NLSREN				
1	50.675	112.964	54.214	38.484	878.35425	1.72300				
2	44.560	113.826	55.076	31.582	720.82373	1.41399				
3	38.556	112.817	54.067	26.634	605.04004	1.19471				
4	39.255	111.153	52.403	28.488	650.21069	1.27547				
5	39.177	109.537	50.787	29.992	684.53101	1.34279				
6	41.253	107.400	48.650	34.597	789.63306	1.54896				
7	34.854	111.567	52.817	24.487	558.89307	1.09634				
8	21.763	111.960	53.210	13.586	310.09229	0.60829				
9	16.512	111.155	52.445	9.988	227.96663	0.44719				
10	21.013	112.574	53.824	12.485	284.95361	0.55897				
11	24.021	113.726	54.976	14.082	321.41113	0.63049				
12	25.530	114.987	56.237	14.779	337.32104	0.66170				
13	27.048	114.789	56.039	15.480	353.30811	0.65306				
14	28.516	115.065	56.319	16.279	371.55200	0.72885				
15	30.689	114.740	55.990	17.980	410.37012	0.80499				
16	33.267	115.004	56.254	19.779	451.43921	0.88556				

REYNOLDS NR = 259876.68750
 VELOCITY = 126.46426
 FREQUENCY = 126.00

STRUCTURAL NR = 2.951
 AMPLITUDE NR = 0.095
 BLADES = 4.0 INCHES

FREQUENCY NR = 8.030×10^{-6}

TABLE II - CONTINUED

RUN NR	31	-	45	DEGREE	MODEL,	LOW	FLOW	RATE	
STRIP	Q	T	DT	H	NUS	NUSREN			
1	48.558	127.711	66.711	26.544	603.47437	1.53127			
2	42.385	123.425	62.425	24.455	555.96436	1.41072			
3	37.004	127.554	66.554	18.545	421.60571	1.06980			
4	38.171	130.399	69.399	18.338	416.90308	1.05786			
5	37.052	130.849	69.849	17.637	400.96411	1.01742			
6	39.788	128.454	67.454	20.643	469.29956	1.19082			
7	33.655	127.422	66.422	17.145	389.78467	0.98905			
8	20.488	124.288	63.288	10.252	233.08624	0.59144			
9	14.687	132.157	71.157	5.434	123.52975	0.31345			
10	18.591	131.580	70.580	7.435	169.03079	0.42890			
11	22.106	128.252	67.252	9.643	219.22972	0.55628			
12	24.552	128.646	67.646	10.742	244.21631	0.61968			
13	25.702	129.301	68.301	10.940	248.72733	0.63113			
14	26.661	129.408	68.408	11.240	255.54139	0.64842			
15	29.125	127.674	66.674	13.044	296.55908	0.75250			
16	31.208	127.733	66.733	14.144	321.56372	0.81595			

TABLE II - CONTINUED

RUN NR	32	- 45 DEGREE	MODEL, HIGH FLOW RATE						
STRIP	Q	T	DT	H	NUS	NUSREN			
1	46.855	114.558	52.958	35.172	798.24097	1.77058			
2	41.337	111.126	49.126	32.581	748.51318	1.66028			
3	36.474	111.933	49.933	27.079	614.56958	1.36318			
4	36.758	112.408	50.408	27.178	616.81421	1.36815			
5	36.374	114.489	52.489	25.373	575.85303	1.27730			
6	38.544	115.163	53.163	27.172	616.66870	1.36783			
7	32.856	113.347	51.347	23.176	525.98339	1.16668			
8	19.518	111.045	49.045	13.281	301.42285	0.66859			
9	14.027	114.358	52.358	7.774	176.42496	0.39133			
10	18.301	115.282	53.282	10.272	233.11400	0.51707			
11	21.350	113.029	51.029	13.177	295.04907	0.66332			
12	23.770	114.782	52.782	14.173	321.65161	0.71346			
13	24.755	116.155	54.195	14.069	319.30713	0.70825			
14	25.846	115.671	53.671	14.971	339.76074	0.75362			
15	28.570	117.568	55.568	16.366	371.43286	0.82387			
16	30.760	117.880	55.880	17.465	356.38086	0.87921			

KEYNOLUS NR = 203253.43750
 VELOCITY = 100.68649 FT/S
 FREQUENCY = 10.00 CPS

STRUCTURAL NR = 0.294
 AMPLITUDE NR = 0.115
 BLADES = 4.0 INCHES

FREQUENCY NR = 1.023×10^{-6}

TABLE II - CONTINUED

RUN NR	33	- 45	DEGREE	MODEL,	LOW	FLOW	RATE	
STRIP	Q	T	DT	H	NUS	NUSREN		
1	48.552	120.021	59.521	31.864	725.03931	1.83722		
2	43.392	121.658	61.158	25.860	588.42480	1.49105		
3	38.110	121.967	61.467	21.659	492.83960	1.24884		
4	38.483	123.648	63.148	21.255	483.64673	1.22554		
5	37.857	123.945	63.445	20.854	474.52905	1.20244		
6	40.144	124.071	63.571	22.754	517.75586	1.31198		
7	34.714	125.694	65.194	18.250	415.27271	1.05229		
8	21.393	124.987	64.487	10.252	233.27626	0.59111		
9	15.060	128.257	67.757	6.044	137.52956	0.34850		
10	19.360	126.757	66.257	8.448	192.22200	0.48708		
11	23.252	125.561	65.061	10.751	244.62231	0.61986		
12	25.217	126.003	65.503	11.549	262.80176	0.66593		
13	26.362	126.355	65.855	11.949	271.88428	0.68895		
14	27.246	126.460	65.960	12.248	278.70483	0.70623		
15	29.870	125.742	65.242	13.850	315.15112	0.75858		
16	31.800	124.148	63.648	15.554	353.91992	0.89682		

REYNOLDS NR = 155739.25000
 VELOCITY = 76.52080 FT/S
 FREQUENCY = 10.00 CPS

STROUHAL NR = 0.387
 AMPLITUDE NR = 0.090
 BLADES = 4.0 INCHES

FREQUENCY NR = 1.757×10^{-6}

TABLE II - CONTINUED

RUN NR	34	-	45	DEGREE	MODEL,	LOW	FLOW	RATE	
STRIP	Q	T	DT	H	NUS	NUSREN			
1	50.846	130.074	69.074	26.839	610.16504	1.54825			
2	44.056	125.701	64.701	24.349	553.56763	1.40464			
3	38.662	125.255	64.255	20.750	471.74707	1.19703			
4	38.561	125.810	64.810	20.949	476.26367	1.20849			
5	38.517	128.379	67.379	19.843	451.11572	1.14468			
6	41.339	128.322	67.322	21.843	496.58813	1.26006			
7	35.021	132.526	71.526	16.133	366.76953	0.93065			
8	21.651	129.532	68.532	9.540	216.88617	0.55033			
9	15.485	133.751	72.751	5.530	125.71498	0.31899			
10	19.575	129.070	68.070	8.541	194.17686	0.49271			
11	23.587	127.480	66.480	10.745	244.28004	0.61984			
12	25.732	127.658	66.658	11.644	264.73145	0.67174			
13	26.997	128.369	67.369	12.043	273.78638	0.69471			
14	27.537	127.490	66.490	12.645	287.47510	0.72945			
15	30.550	126.010	65.010	14.548	330.75171	0.83926			
16	33.058	126.797	65.797	15.646	355.71680	0.90261			

REYNOLDS NR =	155314.12500	STROUHAL NR =	0.0
VELOCITY =	76.52080	AMPLITUDE NR =	0.0
FREQUENCY =	0.0	BLADES =	4.0
			INCHES

FREQUENCY NR = 0.0

TABLE II - CONTINUED

RUN NR	35	- 45 DEGREE	MODEL, LOW FLOW RATE						
STRIP	Q	T	DT	H	NUS	NUSREN			
1	51.573	138.359	77.109	23.318	525.89136	1.59122			
2	46.857	142.851	81.601	18.807	427.37720	1.28338			
3	40.652	140.902	79.652	16.212	368.40259	1.10628			
4	41.126	140.731	79.481	16.712	379.77466	1.14043			
5	40.504	141.464	80.214	16.310	370.64355	1.11301			
6	39.289	142.244	80.994	15.608	354.69238	1.06511			
7	34.482	142.370	81.120	13.308	302.41846	0.90814			
8	22.621	137.327	76.077	8.820	200.44046	0.60191			
9	17.176	137.771	76.521	6.119	139.05881	0.41758			
10	21.075	139.958	78.708	7.314	166.20593	0.49910			
11	24.721	141.982	80.732	8.409	191.08907	0.57383			
12	26.561	142.305	81.055	9.208	209.25060	0.62836			
13	27.533	141.528	80.678	9.509	216.08937	0.64890			
14	29.528	142.492	81.242	9.908	225.14740	0.67610			
15	31.707	140.018	78.768	11.414	259.37378	0.77888			
16	34.514	139.171	77.921	12.916	293.50854	0.88138			

REYNOLDS NR = 110894.53750
 VELOCITY = 54.71074
 FREQUENCY = 10.00

STROKAL NR = 0.541
 AMPLITUDE NR = 0.440
 BLADES = 6.0 INCHES

FREQUENCY NR = 3.452×10^{-6}

TABLE II - CONTINUED

RUN NR	36	-	45	DEGREE	MODEL,	LOW	FLOW	RATE		
STRIP	Q	T	DT	H	NUS	NUSREN				
1	52.266	130.572	68.572	28.235	640.80176	1.65571				
2	46.181	133.065	71.065	22.529	511.30176	1.32111				
3	40.108	133.317	71.317	18.528	420.50732	1.08651				
4	40.587	132.334	70.334	19.731	447.79541	1.15702				
5	40.199	132.574	70.574	19.330	438.70435	1.13353				
6	39.733	129.251	67.251	20.638	468.39111	1.21023				
7	33.205	131.138	69.138	15.834	359.35059	0.92849				
8	22.290	129.079	67.079	10.239	232.37079	0.60040				
9	17.073	129.573	67.573	7.238	164.25810	0.42441				
10	20.904	132.966	70.966	8.329	189.03600	0.48843				
11	24.358	133.490	71.490	9.828	223.04982	0.57632				
12	26.390	134.059	72.059	10.527	238.90497	0.61728				
13	27.671	134.708	72.708	10.825	245.67758	0.63478				
14	29.219	134.457	72.457	11.526	261.57788	0.67587				
15	31.334	133.260	71.260	12.929	293.41748	0.75813				
16	34.035	132.914	70.914	14.429	327.47949	0.84614				

REYNOLDS NR = 149788.75000
 VELOCITY = 74.20145
 FREQUENCY = 20.00
 STROUFAL NR = 0.798
 AMPLITUDE NR = 0.240
 BLADES = 6.0 INCHES

FREQUENCY NR = 3.769×10^{-6}

TABLE II - CONTINUED

RUN NR	37	- 45 DEGREE MODEL, LOW FLOW RATE							
STRIP	Q	T	DT	H	NUS	NLSREN			
1	53.016	141.743	81.243	22.711	516.77808	1.57643			
2	46.527	146.291	85.791	17.500	358.19727	1.21470			
3	40.594	147.958	87.458	14.196	323.01245	0.98535			
4	40.845	148.226	87.726	14.495	329.82349	1.00613			
5	40.805	150.429	89.929	14.089	320.59497	0.97798			
6	40.524	150.572	90.072	14.089	320.58667	0.97795			
7	34.506	148.069	87.569	12.095	275.22192	0.83957			
8	25.211	147.398	86.898	8.397	191.06900	0.58286			
9	23.574	150.672	90.172	7.189	163.57559	0.49899			
10	24.934	147.960	87.460	7.996	181.93509	0.55499			
11	25.849	145.277	84.777	8.602	195.74097	0.59711			
12	28.249	145.833	85.333	9.301	211.63737	0.64560			
13	27.901	145.092	84.592	9.103	207.12868	0.63185			
14	29.447	146.626	86.126	9.199	209.31665	0.63852			
15	31.943	146.089	85.589	10.300	234.37718	0.71497			
16	37.590	147.118	86.618	12.498	284.37793	0.86750			

REYNOLDS NR = 107462.31250
 VELOCITY = 52.80045 FT/S
 FREQUENCY = 5.00 CPS
 STROUHAL NR = 0.280
 AMPLITUDE NR = 0.650
 BLADES = 6.0 INCHES

FREQUENCY NR = 1.846×10^{-6}

TABLE II - CONTINUED

KUN NR	38	- 45 DEGREE MODEL, LOW FLOW RATE							
STRIP	Q	T	DT	H	NUS	NUSREN			
1	32.442	125.150	67.150	15.257	348.68091	1.05635			
2	30.469	131.713	73.713	12.241	279.76001	0.84755			
3	28.814	132.420	74.420	11.340	259.15259	0.78512			
4	31.075	130.363	72.363	13.445	307.25903	0.93086			
5	33.473	131.416	73.416	14.642	334.62549	1.01377			
6	34.772	130.197	72.197	16.045	366.68799	1.11090			
7	29.875	129.655	71.655	13.646	311.86865	0.94482			
8	23.294	129.096	71.096	10.448	238.76730	0.72336			
9	19.118	132.511	74.511	7.539	172.30309	0.52200			
10	19.457	134.086	76.086	7.236	165.35962	0.50097			
11	20.444	131.543	73.543	7.942	181.49808	0.54986			
12	22.404	130.783	72.783	8.944	204.39380	0.61922			
13	23.269	131.118	73.118	9.043	206.66077	0.62609			
14	24.081	130.806	72.806	9.243	211.24872	0.63959			
15	26.719	130.908	72.908	10.343	236.38231	0.71613			
16	31.352	132.146	74.146	12.340	282.02148	0.85440			

REYNOLDS NR = 108953.50000
 VELOCITY = 52.80045
 FREQUENCY = 55.00
 FREQUENCY NR = 20.024 x 10⁻⁶
 STROUHAL NR = 3.085
 AMPLITUDE NR = 0.410
 BLADES = 6.0 INCHES

TABLE II - CONTINUED

RUN NR STRIP	35 Q	- 45 T	DEGREE DT	MODEL, H	LOW FLOW RATE NUS	NUSREN
1	40.059	117.456	57.956	25.072	571.48999	1.71805
2	35.522	121.839	62.339	19.162	436.77051	1.31305
3	29.664	123.584	64.084	14.457	329.54395	0.99070
4	29.002	122.342	62.842	14.760	336.44946	1.01146
5	28.579	123.285	63.785	14.358	327.26076	0.98390
6	28.555	123.010	63.510	14.859	338.69287	1.01820
7	23.525	125.013	65.513	11.054	251.96687	0.75748
8	17.259	124.055	64.555	7.956	181.35721	0.54521
9	11.327	126.661	67.161	4.350	99.15692	0.29809
10	14.511	126.299	66.799	5.951	135.64716	0.40779
11	18.780	123.945	64.445	8.357	190.48082	0.57264
12	21.814	127.513	68.013	8.948	203.96310	0.61317
13	22.606	126.777	67.277	9.350	213.12097	0.64070
14	23.012	125.406	65.906	9.753	222.31319	0.66833
15	25.883	126.321	66.831	10.951	249.61577	0.75041
16	29.661	127.977	68.477	12.547	285.99634	0.85978

REYNOLDS NR = 110647.87500
 VELOCITY = 54.06801
 FREQUENCY = 0.0

F1/S
 CPS

CIRCULAR NR = 0.0
 AMPLITUDE NR = 0.0
 BLADES = 6.0 INCHES

FREQUENCY NR = 0.0

TABLE II - CONTINUED

RUN NR	40	-	45 DEGREE MODEL, LOW FLOW RATE						
STRIP	Q	T	DT	H	NUS	NUSREN			
1	37.622	156.425	57.675	10.878	248.28012	1.31532			
2	28.429	162.076	103.326	6.663	152.08690	0.80571			
3	24.204	162.875	104.125	5.361	122.36848	0.64827			
4	24.212	161.130	102.380	5.766	131.60141	0.69719			
5	23.401	158.436	99.686	6.073	138.60748	0.73430			
6	20.776	160.590	101.840	5.067	115.65665	0.61272			
7	16.843	163.911	105.161	3.659	83.50626	0.44239			
8	13.679	162.714	103.964	2.962	67.60071	0.35813			
9	10.705	158.964	100.214	2.372	54.12794	0.28675			
10	15.083	159.357	100.607	3.571	81.49353	0.43173			
11	18.857	159.486	100.736	4.570	104.30984	0.55260			
12	21.438	161.108	102.358	4.966	113.34360	0.60046			
13	22.076	160.040	101.290	5.169	117.97145	0.62498			
14	22.642	161.533	102.783	4.865	111.03604	0.58824			
15	25.642	160.913	102.163	5.767	131.61427	0.69726			
16	31.665	160.304	101.554	7.868	179.58044	0.95137			

REYNOLDS NR = 35630.42569
 VELOCITY = 17.33890 FT/S
 FREQUENCY = 0.0 CPS
 STRUCTURAL NR = 0.0
 AMPLITUDE NR = 0.0
 BLADES = 6.0 INCHES

FREQUENCY NR = 0.0

TABLE II - CONTINUED

RUN NR	41	- 90 DEGREE MODEL, LOW FLOW RATE						
STRIP	Q	T	DT	H	NUS	NUSREN		
1	47.841	120.612	53.612	35.448	797.57617	2.05668		
2	40.280	119.253	52.253	28.651	644.64941	1.66233		
3	35.640	117.988	50.988	25.154	565.96680	1.45943		
4	36.611	118.225	51.225	26.154	588.45410	1.51742		
5	35.711	121.608	54.608	23.046	518.52344	1.33709		
6	33.508	120.930	53.930	22.047	496.05981	1.27917		
7	25.627	117.922	50.922	16.754	376.97046	0.97208		
8	19.502	118.598	51.598	11.653	262.18506	0.67609		
9	14.583	118.025	51.025	8.254	185.71577	0.47890		
10	17.667	118.192	51.192	10.254	230.70679	0.59491		
11	21.569	120.565	53.565	12.348	277.83008	0.71643		
12	23.840	120.237	53.237	13.749	305.34741	0.79770		
13	25.138	120.821	53.821	14.347	322.81616	0.83243		
14	25.583	120.551	53.551	14.848	334.08057	0.86148		
15	28.654	120.358	53.358	16.949	381.34058	0.98335		
16	31.303	120.594	53.594	18.948	426.32764	1.09935		

REYNOLDS NR = 150387.68750
 VELOCITY = 76.52080
 FREQUENCY = 22.00

STRUCTURAL NR = 0.602
 AMPLITUDE NR = 0.110
 BLADES = 6.0 INCHES

FREQUENCY NR = 4.004×10^{-6}

TABLE II - CONTINUED

RUN NR	42	- 90 DEGREE MODEL, LOW FLOW RATE							
STRIP	Q	T	DT	H	NUS	NUSREN			
1	40.620	130.117	61.117	23.121	518.42676	1.68750			
2	34.835	129.072	60.072	19.323	433.27710	1.41034			
3	32.644	128.350	59.350	18.225	408.65112	1.33018			
4	35.114	127.918	58.918	20.526	460.24731	1.49812			
5	37.384	129.473	60.473	21.722	487.06982	1.58543			
6	38.057	130.309	61.309	22.020	493.75122	1.60718			
7	31.466	132.145	63.145	16.516	370.32471	1.20542			
8	24.358	130.867	61.867	12.519	280.70410	0.91370			
9	23.387	133.496	64.496	11.012	246.92560	0.80375			
10	21.172	131.562	62.562	10.017	224.60912	0.73111			
11	23.472	132.956	63.956	10.814	242.47075	0.78925			
12	23.079	130.118	61.118	11.221	251.59557	0.81895			
13	24.686	129.995	60.995	12.021	269.54053	0.87737			
14	25.252	129.748	60.748	12.321	276.28076	0.89931			
15	28.126	129.920	60.920	13.921	312.14795	1.01605			
16	29.835	129.460	60.460	15.122	335.08032	1.10372			

REYNOLDS NR = 94381.43750
 VELOCITY = 48.53128
 FREQUENCY = 55.00

STROUHAL NR = 2.374
 AMPLITUDE NR = 0.330
 BLADES = 6.0 INCHES

FREQUENCY NR = 25.149 x 10⁻⁶

TABLE II - CONTINUED

RUN NR	43	- 90 DEGREE MODEL, LOW FLOW RATE							
SIRIP	Q	T	DT	H	NUS	NUSREN			
1	44.754	127.623	57.623	29.124	651.93115	2.00679			
2	39.042	129.738	59.738	22.919	513.03223	1.57923			
3	33.903	129.256	59.256	19.220	430.23608	1.32436			
4	35.593	130.539	60.539	20.117	450.31226	1.38616			
5	32.806	131.994	61.994	17.514	392.03320	1.20677			
6	21.839	131.967	61.967	17.114	383.08081	1.17921			
7	26.721	132.073	62.073	13.813	309.20654	0.95181			
8	21.097	129.881	59.881	11.019	246.65025	0.75924			
9	17.376	132.276	62.276	8.113	181.60420	0.55902			
10	19.516	131.322	61.322	9.415	210.75629	0.64875			
11	22.668	129.836	59.836	11.619	260.08325	0.80059			
12	23.819	129.593	59.593	12.220	273.52710	0.84198			
13	24.768	129.900	59.900	12.519	280.22583	0.86260			
14	26.046	129.692	59.692	13.219	295.90625	0.91087			
15	28.214	129.834	59.834	14.419	322.75977	0.99353			
16	30.903	129.364	59.364	16.420	367.55396	1.13141			

REYNOLDS NR = 105535.81250
 VELOCITY = 54.55077 FT/S
 FREQUENCY = 10.00 CPS

STROUHAL NR = 0.384
 AMPLITUDE NR = 0.290
 BLADES = 6.0 INCHES

FREQUENCY NR = 3.638×10^{-6}

LIST OF REFERENCES

1. F.J. Bayley, P.A. Edwards, and P.P. Singh, "The Effect of Flow Pulsations on Heat Transfer by Forced Convection from a Flat Plate", International Developments in Heat Transfer, International Heat Transfer Conference, 2d 1961.
2. Miller, J.A., "Heat Transfer in the Oscillating Turbulent Boundary Layer", Journal of Engineering for Power, p 239, October 1969.
3. Feiler, C.E. and Heager, E.B., NASA Technical Report R-142, "Effect of Large - Amplitude Oscillations on Heat Transfer", 1962.
4. Miller, J.A. and Pucci, P.F., "Heat Transfer to an Airfoil in Oscillating Flow", Journal of Engineering for Power, p 461, October 1971.
5. Kezios, S.P. and Prasanna, K.V., "Effect of Vibration on Heat Transfer from a Cylinder in Normal Flow", ASME Paper G6-WA/HT-43, December 1966.
6. Seban, R.A., "The Influence of Freestream Turbulence on the Local Heat Transfer from Cylinders", Journal of Heat Transfer, May 1960, p. 101.
7. Kestin, J., Maeder, P.F., and Sogin, H.H., "The Influence of Turbulence on the Transfer of Heat to Cylinders Near the Stagnation Point", Zamp, Vol XII, 1961, p 115.
8. Van Der Hegge Zijnen, B.G., "Heat Transfer from Horizontal Cylinders to a Turbulent Air Flow", Applied Scientific Research, Section A, Vol 7, August 1957.
9. Boulos, M.I. and Pei, D.C.T., "Dynamics of Heat Transfer from Cylinders in a Turbulent Air Stream", International Journal of Heat and Mass Transfer, Vol 17, p 767, July 1979.
10. Viteri, M.A., "Experimental Determination of the Average Heat Transfer Coefficient for Yaw Cylinders", M.S. Thesis, Naval Postgraduate School, Monterey, California, 1969.

11. Kraabel, J.S., "Heat Transfer to Air from a Yawed Iso-thermal Cylinder", Ph.D. Thesis, University of California, Davis, 1979.
12. Despard, R.A., "Laminar Boundary Layer Separation in Oscillating Flow", Ph.D. Thesis, Naval Postgraduate School, Monterey, California, June 1969.
13. Banning, R.M., "The Unsteady Normal Force on an Airfoil in Oscillating Flow", Engineer's Thesis, Naval Postgraduate School, Monterey, California, December 1969.
14. Nickerson, R.J., The Effect of Freestream Oscillations on the Laminar Boundary Layer on a Flat Plate, ScD Thesis, MIT, 1958.
15. Hori, E., "Experiments on the Boundary Layer of an Oscillating Circular Cylinder", Bulletin of the Japan Society of Mechanical Engineers, V.G., NR22, p 201-209, 1963.
16. Hill, P.G., Laminar Boundary Layers in Oscillatory Flow, Sc.D. Thesis, MIT, 1958.
17. Feiler, C.E. and Yeager, E.B., "Effect of Large Amplitude Oscillations on Heat Transfer", NASA Technical Report R-142, 1962.
18. Karlsson, S.F., An Unsteady Turbulent Boundary Layer, Ph.D. Thesis, Johns Hopkins University, 1958.
19. Miller, J.A., Transition in Oscillating Blasius Flow, Ph.D. Thesis, Illinois Institute of Technology, June 1963.
20. Miller, J.A., "A Simple Linearred Hot-Wire Anemometer", Journal of Fluids Engineering, V. 98, p 749-752, December 1976.
21. Sandborn, V.A., Resistance Temperature Transducers, Meteorology Press, 1972.
22. Toullokian, Y.S. et al, Thermophysical Properties of Matter, Thermophysical Properties Research Center, Purdue University, IFI/Plenum, New York, 1970.
23. Kline, S.J. and McClintock, F.A., "Describing Uncertainties in Single Sample Experiments", Mechanical Engineering, V 75, p 3-8, January 1953.
24. Froessling, N. in Schlichting, H., Boundary Layer Theory, Translated by J. Kestin, McGraw-Hill, 1955, p 305.

25. Schmidt, E. and Wenner, K. in Schlichting, H., Boundary Layer Theory, Translated by J. Kestin, McGraw-Hill 1955, p 312.

INITIAL DISTRIBUTION LIST

	No. of Copies
1. Defense Technical Information Center Cameron Station Alexandria, Virginia 22314	2
2. Library, Code 0142 Naval Postgraduate School Monterey, California 93940	2
3. Department Chairman, Code 69 Department of Mechanical Engineering Naval Postgraduate School Monterey, California 93940	1
4. Professor J.A. Miller, Code 67Mo Department of Aeronautics Naval Postgraduate School Monterey, California 93940	1
5. Professor P.F. Pucci, Code 69Pc Department of Mechanical Engineering Naval Postgraduate School Monterey, California 93940	1
6. Fred W. Bunson, Jr. 1524 Kiskiak Circle, NWS Yorktown, Virginia 23691	1

Thesis

B82675 Brunson

c.1

Local heat transfer
coefficients around a
cylinder in oscil-
lating flow.

Thesis

B82675 Brunson

c.1

Local heat transfer
coefficients around a
cylinder in oscil-
lating flow.

thesB82675

Local heat transfer coefficients around



3 2768 002 07844 6

DUDLEY KNOX LIBRARY